MARS ORBITAL SURVEY AND IMAGING CARTOGRAPHER

2025 AIAA Request for Proposal Response
Space Design Competition

Submitted by:

Adi Arora
Olivia Caper
Sana Churi
Catherine Fang
Kaleigh Griswell
Cheyenne Halverson
Devi "Diya" Patel
Tobias Roule

Faculty Advisor:

Dr. Yashwanth Nakka

Adi Arora

AIAA #: 1799633

Kaleigh Griswell

AIAA #: 1799632

Olivia Caper

AIAA #: 1341806

Cheyenne Halverson

AIAA #: 1799631

Sana Churi

AIAA #: 1603465

Devi "Diya" Patel

AIAA #: 1744692

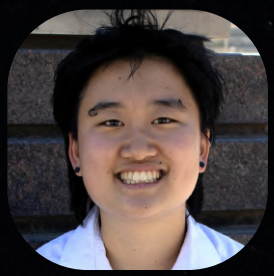

Catherine Fang

AIAA #: 1405486

Tobias Roule

AIAA #: 1326080

MOSAIC Team

Dr. Yashwanth Nakka

AIAA #: 1375180

Contents

I. Executive Summary

The Mars Orbital Survey and Imaging Cartographer (MOSAIC) was created to answer the question "what untapped resources does Mars hold and how viable is the planet for future human settlement?" Following the AIAA Undergraduate Team Space Design Competition, MOSAIC was formulated to efficiently map the surface of Mars and determine future human outposts to enable scientific exploration and a human presence on Mars. The MOSAIC Team has broken the mission into two stages: first, the Orbiter for Planetary Understanding and Sensing (OPUS) shall orbit Mars at an inclination allowing for mapping of at least 75% of the Martian surface to determine future landing sites, and second, the probes, Terrestrial Investigation of Landscape Erosion and Space weather (TILES), shall be deployed at 2 landing sites that meet mission requirements for environmental data gathering. The mission planning began with launch and trajectory calculations.

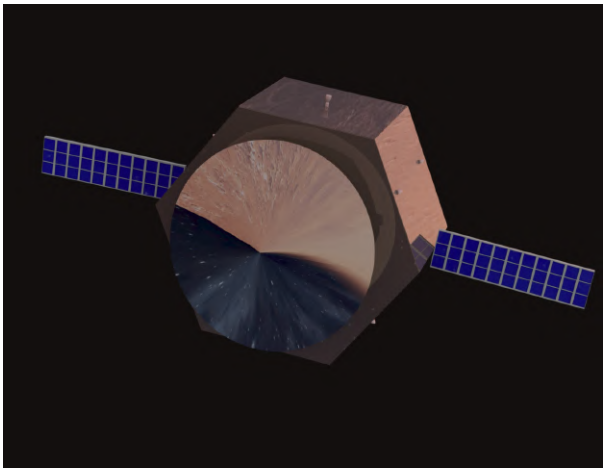

Fig. 1 OPUS and TILES Assembly and Render

As the primary mission objectives need to be met by January of 2033, MOSAIC is set to launch on December 31, 2028 entering a 28° inclination and 400 km altitude Low Earth Orbit (LEO), where it will then depart for Mars. The transit period is projected to be 240 days, and it is planned to arrive to the Martian sphere of influence on August 28, 2029. To increase efficiency, as opposed to injecting straight into a circular orbit around Mars for the science orbit, the orbiter enters an aerobraking phase to conserve the amount of ΔV needed for the mission. The aerobraking orbit starts as a highly elliptical orbit with an apoapse of 50,000 km and a periapse of 3,506 km. Over time, the Martian atmosphere, though relatively thin, will provide enough of a drag force in order to lower the apoapse. The aerobraking phase will end once a desired apoapse of 250 km is met, and at that point, a circularization and inclination change burn is performed to put the vehicle at the desired orbit, 50° inclination, of a circular 250 km altitude orbit. On February 7, 2030, the primary science mission begins as OPUS enters its desired orbit for imaging data to be collected. One map at 75% coverage takes 119 days, accounting for the orbital time in umbra and penumbra, to complete. Thus, the primary science mission concludes on June 6, 2030. At a minimum, the team decided to make at least three more maps of the planet before January 2033 to account for any topological or atmospheric changes, and to create more detailed maps per iteration. OPUS will continue to orbit and map Mars' surface after the TILES probes are dropped, continuing past 2033.

The ADCS system was designed to enable science instrument data collection, solar panel power generation, and ensure proper trajectory course. Two types of actuators are used: momentum wheels for most rotational motion, and

thrusters for momentum dumping and translational motion. A sensor suite is also used to determine the attitude and location of OPUS. The sensor suite is comprised of 5 sun sensors, 2 star trackers, and 2 inertial measurement units. Actuator and sensor configurations were designed for maximum redundancy, in case of failure from any individual sensor or actuator. During a normal operating cycle, the ADCS system will be equipped for the following modes: science, earth relay, TILES relay, and safe modes. In addition, the ADCS system is designed for the capability to perform trajectory correction maneuvers, as well as orient OPUS for its aerobraking campaign and release of the TILES.

To provide MOSAIC with a means of relaying its scientific data back to Earth, a communications system was chosen based on heritage and reliability. Using NASA's three Deep Space Network stations, the orbiter OPUS will relay science data across X-band frequencies, and mission control will ensure proper commands are sent to each subsystem. Once the TILES probes are launched to the Martian surface, they will communicate with OPUS using the Ultra-High Frequency range, and OPUS will relay this information back to Earth once again. OPUS is equipped with a 2.5 m high-gain antenna, two smaller low-gain antennas, and an ultra-high frequency antenna for redundancy and a strong link between all subsystems involved. TILES has its own ultra-high frequency antenna to communicate with OPUS, as well as a medium-gain antenna for emergency communications directly to Earth. The most intensive communications operation will be the relay of high-resolution images from the High-Resolution Imaging Camera (HiRIC), where one full-size image takes roughly 40 minutes to downlink from Mars at a rate of 10 MBps. Thus, image data relay will occur during OPUS's designated science mode.

Once the landing locations have been determined, the Entry, Descent, and Landing (EDL) of the two TILES will begin on January 14, 2034. To begin the EDL sequence, both TILES will be ejected from OPUS using pyrotechnic bolts and loaded springs. After release, the aeroshell will be used to slow the initial descent velocity and protect the instruments aboard the TILES. A disk-band gap parachute will be deployed when the probe reaches about Mach 2. Shortly afterwards, the aeroshell will be ejected, using a similar pyrotechnic bolt configuration as before. When descent velocity reaches around 60m/s, 4 descent thrusters will be enabled and the parachute will be detached from the TILES. About 20 meters above the Martian surface, telescoping landing legs will be deployed. Finally about an hour after the TILES is safely landed and communication with Earth is confirmed, the TILES will be unfolded to release the science instruments. This EDL sequence will ensure the safe landing of the instruments aboard the TILES and land the probe within a 50km radius of the target landing location.

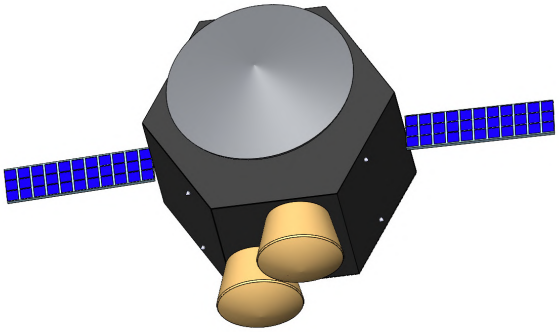

Fig. 2 OPUS and TILES Assembly, Bottom View

For the OPUS to reach the correct orientation, 9 hydrazine thrusters were chosen to enable correct pointing requirements for communications, power acquisition, attitude and control determination, and trajectory. The propulsion system has one large thruster mainly used for trajectory corrections and 8 smaller thrusters for attitude control. All of the fuel for these thrusters are located in one main storage tank aboard the OPUS. The amount of hydrazine was determined by the necessary delta-v for the orbit insertion maneuvers it requires, as well as for the predicted attitude control maneuvers required over the lifetime of the project.

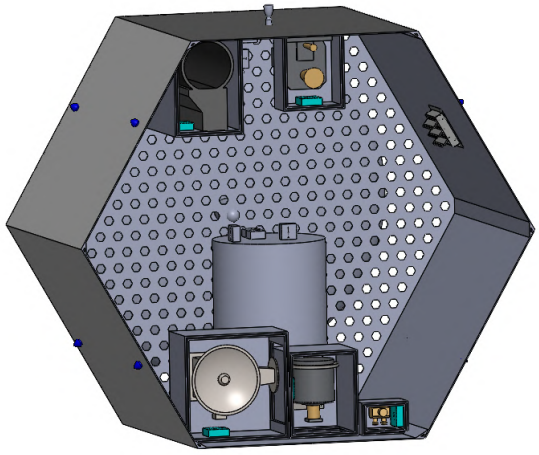

Fig. 3 OPUS Open-Case Subsystem View

To meet the ambitious science objectives of the MOSAIC mission, the OPUS and TILES were both equipped with a variety of flight-proven and novel instruments, selected to balance the novelty of scientific data, level of flight heritage, and constraints from other subsystems. The OPUS is tasked with surveying at least 75% of the Martian surface; to do so, it carries four key instruments. The Gamma-Ray and Neutron Spectrometer (GRNS), adapted from the Psyche mission, provides both gamma-ray and neutron flux data to determine elemental abundances and detect organic and inorganic compounds on the Martian surface. This marks the first use of a neutron spectrometer in Martian orbit, offering unprecedented insight into Mars' subsurface composition and presence of water ice. Second, it carries a laser altimeter modeled after LOLA on NASA's Lunar Reconnaissance Orbiter. This instrument produces high-resolution elevation maps and supports landing site selection by characterizing terrain stability and levelness. Its high accuracy and fast sampling rate provide a significant upgrade over similar instruments on prior Mars missions.

Third, a visual camera with the same design as HiRIC is also included in the science payload. With a 0.5-meter resolution at 265 km altitude, this camera enables detailed imaging of Martian surface features. Selected for its balance between resolution and reduced mass/volume requirements, HiRIC will support identification of landing zones across seasons. Lastly, a Fourier Transform Infrared Spectrometer will provide data on temperature, wind, and gaseous composition of the Martian atmosphere, which is critical for understanding the conditions faced by future missions and potentially supporting future on-site resource utilization. Though this novel CIRS-LITE design has a lower Technology Readiness Level (TRL 5) than the other instruments aboard OPUS, its heritage from Cassini's CIRS and Voyager's IRIS instruments supports its viability on this mission.

Additionally, each of the two TILES carries a targeted suite of environmental sensors aimed at assessing the Martian

surface's habitability. The first of these is the Radiation and Dust Sensor (RDS), which was originally deployed on the Perseverance rover. The RDS monitors airborne dust properties and seasonal cloud cover, critical for evaluating environmental hazards at potential landing sites. Its consistent operation on Mars since 2021 justifies its selection with a TRL of 8. The second is the Radiation Assessment Detector (RAD). A veteran of the Curiosity rover mission, RAD collects radiation from cosmic rays and solar particles on the Martian surface, essential data for ensuring the safety of sensitive electronics and human missions. With over a decade of reliable performance beyond its expected lifespan, RAD is rated TRL 9.

Collectively, the instruments aboard OPUS and TILES ensure that the science goals of the MOSAIC mission are fulfilled, with special attention paid to balancing reliability and novelty. The combined data from the orbital and surface mission components will directly inform human exploration and deepen our understanding of Mars' geology, climate, and surface.

In order to power the various instruments and systems on OPUS and TILES, a power system consisting of solar panels and batteries is used. The power system was designed to support all operations at various phases of the mission. The solar panels are used during the hours when OPUS is illuminated and during the Martian day when TILES is illuminated. The solar panels were sized to collect a sufficient amount of power to power all systems during the hours of light and store enough power to power the system during the hours of darkness. Lithium ion batteries are used on both OPUS and TILES to store power. The size of the solar panels and batteries were determined by the required power for all systems during the various phases of the mission and the time the system will have these power requirements with some margin. As a result, the power system has the capability to operate all necessary operations for powered systems for instrumentation, ADCS, thermal control, and communication.

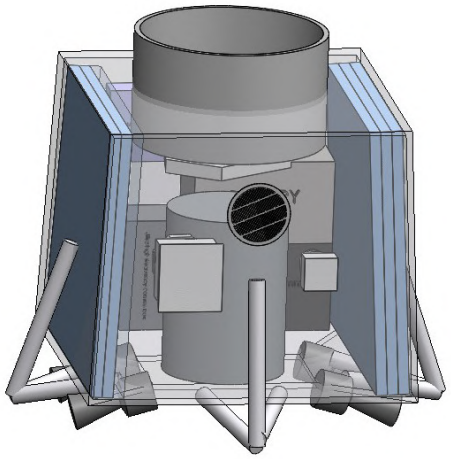

Fig. 4 TILES with Transparent Outer-layer for Visualization

The OPUS and TILES missions implement tailored thermal control systems to manage extreme environmental conditions throughout their Mars mission phases. OPUS utilizes a multilayer insulation (MLI) structure with graphite composite, aluminum honeycomb, Kapton, and coatings to withstand aeroheating during aerobraking. Passive control is supplemented by loop heat pipes and resistive heaters, while sensitive instruments use cryocoolers. Deep space protection is enhanced with MEMLI insulation.

TILES utilizes an ablative aeroshell with PICA and SLA-561V for EDL protection. On the Martian surface, it

combines MLI, aerogel insulation, and RHUs to maintain thermal balance. RHUs were chosen over RTGs for their simplicity and suitability for the probe's low power and thermal needs. Both systems ensure operational temperatures are maintained for mission success.

The dimensionality of this mission was determined by minimizing the volume requirements of the OPUS and TILES all assembled within the payload bay of our launch vehicle, the Falcon Heavy. Using the constraints of this vehicle's payload bay, the dimensions of the OPUS were determined to be 3.520x2.880x2.975 m^3, including the communications dish and folded solar panels. Once in orbit, the fully expanded orbiter will have a wingspan of 7.24 m. The TILES were also sized to minimize volume but maximize area when unfolded on Mars to enable high solar power production. This amounted to a folded dimensionality of 0.80x0.60x0.60 m^3 and an unfolded configuration of 1.97x1.53x0.31 m^3. Both structures where primarily created with an Aluminum Lithium alloy for structural, cost and novelty reasoning.

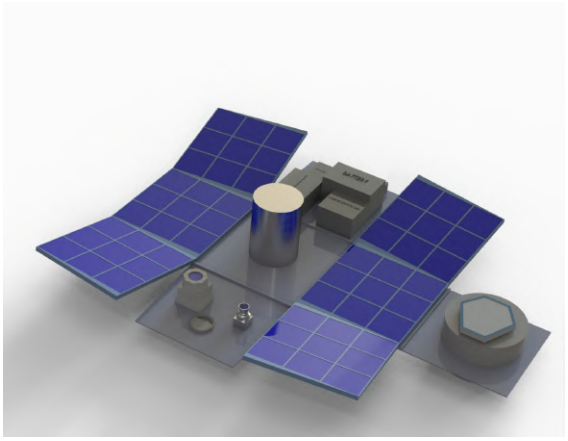

Fig. 5 Unfolded TILES Render

Overall, MOSAIC Team first based all design decisions around a preliminary mass budget that used 70% of the Falcon Heavy payload fairing to provide an upper limit for mass. As subsystems were researched and designed, the actual mass estimate resulted in being about 30% of the total launch vehicle capacity, which allows for the opportunity for costs to be mitigated by another mission sharing the payload fairing alongside MOSAIC. Since the budget calculations estimate MOSAIC to be a little less than the $1 billion limit established in the RFP, this option may be necessary.

A risk analysis was also conducted along with pre-launch mitigation strategies. These mitigation strategies were implemented into the research and development of each subsystem.

The mission from Phase A through E has a duration of 15 years, with the Operations phase (Phase E) lasting 10 years. With an optimized launch date of December 31, 2028, all phases were designed around that date, including margins to allow for unexpected delays. Should the initial launch window be missed, January 16, 2029 is the next available window. All of OPUS's mapping will be concluded by the end of 2033, and the TILES will deploy at their POFMOs and record data through 2039.

The Mars Orbital Survey and Imaging Cartographer (MOSAIC) mission represents a comprehensive and innovative step forward in Martian exploration, and it will be vital to future manned missions to Mars and further exploration of the planet.

II. Nomenclature

ATLO	=	Assembly, Testing, Launch, & Operations (Phases D & E)
CBE	=	Current Best Estimate
CER	=	Cost Estimating Relationships
DSN	=	Deep Space Network
ΔV	=	Change in velocity across all phases of the mission
HGA	=	High-Gain Antenna
IA&T	=	Integration, Assembly, & Test
LGA	=	Low-Gain Antenna
LEO	=	Low Earth Orbit
Level 1 Components	=	High-level categories for mission systems, like spacecraft dry mass and propellant
Level 2 Components	=	Subcategories of the Level 1 Components, such as OPUS and both TILES
MGA	=	Medium-Gain Antenna
MOSAIC	=	Mars Orbital Survey and Imaging Cartographer
MRO	=	Mars Reconnaissance Orbiter
NASA	=	National Aeronautics and Space Administration
OPUS	=	Orbiter for Planetary Understanding and Sensing
POFMO	=	Potential Outposts for Future Martian Occupation
R&D	=	Research and Development
RFP	=	Request-for-Proposal (2024–2025 AIAA Undergraduate Team Space Design Competition Guidelines) [1]
SDST	=	Small Deep Space Transponder
SEE	=	Standard Error of the Estimate
Spacecraft	=	Combined assembly of OPUS, the two TILES, and propellant
Spacecraft Dry Mass	=	Combined assembly of OPUS and the two TILES
TILES	=	Terrestrial Investigation of Landscape Erosion and Space weather (formerly "the probes")
TRL	=	Technology Readiness Level
UHF	=	Ultra High Frequency
WBS	=	Work Breakdown Structure

Introduction

Mars is known to be a planet of scientific interest and untapped potential, with resources and landscapes not yet understood enough to ensure human success on the planet. With relevant technology improving every day, the race to identify human landing sites on Mars has only intensified. However, in order to safely send crewed missions to the Red Planet, we must know more about where these crews may land, specifically by mapping and studying the environment of potential landing sites. Given the need for creative solutions, the American Institute of Aeronautics and Astronautics (AIAA) has asked undergraduate students to design a Mars mission that will map 75% of the Martian surface while also conducting a specific environmental study of potential landing sites. Given the AIAA request for proposal, we created the MOSAIC mission.

The purpose of the MOSAIC mission, the Mars Orbital Survey and Imaging Cartographer (MOSAIC), is to create a highly detailed geographic survey of at least 75% of the Martian surface, including elevation profiles, landing sites, and traverse paths to inform future missions to the planet. Phase 1 will be achieved by an orbiter in a high-inclination semi-synchronous orbit that will use laser altimeters, spectrometers, and high-resolution imaging to collect data regarding potential landing sites. Phase 2 shall be achieved by landing two probes at two landing sites chosen to collect dust accumulation and radiation data, marking the locations for future manned missions and colonies.

The orbiter, OPUS (Orbiter for Planetary Understanding and Sensing), is tasked with carrying the mapping aspect of the MOSAIC mission, while the probes, TILES (Terrestrial Investigation of Landscape Erosion and Space weather), shall conduct surface testing. After separation from the launch vehicle, OPUS will conduct an aerobraking maneuver to enter the appropriate science orbit. Once the orbiter has completed initial mapping, the TILES probes will separate from the OPUS body and descend to the Martian surface where they will relay information about the environmental states of these sites.

III. Mission Overview

A. RFP Design Requirements and Constraints

Below is a table of the mission requirements from the AIAA RFP:

Table 1 High-Level RFP Requirements

Req ID	Requirement Description
RFP-1	Design an integrated comprehensive mission to send one or more exploration assets to Mars vicinity with the primary objective to accurately characterize the atmospheric composition, conduct a detailed geographic survey, and/or determine the potential subsurface resources that may exist on Mars. The designed mission must address at minimum one of these primary objectives: a. Characterization of the atmospheric composition and detailed density profile will provide mission planners the necessary data to plan and design the entry, descent, and landing system to support human exploration. b. Detailed geographic survey, including terrain and elevation profile of the entire Martian surface will provide mission planner the ability to pinpoint potential landing location and traverse paths for each mission to maximize the potential to achieve exploration objectives. c. Investigation, identification, and quantification of potential surface and subsurface resources will enable mission planners to determine the potential of utilizing such resources in support of the human exploration activities.
RFP-2	The designed mission must be able to provide data on at least one primary objective area with minimum of 75% coverage of the entire Mars globe at the conclusion of the primary mission phase.
RFP-7	The cost for the mission and capability development in support of its activities shall not exceed $1.0 Billion US Dollars (in FY24), including development, hardware, launch, and operation cost of the mission through the primary mission phase.
RFP-8	The mission should complete deployment and primary data gathering activities no later than December 31, 2033, with the system designed to operate into the late 2030s, though operation cost past the primary mission phase will be outside the scope of this RFP.

Additional requirements and their compliance regarding the format and content of this report can be found in Table XII at the end of this document.

The MOSAIC Team aimed to achieve all three sub-requirements in RFP-1, but the first question was clear: how could one asset meet all three goals? After further analysis of previous Martian missions and some preliminary calculations, it was determined that an orbiter would achieve RFP-1a and RFP-1b through various types of mapping data, while surface probes would have to be released in order to fulfill RFP-1c. Therefore, this mission would have three assets: an orbiter (OPUS) and two probes (TILES).

B. Mission and System Requirements

From the RFP Requirements in Table 1, the MOSAIC Team then established the framework of the mission into ten primary requirements:

Table 2 Mission Requirements

Req ID	Requirement Description
MR-1.0	This mission and development for the primary mission phase shall not cost over $1.0 billion USD.
MR-2.0	The mission shall launch from Kennedy Space Center on December 31, 2028, and no later than January 16, 2029.
MR-3.0	All phases of the mission shall be completed by December 31, 2039.
MR-3.1	The primary phase of the mission shall be completed no later than December 31, 2033.
MR-3.2	The secondary phase of the mission shall be completed no later than December 31, 2038.
MR-4.0	The OPUS and TILES shall remain operational through the primary and secondary phases of the mission.
MR-5.0	The orbiter, OPUS (Orbiter for Planetary Understanding and Sensing), shall map at least 75% of the Martian surface during the primary phase of the mission.
MR-6.0	The Ground Station shall analyze the data from the OPUS to determine Potential Outposts for Future Martian Occupation (POFMOs) for the second phase of the mission.
MR-7.0	The OPUS shall be able to carry two TILES (Terrestrial Investigation of Landscape Erosion and Space weather) to be released over and land at two identified POFMOs.
MR-8.0	The TILES shall gather environmental data at their POFMO during the secondary phase of the mission.
MR-9.0	The launch vehicle shall ensure the survival of the OPUS and two TILES (a.k.a. "the spacecraft") in transit from Earth to Mars.
MR-10.0	The launch vehicle, OPUS, and TILES shall be able to communicate with the Ground Station during all phases of the mission.

From these requirements in Table 2 and the launch vehicle determined in Section IV, the MOSAIC Team was then able to determine more specific requirements for the mission architecture and system as a whole:

Table 3 System Requirements

Req Name	Parent Req	Traceability	Requirement	Rationale
SYS-1.0	LV-1.0	MR-9.0 - LV-1.0 - SYS-1.0	The total payload shall not exceed 16,800 kilograms.	From the Falcon Heavy User Guide [2]. Provides mass limit for the spacecraft.
SYS-2.0	LV-1.0	MR-9.0 - LV-1.0 - SYS-2.0	The spacecraft shall fit within the payload fairing envelope of 4.5 meters in diameter and 12.1 meters in height. Any additional height must fit within the conical nose of the payload fairing in accordance to the payload fairing	From the Falcon Heavy User Guide[2]. Ensures that the spacecraft can be able to fit inside the Falcon Heavy's payload fairing.
SYS-3.0	LV-1.0	MR-9.0 - LV-1.0 - SYS-3.0	The spacecraft shall be compatible with the maximum, worst-case flight environment of the Falcon Heavy.	From the Falcon Heavy User Guide[2]. Ensures that the spacecraft can survive the conditions experienced during launch.
SYS-3.1	SYS-3.0	MR-9.0 - LV1.0 - SYS-3.0 - SYS-3.1	The spacecraft shall be compatible with the Falcon Heavy radio-frequency environment of 140 decibel-microvolts per meter.	From the Falcon Heavy User Guide[2]. Ensures that the spacecraft can withstand radio-frequencies emitted by the Falcon Heavy during launch.
SYS-3.2	SYS-3.0	MR-9.0 - LV-1.0 - SYS-3.0 - SYS-3.2	The spacecraft shall not emit radiation more than 48 decibels-microvolts per meter, as measured at the top of the payload attach fitting.	From the Falcon Heavy User Guide[2]. Ensures that the spacecraft will not emit radiation at a level that would interfere with the launch vehicle's operations.
SYS-3.3	SYS-3.0	MR-9.0 - LV-1.0 -SYS-3.0 - SYS-3.3	The spacecraft inside the payload attach fitting shall be able to withstand quasi-static loads, sine, acoustic, shock, and random vibration, pressure, and thermal limits experienced during flight.	From the Falcon Heavy User Guide[2]. Ensures that the spacecraft can endure other conditions experienced during launch.
SYS-3.4	SYS-3.0	MR-9.0 - LV-1.0 - SYS-3.0 - SYS-3.4	The spacecraft shall be compatible with the mechanical and electrical interfaces of the Falcon Heavy.	From the Falcon Heavy User Guide[2]. Ensures that the spacecraft will be able to connect to the mechanical and electrical connections of the Falcon Heavy.
SYS-4.0	MR-6.0	MR-6.0 - SYS-4.0	A POFMO shall have the following characteristics within a 1 kilometer radius (in descending importance): a) Elevation differential of +- 2 meters b) Low rock abundance c) Within an equatorial latitude +- 30 degrees d) Mean wind speeds below 10 meters per second e) At/within 10 kilometers from a significant crater. A "significant crater" is defined as being at least 1 kilometer in diameter, regardless of depth.	Details the characteristics that would be the most advantageous for future manned Mars missions and potential outposts. This ensures that the locations chosen by the Ground Station will a) be relatively flat (not on a hilly terrain), b) have minimal rocks, c) be within the warmest regions of Mars, d) minimize winds to ensure outpost integrity, and e) be within walking distance of (presumably) aerologically important locations for future research.
SYS-4.1	SYS-4.0	MR-6.0 - SYS-4.0 - SYS-4.1	If no locations on Mars satisfy SYS-4.0, the Ground Station shall conduct additional analysis to choose POFMOs based on locations that are the closest to the original requirements.	Ensures that POFMOs will be chosen if the initial requirements are not met.
SYS-5.0	MR-5.0	MR-5.0 - SYS-5.0	The OPUS shall collect chemical composition, elevation, and visual-spectrum imaging data.	Describes what data - and therefore what kind of instruments needed - OPUS will gather for the Ground Team to form into maps of the Martian surface.
SYS-6.0	MR-8.0	MR-8.0 - SYS-6.0	The TILES shall collect radiation, dust composition and density, and meteorology data at its POFMO.	Describes what data - and therefore what kind of instruments needed - the TILES will gather for the Ground Team to analyze to characterize Martian weather and conditions.
SYS-7.0	MR-4.0	MR-9.0 - MR-4.0 - SYS-7.0	The data collecting instruments for both the OPUS and TILES shall function when the region of focus is not eclipsed.	Ensures that the OPUS is not scanning or that the TILES are not imaging when there is no sunlight to illuminate the area. Saves power and data cleaning.
SYS-8.0	MR-2.0	MR-2.0 - SYS-8.0	All spacecraft integration, assembly, and testing shall occur at a Kennedy Space Center Facility.	Since MOSAIC will launch from there, it lowers transportation costs to have IA&T occur there too.

Throughout the report, subsystem requirements will be placed at the beginning of their sections with the understanding that they were determined based on the calculations and discussion following it. These subsystem requirements (from Tables 5, 10, 12, 13, 14, 19, 20, 21, 30, 31, and 38) have been summarized in the Requirements Tree in Figure 6 for

visualization purposes:

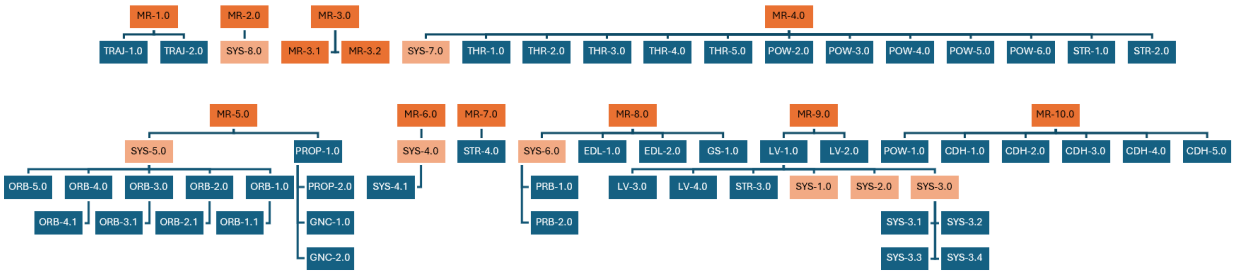

Fig. 6 Requirements Tree

C. Science Traceability Matrices

The MOSAIC Team then defined the goals, objectives, and measurements of each asset of the mission. Below is the STM for the OPUS:

Decadal Survey Question	Science/Technology Goals	Science/Technology Objectives	Measurement Requirements		Instrument Requirements		Projected Performance	Mission Requirements (Top Level)
			Physical Parameters	Observables				
Q4.3e What exogenic volatile and nonvolatile materials are delivered to planetary bodies?	Characterize type and amount of material delivered to Mars via comets, asteroids, and other impacts	Obtain chemical composition of Mars surface close to impact sites	Relative presence of inorganic materials (Fe, Cl, Na, etc); Relative presence of organic materials (C, H, O, N, P, S, and molecules made up of these elements) near impact sites	Numbers and energies of gamma rays, neutrons	Gamma Ray and Neutron Spectrometer (GRNS)	Spectrum range from 0.3 eV to 100 MeV; detection of cosmic-ray generated gamma-rays	Neutron energy ranges delineated as follows: thermal (<0.3 keV), low-energy epithermal (0.3 eV–1 keV), and high-energy epithermal (up to 100 keV); Gamma-rays detected in 0.1- to 10-MeV range	Polar orbit of 45° inclination to maximize time observing impact sites >1km; 45° FOV
Q10.5b What processes govern the inventories, forms, and distribution of life-supporting elements on planetary bodies?	Determine characteristics of certain locations on the Martian surface that will be potentially favorable to future habitation or exploration	Generate elevation profiles of at least 75% of surface; identify resources (ice, regolith, oxygen, etc)	Flat terrain w/ minimal loose regolith, equatorial, low rock abundance, proximity to significant(>1km) craters	time of flight (determines range), pulse spreading (determines surface roughness)	Laser Altimeter	Radial accuracy <10m; Spatial accuracy <130 m; Timing resolution of <1 ns	Radial accuracy ~5m; Spatial accuracy ~100 m; Timing resolution of 0.5 ns	250-km science orbit of 45° inclination
		Map traverse paths between landing sites (ie crater to avoid, craters to explore)	Observe uneven/unstable terrain, map extreme elevation changes	time of flight (determines range), pulse spreading (determines surface roughness)	Laser Altimeter	Radial accuracy <10m; Spatial accuracy <130 m; Timing resolution of <1 ns	Radial accuracy ~5m; Spatial accuracy ~100 m; Timing resolution of 0.5 ns	250-km science orbit of 45° inclination
		Identify potential landing sites	High-resolution optical images, multispectral imaging capability for supplemental surface composition analysis; ability to detect changes over time	Surface and terrain features, albedo variations, landing site characteristics (rock abundance, obvious elevation changes)	High Resolution Imaging Camera	5-m optical system, focal length of 2.5 m, aperture of 0.5 m; multispectral imaging covering 400–1000 nm	Spatial resolution of <5 m/pixel at nadir; (SNR) >100 in bright terrain and >50 in low-light	250-km science orbit ensuring resolution requirements; trajectory that allows for image cadence of <30 days
Q4.4b What materials ejected from impact craters are deposited on planetary surfaces?	Determine how the composition of Mars' surface and atmosphere can affect the future of exploratory missions to the planet's surface	Chemical composition of ejected materials in Mars caters; dectect radition levels of ejected materials	Radiation Rates; Particle Flux	Numbers and energies of gamma rays, neutrons	Gamma Ray and Neutron Spectrometer (GRNS)	Spectrum range from 0.3 eV to 100 MeV; detection of cosmic-ray generated gamma-rays	Neutron energy ranges delineated as follows: thermal (<0.3 keV), low-energy epithermal (0.3 eV–1 keV), and high-energy epithermal (up to 100 keV); Gamma-rays detected in 0.1- to 10-MeV range	Polar orbit of 45° inclination to maximize time observing impact sites >1km; 45° FOV
		Obtain chemical and temperature composition of Mars atmosphere	Relative presence of different gases in atmopshere (incl. CO2, N, Ar, O, methane, …)	Infrared-light energy (radiance) emitted by particles in atmosphere	Infrared Spectrometer (CIRS-Lite)	Wavelength range from 7 to 333 μm; spectral resolution < 2 cm^-1	Multiple detector arrays sampling varied wavelengths: high Tc superconductor, 16-333μm; photoconductive HgCdTe, 9-16μm; photovoltaic HgCdTe, 7-9μm. Spectral resolution of 0.125 cm^-1	Optics temperatures of 140K, detectors near 70-90K
		Search for presence of water or ice	Presence of surface or near-surface ice reservoirs	Numbers and energies of gamma rays, neutrons	Gamma Ray and Neutron Spectrometer (GRNS)	Spectrum range from 0.3 eV to 100 MeV; detection of cosmic-ray generated gamma-rays	Neutron energy ranges delineated as follows: thermal (<0.3 keV), low-energy epithermal (0.3 eV–1 keV), and high-energy epithermal (up to 100 keV); Gamma-rays detected in 0.1- to 10-MeV range	Polar orbit of 45° inclination to maximize time observing impact sites >1km; 45° FOV

Fig. 7 OPUS Science Traceability Matrix

Below is the STM for each of the TILES:

Decadal Survey Question	Science/Technology Goals	Science/Technology Objectives	Measurement Requirements		Instrument Requirements		Projected Performance	Mission Requirements (Top Level)
			Physical Parameters	Observables				
Q10.7b What Endogenous Factors Control the Continuity of Habitability?	Determine the rate and distribution of Martian dust accumulation to assess risks to surface infrastructure, spacecraft, and human habitat and develop mitigation strategies for future missions	Characterize dust deposition rates, grain size distribution, and electrostatic properties over an extended period of time	Dust accumulation rate over a given area (g/m²/day), grain size (μm), electrostatic charge (V/m)	Surface dust layer thickness changes, dust particle size distribution, charge variations	Radiation and Dust Sensor (RDS)	Skycam: take images in visible to near-infrared range Photodetectors: Zenith-pointing detect discrete wavelengths from 245-1100 nm; lateral detectors centered on 750nm	Skycam: images within 600-800nm, >2 images per day Photodetectors: Zenith pointing detectors individually will image 245, 295, 250–400, 450, 650, 750, 950, and 110–1100 nm Lateral detectors image from 740-760 nm	Multiple locations monitored over at least one Martian year; locations chosen such that dust accumulation will not be quick enough to cut mission short
Q10.7a What Exogenous Factors Control the Continuity of Habitability?	Determine the influence of space weather phenomena on the Martian surface environment to evaluate their potential impact to communication systems, power generation, and safety	Monitor solar wind, cosmic radiation levels, and induced atmospheric effects on Mars	Particle flux (particles/cm²/s), radiation dose rate (mSv/day), timing of solar weather events	Solar wind interactions with atmosphere, changes in surface radiation, event frequency	Radiation Assessment Detector (RAD)	36.7° FOV; Detect particles with energies ranging from 0.15-270 MeV	The following particles will be detected in the following energy ranges (all MeV): Protons: 4.3-270 (largest flux) Neutrons: 2-100 (high safety concern) Electrons: 0.15-15 (precursor to solar events) Gamma, x-rays: <1.5 (solar flare indicators, relevant geologically)	Multiple locations of continuous radiation monitoring for at least one Martian year; solar event tracking from ground station; instrument shielding intended for long-duration operation

Fig. 8 TILES Science Traceability Matrix

D. Mission Statement and Vision

With the determination of the mission requirements and STMs, MOSAIC's mission statement is as follows:

> "MOSAIC is a pioneer of future Martian research and occupation for the advancement of humanity in space.
>
> MOSAIC's OPUS will create a highly-detailed map of surface composition, elevation, radiation and visual spectra, which will then be used to choose two potential occupation locations. The TILES will then land at those locations and collect meteorological and atmospheric data over time so future Martian colonies understand the environment and can establish outposts effectively."

MOSAIC's vision statement:

> "Piecing together our future on Mars"

MOSAIC aims to not only gather data on Mars but to also inspire future missions to find a second home on Earth's sibling planet.

E. Concept of Operations

The MOSAIC mission begins at Cape Canaveral, launching on December 31st, 2028 on the Falcon Heavy rocket. The rocket inserts into a Low-Earth Orbit at about 400 km in altitude. From here, it begins its 240 day transfer to the Martian sphere of influence, where OPUS will be deployed and will execute an aerobraking maneuver. The aerobraking saves critical propellant mass and ΔV by using drag from the Martian atmosphere to slowly bring OPUS closer to its target science orbit. By February 7th, 2030, MOSAIC will have reached its target science orbit. This orbit is nearly circular and 250 km above the Martian surface - just high enough to avoid atmospheric drag, but close enough to the surface to take high quality pictures and collect valuable science data.

Over the next 3 years, OPUS will continue to collect elevation profiles, surface composition, and atmospheric composition data of Mars. By 2033, it will have mapped about 80% of the Martian surface, gleaning information that

will be used to determine two Potential Outposts for Future Martian Occupation (POFMOs). These POFMOs will consist of areas with flat elevation profiles, water ice deposits nearby, or other interesting features for further exploration. Once the POFMOs have been identified, OPUS will release a TILES to each site, where they will gather long-term radiation and dust accumulation data to assess the viability of human habitats in each region. By doing so, the TILES would carry out the first long-term survey of space weather on the Martian surface, particularly at regions of interest for human settlement.

The TILES are designed to run for roughly 5 years, with the potential to outlast this limit. Regardless, at end-of-life, the TILES will be shut down and powered off. Since both TILES will be handled cleanly on Earth and do not interact with potential organic material, powering down each is in the best interest for planetary protection protocols. While the TILES are collecting data, OPUS will also continue to collect data on the Martian surface and act as a relay point for the TILES (and other existing Mars rovers and landers) to transmit back to the Ground Station. Once OPUS reaches its end-of-life, it will also be powered off.

Below is the Concept of Operations diagram with a visualization of MOSAIC's mission.

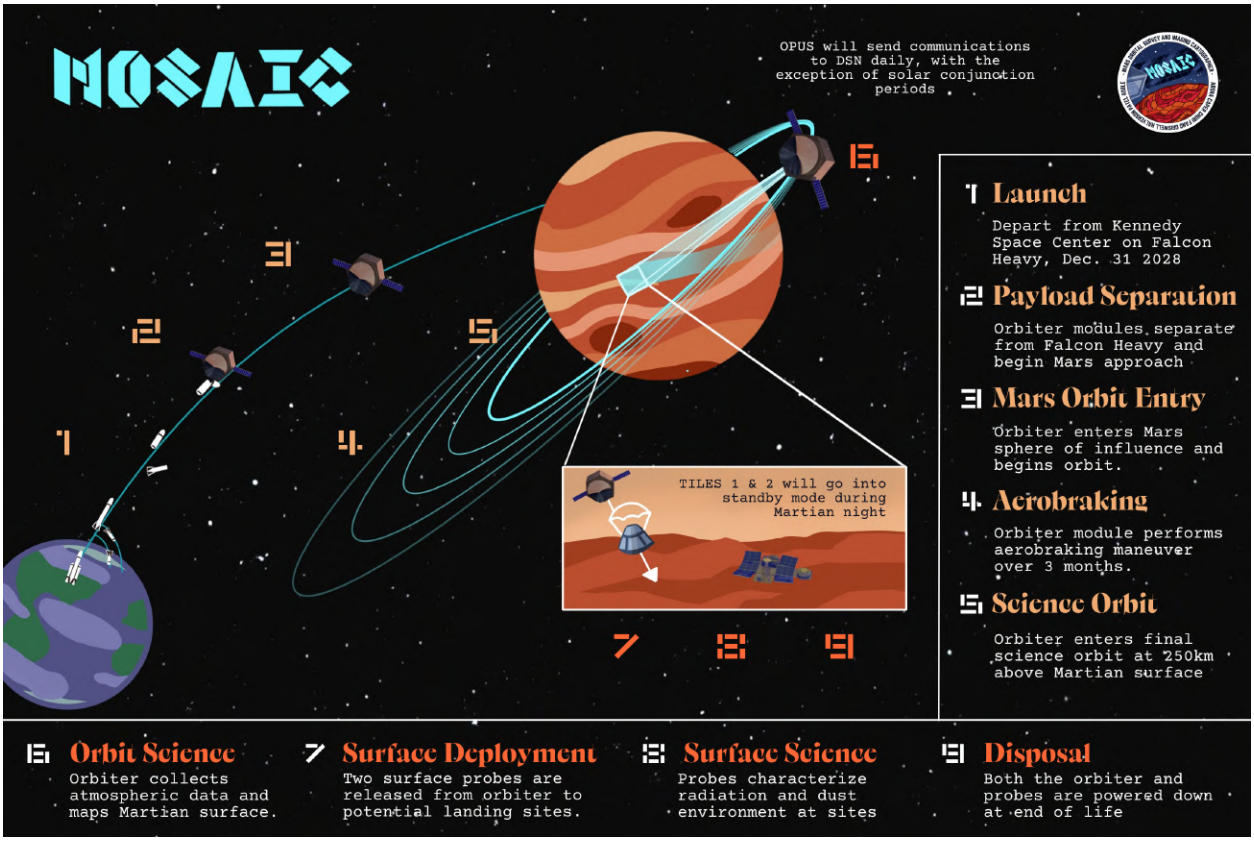

Fig. 9 MOSAIC Concept of Operations

F. Determination of POFMOs

The TILES will land at two Potential Outposts for Future Martian Occupation, called POFMOs, which will be determined by the Ground Station based on the data received from OPUS's mapping. The criteria for the POFMOs were determined based on a) relevance to potential Martian colonies and b) the resources available on Mars. The criteria and their rationale are as follows:

Table 4 POFMO Criteria and Rationale

POFMO Req	Rationale
Elevation differential of +- 2 meters	Area is relatively level
Low abundance of loose rocks/boulders	Area is devoid of large rocks
Within an equatorial latitude +- 30 degrees	Area is within the warmest region of the planet for power and thermal requirements
Mean wind speeds below 10 meters per second	Area does not have extreme weather that could destroy equipment
At/within 10 kilometers from a "significant crater". A "significant crater" is defined as being at least 1 kilometer in diameter, regardless of depth.	Area is near potential landmarks for research

These criteria must apply within a 1 kilometer radius, and are listed in descending importance. If no location meets these criteria, then locations will be chosen based on the closest match at the discretion of the Ground Station.

IV. Launch Vehicle & Trades

A critical part in mission design is selecting the optimal rocket to deliver the payload to Mars. The MOSAIC team analyzed several rockets that would adequately support this mission, attempting to minimize cost, utilize readily available rocketry, ensure reliability, and support payload sizing to Mars. In early investigation, the Polar Satellite Launch Vehicle (PSLV) and Vulcan Centaur were considered because of their low prices, but they have not completed Martian missions, therefore were immediately ruled out [3] [4]. Considering a payload of 8,400 kg needed for the MOSAIC mission, the Falcon 9 would fail to meet the requirement due to its payload to Mars only supporting 4,020 kg [5]. On the opposite end of the spectrum, the Starship carries a payload much greater than necessary of 90,718 kg [6].

A trade study necessary for deciding the ideal launch vehicle was based on the required ΔV from launch to Low Earth Orbit (LEO). The ideal rocket equation,

$$\Delta V = I_{\text{sp}} g_0 \ln\left(\frac{m_w}{m_d}\right), \tag{1}$$

where ΔV, I_{sp}, g_0, m_w, and m_d are the change in velocity, specific thrust of the launch vehicle engines, gravitational acceleration of Earth, wet mass, and dry mass of the bus, respectively. For an initial launch to LEO burn, ΔV,

$$\Delta V = \sqrt{\frac{GM}{(R+h)}}, \tag{2}$$

could be found with G, M, R, and h being the gravitational parameter, the mass of the Earth, the radius of the Earth, and the altitude of the LEO orbit, 400 km, respectively. This gave an initial estimate for the necessary launch ΔV of 7.9 km/s. Knowing this value, the mass ratio could be solved for by rearranging Equation 1. Assuming the Merlin engines on the Falcon Heavy rocket have an I_{sp} of 282 seconds, the mass ratio needed for wet mass to dry mass is 1.003. According to literature, when utilizing a two-stage rocket as opposed to a single stage rocket, more of the overall mass can be used for the payload as opposed to the propellant needed for ΔV which was a favorable option [7] for the MOSAIC mission. All things considered, the rocket chosen for the MOSAIC mission was the Falcon Heavy as it met the Team's specifications.

Based on the selection of the Falcon Heavy, the following requirements were recorded:

Table 5 Launch Vehicle Requirements

Req Name	Parent Req	Traceability	Requirement	Rationale
LV-1.0	MR-9.0	MR-9.0 - LV-1.0	The launch vehicle shall be a SpaceX Falcon Heavy.	The Falcon Heavy was chosen to allow for the most mass margin and contingency during the mission. The OPUS and TILES are anticipated to have a relative high mass.
LV-2.0	MR-9.0	MR-9.0 - LV-2.0	The launch vehicle shall deliver the spacecraft to a distance outside of Earth's atmosphere and pointed towards Mars.	Describes the point where the launch vehicle releases the spacecraft to begin insertion into the science orbit.
LV-3.0	LV-1.0	MR-9.0 - LV-1.0 - LV-3.0	SpaceX shall receive the following information during the launch vehicle development phase: a) Verification of mass properties in accordance to data given for the SpaceX payload attach fitting b) Attitude of the second-stage burn c) Rate of spin of launch vehicle separation d) Temperature limits of the spacecraft e) Verification of environmental , mechanical, and electrical compatibility f) Specifications of the customer-provided payload adapter g) Specifications of customer-provided electrical ground support equipment h) CAD model of spacecraft i) spacecraft safety data j) Inputs to the Interface Control Document k) Launch site operations plans and procedures l) Mission data m) Compliance and proof of FAA review n) Launch site visitor and GSE details information o) Compliance with AFSPCMAN 91-710 Range User's Manual and FAA 14 CFR Part 400	From the Falcon Heavy User Guide[2]. Describes the information needed from the MOSAIC Team to give to SpaceX for development and fabrication of the launch vehicle.
LV-4.0	LV-1.0	MR-9.0 - LV-1.0 - LV-4.0	As part of the Falcon Heavy launch service, SpaceX will: a) Provide personnel, services, hardware, equipment, documentation, analyses and facilities to support mission planning, launch vehicle production and acceptance, payload integration, and launch. b) Secure required launch licensing, including Federal Aviation Administration (FAA) and State Department licenses, with input from the payload customer. c) Secure third-party liability insurance for the launch d) Provide all range and safety documents for the payload provider to complete (per AFSPCMAN 91-710 and 14 CFR Part 400). e) Facilitate the range and range safety integration process. f) Provide up to three sets of 37- or 61-pin satellite-to-launch vehicle in-flight disconnect electrical connectors, or integrate customer-provided mission-unique connectors. g) Provide a 1,575-mm bolted interface compatible with the 62.01-in. diameter Medium Payload Class mechanical interface defined in the EELV Standard Interface Specification, or a 2,624-mm bolted interface as defined in section 5.1.1. h) Provide one 937-mm or 1,194-mm or 1,666-mm (36.89-in. or 47.01-in. or 65.59-in.) adapter and low-shock clampband separation system, or integrate a customer-provided mission-unique separation system. i) Provide an adapter and technical support for a mechanical interface compatibility verification test at a facility of the customer's choosing. j) Provide transportation for the customer's spacecraft container and all ground support equipment (GSE) from the launch site landing location to the spacecraft processing location, if necessary. k) Provide ISO Class 8 (Class 100,000 cleanroom) integration space for the payload and GSE prior to the scheduled launch date, including facilities and support to customer's hazardous operations. l) Provide certified mechanical GSE to support physical mating of the payload to the payload adapter, perform fairing encapsulation, and integrate the encapsulated system with the launch vehicle. m) Process the launch vehicle, integrate and encapsulate the payload within the fairing, and test electrical interfaces with the payload. n) Provide conditioned air into the fairing during encapsulated ground processing. o) Provide one payload access door in the fairing, located at a fixed pre-defined location. p) Conduct a countdown dress rehearsal for customer launch team members supported by SpaceX Mission Management. q) Launch the payload into the specified orbit within the specified environmental constraints. r) Perform 3-axis attitude control or spin-stabilized spacecraft separation. s) Perform a collision avoidance maneuver (as required). t) Verify spacecraft separation from the launch vehicle and provide an orbit injection report. u) Deliver a final post-flight report, which will include payload separation confirmation, ephemeris, payload environment, significant events and any mission-impacting anomalies.	From the Falcon Heavy User Guide[2]. Outlines the services provided by SpaceX.

V. Preliminary Mass Budget

One of the first constraints identified for the mission is determining a maximum mass for OPUS, the TILES, and other components. Table 6 displays the average mass percentages of these components as a percentage of spacecraft dry mass:

Table 6 Average Subsystem Masses as a Percent of Spacecraft Dry Mass [8]

Subsystem (% of Dry Mass)	**No Prop**	**LEO with Prop**	**High Earth**	**Planetary**
Payload	41%	31%	32%	15%
Structure and Mechanisms	20%	27%	24%	25%
Thermal Control	2%	2%	4%	6%
Power (incl. harness)	19%	21%	17%	21%
TT&C	2%	2%	4%	7%
On-Board Processing	5%	5%	3%	4%
Attitude Determination and Control	8%	6%	6%	6%
Propulsion	0%	3%	7%	13%
Other (balance + launch)	3%	3%	3%	3%
Total	100%	100%	100%	100%
Propellant	0%	27%	72%	110%

For MOSAIC, the "Planetary" column in Table 6 will be used for further calculations. In the first stage in the mission development process, a mass margin of 30% is ideal to allow room for elements that may be added later as the mission design is finalized. The theoretical mass budget was calculated by working backwards from this targeted mass margin and the 16,800-kilogram payload capacity of the Falcon Heavy. With these quantities, the theoretical mass budget for Level 1 components - and therefore the maximum allowable mass for the spacecraft dry bus - was determined:

Table 7 Theoretical Mass Budget and Excel Formulas for Level 1 Components, Contingency Included

Component #	**Component Name**	**Excel Formula**	**Value**
11.0	Mass % Margin	N/A	30%
10.0	Launch Vehicle Capacity (total allowable mass)	N/A	16800 kg
9.0	Mass Margin	$10.0 \cdot 11.0$	5040 kg
8.0	Boosted Mass	$10.0 - 9.0$	11760 kg
7.0	Launch Vehicle Adapter	$0.0755 \cdot 1.0 + 50.252$ [9]	456.63 kg
6.0	Injected Mass	$8.0 - 7.0$	11303.37 kg
5.0	Kick Stage	N/A	N/A
4.0	Loaded Mass	$6.0 - 5.0$	11303.37 kg
3.0	Propellant	$4.0 \cdot 52.5\%$	5920.81 kg
2.0	Consumables	N/A	N/A
1.0	**Spacecraft Dry Mass**	$4.0 - 3.0 - 2.0$	**5382.55 kg**

It is imperative to note that the formulas in Table 7 only generate if the "enable iterative calculation" option is selected in Excel, which is not available in the web version. The single decimal-place numbers in the "Excel Formula"

column refer to the "Component Number." The formula for the mass of the propellant was simplified from the 110% shown in Table 6 to be 52.5%, which suggests that the other 47.5% of Loaded Mass is attributed to the consumables and spacecraft dry mass.

Of the spacecraft dry mass, the OPUS is targeted to make up 65%, and both TILES and their mounting hardware will make up 35%. The contingency for OPUS and the TILES is 15%, and each subsystem's contingency is 10%. Similar to Table 7, a top-to-bottom approach was used to calculate theoretical masses of each subsystem: divide out contingency from allocated mass to find CBE masses. With a value for spacecraft dry mass and suggested subsystem percentages from Table 6, the mass budget for OPUS, the two TILES, and their subsystems was then estimated:

Table 8 OPUS Theoretical Mass Budget

1.2 OPUS (65% of Spacecraft Dry Mass)				
	% of OPUS CBE	**CBE (kg)**	**Con.**	**Total (kg)**
1.21 Structures	25.00%	795.1501	10%	874.665
1.22 Thermal Control	10.00%	318.0601	10%	349.866
1.23 Power	21.00%	667.9261	10%	734.719
1.24 TT&C	11.00%	349.8661	10%	384.853
1.25 On-Board Processing	9.00%	286.2541	10%	314.879
1.26 ADCS	8.00%	254.448	10%	279.893
1.27 Propulsion	13.00%	769.7053	10%	846.676
1.28 Gamma-Ray and Neutron Spectrometer (GRNS)	0.50%	15.903	10%	17.4933
1.29 CIRS-Lite	0.70%	22.2642	10%	24.4906
1.210 High Resolution Imaging Camera	1.30%	41.34781	10%	45.4826
1.211 LiDAR	0.50%	15.903	10%	17.4933
OPUS Total				3498.66063

Table 9 TILES Theoretical Mass Budget (*Mass values described are for each of the TILES)

1.1: TILES (35% of Spacecraft Dry Mass)				
	% of CBE	**CBE (kg)**	**Con.**	**Total (kg)**
1.11: TILES*	**45%**	**737.176**	**15%**	**847.75**
1.111: Structures	29.50%	197.6971961	10%	217.467
1.112: Thermal Control	15.00%	100.523998	10%	110.576
1.113: Power	23.00%	154.136797	10%	169.55
1.114: TT&C	12.00%	80.41919842	10%	88.4611
1.115: On-Board Processing	9.00%	60.31439882	10%	66.3458
1.116: EDL	10.00%	67.01599868	10%	73.7176
1.117: Radiation and Dust Sensor (RDS)	1.00%	6.701599868	10%	7.37176
1.118: Radiation Assessment Detector (RAD)	0.50%	3.350799934	10%	3.68588
1.13 TILES Mounting Hardware	**10%**	**171.2631**	**10%**	**188.389**
TILES Total				**1883.39**

The values in bold for the Percent of CBE, CBE, contingency, and total quantities in Tables 9, and 8 apply to the

mass total for each of the Level 2 Components of the OPUS and the TILES, respectively. Alternatively, the unbolded quantities are subsystems and in reference to the structure to where it's attached (a.k.a. Level 3 Components). The Percent of CBE for the subsystems - which sum to 100% for each Level 2 Component - are adjusted from Table 6 and redistributed as the instrumentation was determined (see Sections VII.A and VIII.A).

The actual mass budget estimates were determined after all preliminary subsystem analyses were conducted, and they're included in Section X.A with a 10% margin instead of the initial 30%.

VI. Trajectory & Orbit Analysis

A. Trajectory & Orbital Requirements

The trajectory of this mission was designed for minimizing ΔV, as it is a critical concern for the mass constraints for the propulsion and structures subsystem teams. The trajectory and operations design for MOSAIC was developed with an interconnected approach, ensuring alignment with the team's overall mission objectives, as well as ensuring an orbit that will map at least 75% of the Martian surface. Additional requirements were also identified:

Table 10 Trajectory Requirements

Req Name	Parent Req	Traceability	Requirement	Rationale
TRAJ-1.0	MR-1.0	MR-1.0 - TRAJ-1.0	The total delta-v required shall be minimized as much as possible.	Establishes that the change in velocity over the course of the mission will be minimized to save on mass and cost.
TRAJ-2.0	TRAJ-1.0	MR-1.0 - TRAJ-1.0 - TRAJ-2.0	The science orbit determination shall account for parameters such as variable gravity effects and communication ranges.	Ensures that OPUS's orbit allows it to scan Mars and communicate the data back to the Ground Station.

B. Trajectory/Orbit Trades

Minimizing ΔV starts with selecting a launch and Mars arrival window for the mission. Considering 75% of the Martian surface needs to be mapped by 2033, the sooner a launch window appears, the more favorable for this mission timeline without selecting a date too close to the present for feasibility purposes. Knowing a general time frame of the mission, a departure ΔV porkchop plot was created and can be seen in Figure 10 [10]. The lightest shade of blue in the chart exhibits the lowest ΔV requirements. The Team desires that the time of flight should be no longer than one year, so this would make the most ideal window for launch November 13, 2028 to December 31, 2028 with ranges of ΔV from 3.0 km/s to 3.85 km/s. Ultimately, December 31, 2028 was the date chosen for launch and has a departure ΔV of 3.82 km/s with a time of flight of 240 days. While this is on the higher side for the launch window, this date was chosen due to the proximity of the launch date to the present. If this date is missed due to unforeseen circumstances, January 16,

2029 is the next date possible to launch with an increased ΔV of 4.28 km/s. This date must be met, or else the next launch window is in 2031, and while preliminary maps could be made, the timeline of deployment of TILES including surface science would not likely be completed. The NASA Ames Trajectory Browser aided as well in the selection of a launch date, clearly stating the interplanetary path and necessary ΔV [11].

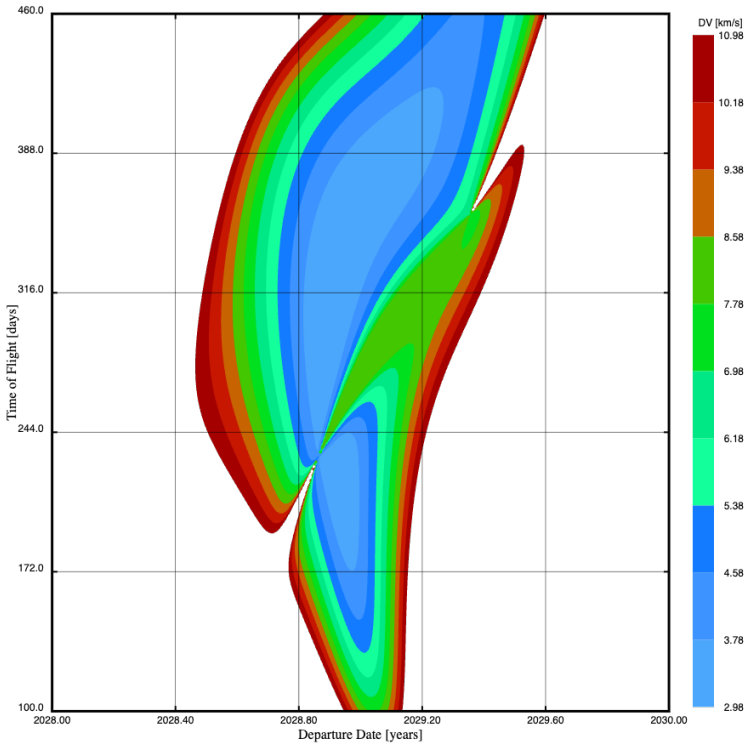

Fig. 10 Porkchop Plot for Departure ΔV from Earth to Mars

The next trade considered was how the payload would enter the Martian orbit. Two methods were considered, a Hohmann transfer and aerobraking from a highly elliptical orbit down to a closer circular orbit followed by re-circularizing. Planning a patched conics Hohmann transfer would require departure from the 400 km Low Earth Orbit, a heliocentric trajectory phase, and a circular arrival capture orbit around Mars at 250 km. Starting with the heliocentric trajectory phase, the state vector for Earth at departure and Mars at arrival are found knowing the time of flight is 240 days (December 31, 2028 to August 28, 2029). The hyperbolic excess velocities of both departure and arrival from/to the respective spheres of influence are

$$v_{\infty_{\text{Departure}}} = \vec{V}_D - \vec{V}_1, \tag{3}$$

$$v_{\infty_{\text{Arrival}}} = \vec{V}_A - \vec{V}_2, \tag{4}$$

with $\vec{V}_D$, $\vec{V}_1$, $\vec{V}_A$, and $\vec{V}_2$ being departure velocity, state velocity of Earth, arrival velocity, and state Mars velocity, respectively. Then at the departure phase, ΔV can be found by

$$\Delta V_{\text{Departure}} = \sqrt{v_{\infty_{\text{Departure}}}^2 + 2\frac{\mu_1}{r_p}} - \sqrt{\frac{\mu_1}{r_p}}, \tag{5}$$

where μ_1 is the standard gravitational parameter of Earth and r_p is the periapsis radius, which is the altitude of the parking orbit added with the radius of the Earth. A similar process was done for the arrival ΔV where

$$\Delta V_{\text{Arrival}} = \sqrt{v_{\infty_{\text{Arrival}}}^2 + 2\frac{\mu_2}{r_p}} - \sqrt{\frac{\mu_2}{r_p}}, \tag{6}$$

and μ_2 is the standard gravitational parameter of Mars with the radius of periapsis, r_p is the altitude of the parking orbit added with the radius of Mars. The departure ΔV is 4.01 km/s, and the arrival ΔV is 3.78 km/s for the Hohmann transfer approach. A more efficient way of Mars capturing that has been historically used is aerobraking. The Mars Orbiter Mission (MOM), Mars Reconnaissance Orbiter (MRO), and Mars Global Surveyor (MGS), are all previous Martian missions that have utilized this tactic [12] [13] [14]. Aerobraking consists of starting in a highly elliptical orbit at a large apoapsis radius and a close periapsis distance and over time, as the spacecraft orbits, the drag from the Martian atmosphere reduces the apoapsis radius until the desired apoapsis is met. Then, a re-circularization burn occurs to raise the periapsis to match the apoapsis to create a nearly circular orbit.

The aerobraking analysis is done by propagating the highly elliptical orbit of 50,000 km by and 3,506 km accounting for two-body acceleration, oblateness, and drag as

$$\mathbf{a}_{\text{2body}} = -\frac{\mu}{r^3}\mathbf{r}, \tag{7}$$

$$a_{J_2} = -\frac{3}{2}J_2\frac{\mu}{r^2}\left(\frac{R_m}{r}\right)^2\begin{bmatrix}\left(1-5\frac{z^2}{r^2}\right)\frac{x}{r}\\ \left(1-5\frac{z^2}{r^2}\right)\frac{y}{r}\\ \left(3-5\frac{z^2}{r^2}\right)\frac{z}{r}\end{bmatrix}, \tag{8}$$

$$\mathbf{a}_{\text{drag}} = -\frac{1}{2}\frac{C_d A}{m}\rho v^2\frac{\mathbf{v}}{v}, \tag{9}$$

where

$$\rho = \rho_0 \exp\left(-\frac{h}{H_0}\right), \quad \text{for } 0 < h < 250 \text{ km}, \tag{10}$$

with μ, $\mathbf{r}$, and r being the standard gravitational constant, position vector of the spacecraft with respect to Mars, and the

magnitude of that position from Equation 7, J_2 and R_m are the oblateness factor of Mars and the radius of Mars for Equation 8, and C_d, A, m, ρ, $\mathbf{v}$, v, ρ_0, h, and H_0 are the coefficient of drag, cross-sectional area of the spacecraft, mass, atmospheric density, the velocity vector of the spacecraft with respect to Mars, the velocity vector's magnitude, the atmospheric density at sea level, altitude of the spacecraft, and the base height for Equations 9 and 10 [15] [16]. The reason for the 250 km orbit selection is that it is at the edge of Mars' atmosphere, so the ΔV for station keeping can be minimized while still orbiting close enough to take high-resolution images necessary for the mapping.

In the aerobraking simulation, the Mars sphere-of-influence arrival ΔV provided by the NASA Ames Trajectory Browser suggests an insertion of 1.28 km/s [11]. With this, the initial elliptical orbit is set and propagated for the amount of time required for it to reach its 3,506 km by 3,646 km orbit. ΔV for the insertion would amount to

$$V_{\text{periapsis target}} = \sqrt{\mu \left(\frac{2}{r_{\text{periapsis}}} - \frac{1}{a_{\text{target}}} \right)}, \tag{11}$$

$$V_{\text{periapsis initial}} = \sqrt{V_{\infty}^2 + \frac{2\mu}{r_{\text{periapsis}}}}, \tag{12}$$

$$\Delta V_{\text{capture}} = V_{\text{periapsis initial}} - V_{\text{periapsis target}}, \tag{13}$$

giving a burn of 0.264 km/s. After 163 days, the spacecraft reaches its target and is ready for the circularization burn calculated by

$$V_{\text{circular}} = \sqrt{\frac{\mu}{r_{\text{final}}}}, \tag{14}$$

$$V_{\text{periapsis final}} = \sqrt{\mu \left(\frac{2}{r_{\text{periapsis}}} - \frac{1}{r_{\text{apoapsis final}}} \right)}, \tag{15}$$

$$\Delta V_{\text{circularization}} = V_{\text{circular}} - V_{\text{periapsis final}}. \tag{16}$$

giving a burn of 0.134 km/s. Figure 11 shows the aerobraking simulation for MOSAIC.

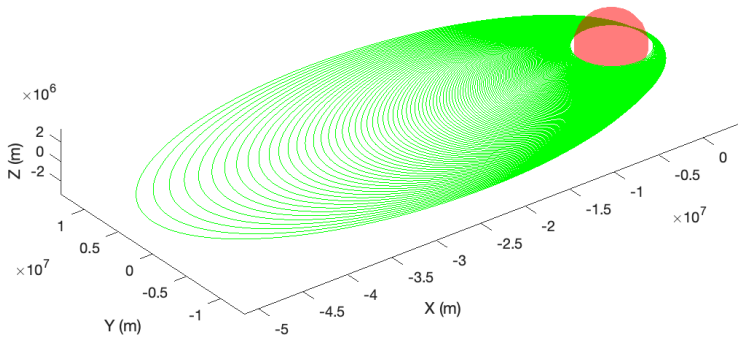

Fig. 11 Aerobraking Simulation

The final burn to consider for both the Hohmann and the aerobraking paths would be the inclination change burn, which occurs in conjunction with the re-circularization burn. It was calculated through geometry that the necessary inclination angle to cover 75% of Mars is approximately 40°. To account for any unexpected errors, the team chose an inclination maximum angle of 50° as to not increase ΔV and a higher inclination would be unnecessary as the goal of the mission is to prepare for human arrival and exploration. It is highly unlikely that the polar regions are a high priority for mapping considering their extreme temperatures. The ΔV required for the inclination change is computed using

$$\Delta V = 2V \sin\left(\frac{\Delta i}{2}\right), \tag{17}$$

where V denotes the velocity the spacecraft is traveling at. The results from this trade study can be seen in Table 11, and it can be noted that aerobraking, while it takes more time, costs less in terms of ΔV, so that is the method selected for MOSAIC. The orbit trimming burn, MOSAIC's station keeping, requires about 0.2-0.6 m/s per week based on literature, which would amount to 0.31 m/s per year maximum, which will total to 0.28 km/s for the entire mission lifespan [17].

Table 11 ΔV Totals for Hohmann Transfer vs. Aerobraking

Burn	**Aerobraking Method**	**Hohmann Transfer Method**
Launch to LEO	9.60	9.60
LEO Departure	3.89	4.01
Mars Arrival	1.28	3.78
Aerobraking Phase		
Aerobraking	0.32	-
Circularization & Inclination Change	0.99	0.98
Final Adjustments		
Orbit Trimming	0.28	0.28
TOTAL	**16.28**	**18.63**

Overall, aerobraking cuts down ΔV needed for the mission considering the 9.60 km/s is covered by SpaceX.

Therefore, the mission requires a ΔV of 6.68 km/s.

C. Selected Trajectory and Orbit

Based on the trade studies and analytical analyses made in the section previous, the ideal trajectory for the MOSAIC mission launches on December 31, 2028, enters a low-inclination (28°) 400 km Low Earth Orbit before departing to Mars, remains in-transit for 240 days until August 28, 2029, enters an aerobraking phase in an ellipse of a 50,000 km apoapse and 3,506 km periapse for 163 days reducing the apoapse until it reaches a 250 km altitude on February 20, 2030, re-circularizes to a nearly circular orbit, and orbits Mars for the rest of the mission timeline with periodic orbit trimming (station keeping).

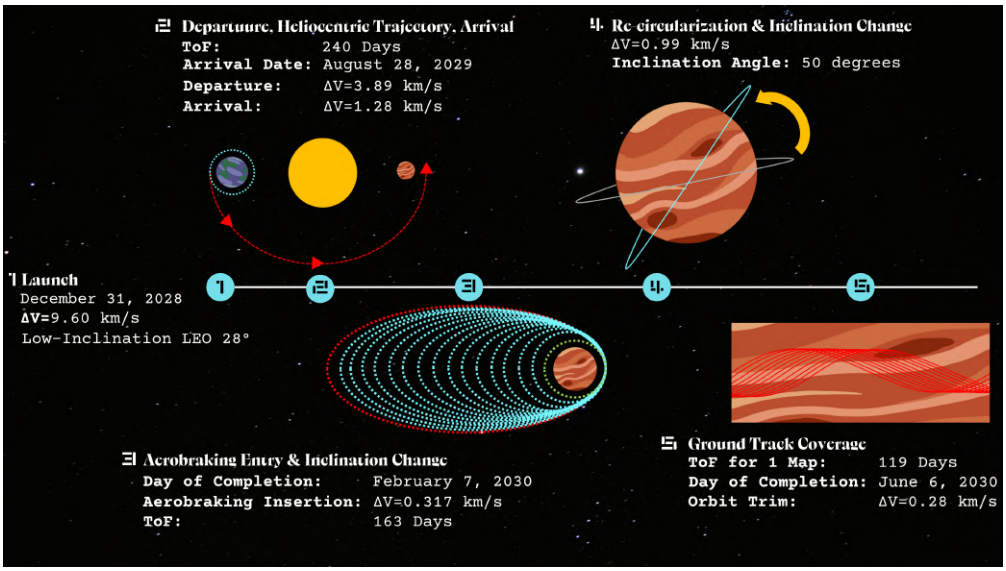

Fig. 12 Selected Trajectory for MOSAIC

D. Coverage and Visibility Analysis

Running a simulation in the General Mission Analysis Tool (GMAT) of the 250 km altitude science orbit, taking into account when OPUS is in umbra, full darkness, and penumbra, partial darkness, a preliminary ground track covering 75% of the Martian surface will be done within 119 days, finishing its first mapping sequence on May 19, 2031 [18]. The goal is to make at least four maps which would last until February 19, 2032 in order to note minor changes in topographical features, polish images, and add detail before sending TILES 1 and 2 to the surface. Images will continue to be taken in order to add more detail past these core maps. In Figure 13 , the coverage of Mars is shown after the 119 day initial mapping period. As the 50° inclination angle suggests, latitudes of ±50° are met. An inclination angle of 48.9° is necessary, but 50° is chosen to account for potential slight incorrect maneuvering.

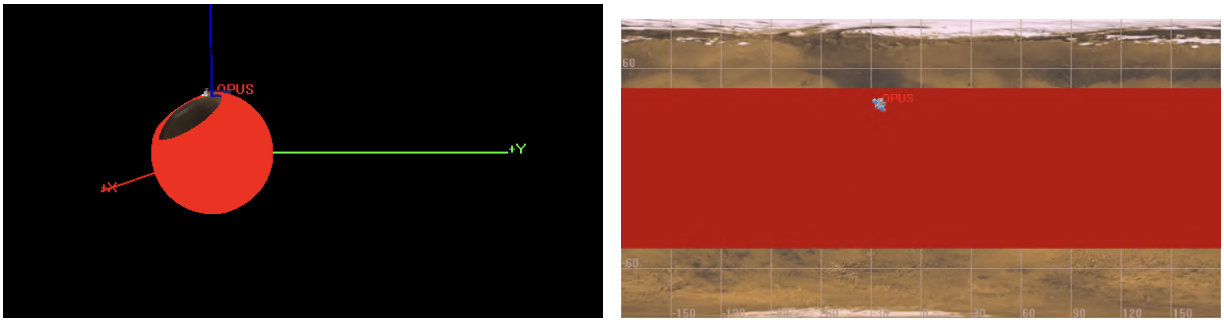

(a) GMAT Orbit View of Ground Coverage

(b) GMAT Ground Track of Plot of Ground Coverage

Fig. 13 Coverage map completed by OPUS

VII. OPUS Design

A. Instrumentation Selection & Trades

The instruments aboard the OPUS will have the following requirements:

Table 12 OPUS Instrumentation Requirements

Req Name	Parent Req	Traceability	Requirement	Rationale
ORB-1.0	SYS-5.0	MR-5.0 - SYS-5.0 - ORB-1.0	The OPUS shall collect surface composition (including hydrology) and radiation data using gamma-ray and neutron spectroscopy.	Details how OPUS will collect surface composition data.
ORB-1.1	ORB-1.0	MR-9.0 - ORB-1.0 - ORB-1.1	The gamma-ray and neutron spectrometer shall collect data at a data rate of 0.122 kilobits per second.	Determined by the instrument manufacturer. Ensures that the spectrometer can collect data at its optimal data rate.
ORB-2.0	SYS-5.0	MR-5.0 - SYS-5.0 - ORB-2.0	The OPUS shall collect low atmospheric data using infrared spectroscopy.	Details how OPUS will collect atmospheric data.
ORB-2.1	ORB-2.0	MR-9.0 - ORB-2.0 - ORB-2.1	The infrared spectrometer shall collect data at a data rate of 6 kilobits per second.	Determined by the instrument manufacturer. Ensures that the spectrometer can collect data at its optimal data rate.
ORB-3.0	SYS-5.0	MR-5.0 - SYS-5.0 - ORB-3.0	The OPUS shall generate elevation profiles of the Martian surface using a laser altimeter.	Details how OPUS will collect elevation data.
ORB-3.1	ORB-3.0	MR-9.0 - ORB-3.0 - ORB-3.1	The laser altimeter shall collect data at a data rate of 10 kilobits per second.	Determined by the instrument manufacturer. Ensures that the altimeter can collect data at its optimal data rate.
ORB-4.0	SYS-5.0	MR-5.0 - SYS-5.0 - ORB-4.0	The OPUS shall take pictures of the Martian surface using a high-resolution imaging camera.	Details how OPUS will generate a detailed visual-spectrum map.
ORB-4.1	ORB-4.0	MR-9.0 - ORB-4.0 - ORB-4.1	The imager shall take pictures at a resolution of at least 0.5 meters (measured at an altitude of 265 kilometers).	Determined by the instrument manufacturer. Ensures that the camera can take pictures at its optimal resolution.
ORB-5.0	SYS-5.0	MR-9.0 - SYS-6.0 - PRB-1.0	All instruments on the OPUS shall be able to function without exposure to the Martian atmosphere.	Ensures that OPUS can function in the vacuum of space.

1. Gamma-Ray and Neutron Spectrometer

OPUS will carry four different instruments to observe and characterize the Martian surface and atmosphere. The first of these instruments is a Gamma-Ray and Neutron Spectrometer (GRNS), specifically following the design of the GRNS currently onboard the Psyche mission. In addition to Psyche, GRNS systems have significant flight heritage; other examples include the instrument suites on the NASA MESSENGER and NEAR missions, which observed Mercury and

the asteroid Eros, respectively.[19] GRNS systems are commonly used to characterize the elemental composition and geology of the bodies they orbit. This is done by collecting gamma-ray and neutron flux from the body itself. While the GRNS will be collecting data over the Martian surface, its primary goal will be to study the relative presence of inorganic materials (e.g. Fe, Cl, Na) and organic materials (e.g. C, H, O, N) in and near impact craters. In addition to this primary mission, the GRNS also is capable of identifying surface water ice and parsing levels of radioactivity within and near impact sites. A GRNS system was chosen for the characterization of the surface of Mars because, although gamma-ray spectrometers have been used in other Mars missions (such as the 2001 Mars Odyssey[20]), no neutron spectrometer has ever been aboard a Mars orbiter. Thus, the OPUS GRNS seeks to combine higher-fidelity gamma-ray measurements with completely novel neutron measurements to best shed light on Mars' composition in areas of interest. While Psyche's specific GRNS model has not been yet reached its body of interest, it has been collecting data since 2023, and its design from Johns Hopkins Applied Physics Lab is based significantly enough in their prior designs with significant flight heritage to justify its use aboard OPUS[19]. Therefore, we have determined this instrument to be TRL 7. CAD models of the GRNS system are shown below in Figures 14(a) and 14(b).

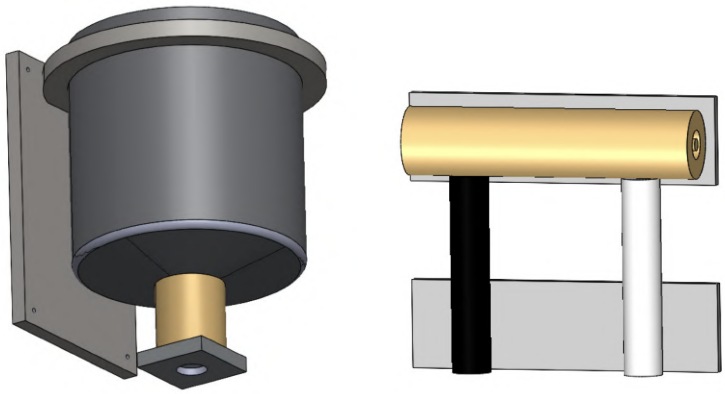

(a) (b)

Fig. 14 Gamma Ray and Neutron Spectrometers

2. Laser Altimeter

The second instrument aboard the OPUS is a laser altimeter of the same design as the Lunar Orbiter Laser Altimeter, or LOLA. LOLA currently orbits the Moon as part of the Lunar Reconnaissance Orbiter mission. This design is a more modern and accurate version of MOLA, the Mars Orbiter Laser Altimeter. [21] Laser altimeters are used to create detailed surface maps of the body they orbit; in the case of OPUS, the laser altimeter will be used to generate elevation profiles of at least 75% of the surface, as well as identify surface resources such as ice or regolith. In turn, this data will be used to observe uneven/unstable terrain and identify extreme elevation changes to aid in the identification of landing sites and potential traverse paths between them. Our CAD model of this laser altimeter design is shown below.

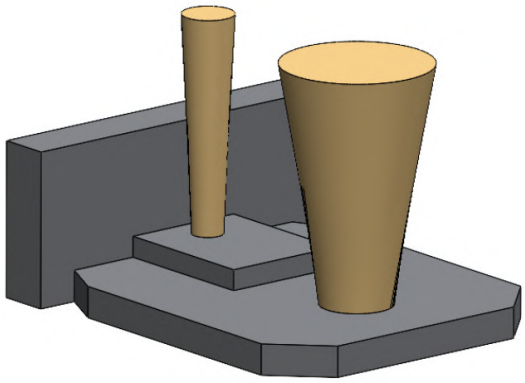

Fig. 15 LOLA CAD Model

The LOLA design was chosen because it strikes a balance between novel and proven technology. Several novel LiDAR technologies were considered, the most significant of which being scanning LiDAR. Scanning LiDAR allows for the capture of broader cross-track area increasing coverage and reducing the amount of repeat sampling. [22] However, this technology has only been used in a planetary context onboard the OSIRIS-REx mission, wherein the scanning laser altimeter only operated at a maximum range of 7 km. [23] Given this technology's unproven nature within OPUS's mission parameters, it is left to a future mission as a technology demonstration. As previously stated, the LOLA design draws significantly upon previous instruments with Mars flight heritage, but it has 3-5 times greater vertical accuracy and takes measurements 32 times more frequently than MOLA[21]. Therefore, it is chosen to fly onboard OPUS due to its combination of high TRL (TRL 7) and collected data that is novel in its fidelity.

3. Imaging Camera

A high-resolution camera will also be a part of OPUS's scientific payload to best identify potential landing sites in conjunction with the laser altimeter. Specifically, this camera will follow the design of HiRIC, or High-Resolution Imaging Camera, that currently is a payload on China's Tianwen-1 orbiter. This design is relatively light but still carries a resolution of 0.5 meters at an altitude of 265 km. [24] This resolution will be more than enough to identify surface features such as rock abundance, elevation changes, and albedo during its initial imaging of Mars to best inform POFMO and future landing site selection. In comparison to HiRISE, the camera on the Mars Reconnaissance Orbiter, the HiRIC design lacks high-end resolution, however, it compensates for this in mass reductions of >20kg, as well as significant volume reductions [24] [25]. These savings alongside a TRL of 8 (as OPUS will orbit at a lower altitude than Tianwen-1) allow for a less complex and expensive science payload overall. Additionally, this mission will prioritize the repeat imaging of landing areas of interest during different seasons, an explicit goal for future missions laid out by the HiRISE team [25]. An image of HiRIC's design is shown below.

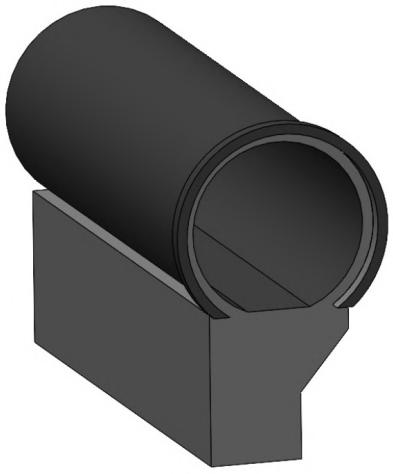

Fig. 16 HiRIC Design

4. Fourier Transform Spectrometer

The final instrument aboard OPUS is a Fourier transform spectrometer, specifically the Composite InfraRed Spectrometer Lite, or CIRS-Lite. This type of spectrometer uses radiance spectra of gaseous species to identify atmospheric composition as well as generate temperature and wind profiles of a terrestrial body's atmosphere [26]. Knowledge of these qualities prove useful to landing site selection, specifically with regards to processes such as in-situ resource utilization. CIRS-Lite was designed to be a lighter, cheaper, and more robust version of its previous iteration, CIRS. CIRS was used aboard Cassini's mission to observe the compositions of Saturn and Titan. Previous examples of infrared spectrometry were used onboard Voyager (IRIS) and many Earth-centric missions [27]. The fact that CIRS-Lite has yet to fly on a mission of its own (or even be tested to do so) is certainly a source of risk. However, its design is almost entirely based on that of its predecessors, saving weight by combining the modern optical design of CIRS with the low complexity of IRIS and using other telescopic components that have been proven in other missions. These factors along with the general reliability of Fourier transform spectrometers made CIRS-Lite the most revelatory option for exploring the composition and dynamics of Mars' atmosphere, despite its TRL of 5 [28]. A CAD image of CIRS-Lite can be seen below.

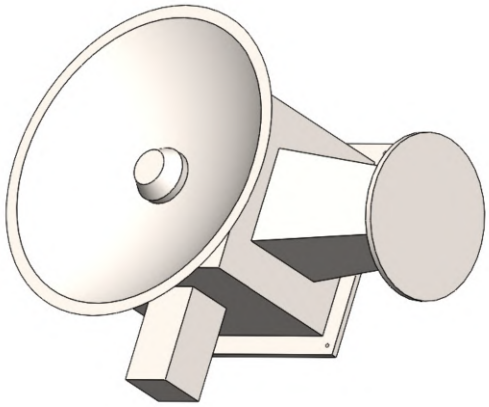

Fig. 17 CIRS-Lite Design

B. Propulsion

The propulsion subsystem shall have the following requirements:

Table 13 Propulsion Subsystem Requirements

Req Name	Parent Req	Traceability	Requirement	Rationale
PROP-1.0	MR-5.0	MR-5.0 - MR-5.0 - PROP-1.0	The OPUS shall carry sufficient and satisfactory fuel to insert into the science orbit and maintain the desired attitude and orientation.	The system must be capable of achieving and keeping desired trajectory.
Prop-2.0	PROP-1.0	MR-5.0 - PROP-1.0 - PROP-2.0	The OPUS propellant shall be hydrazine.	This propellant has a simpler system, long shelf life, and relatively high thrust-to-weight ratio: saves on mass and volume.

1. Thruster Trades

The first trade study conducted for the propulsion system was for the decision between chemical and electric propulsion. A combination of chemical and electric propulsion was considered due to a hybrid architecture allowing for more fuel-efficient trajectories without significantly longer flight times [29]. However, this would greatly increase the complexity of the propulsion system, and the majority of past missions used solely chemical propulsion, so it was more difficult to find information on hybrid systems at this time. As a result, a hybrid propulsion system was ruled out for this mission.Some factors considered in this trade were the specific impulse, timeline, thrust-to-weight ratio, and cost [30]. Electric propulsion has a much higher specific impulse than chemical propulsion. As a result, electric propulsion would be ideal if the mission required a relatively high delta-v. However, this was deemed unnecessary for OPUS. Using electric propulsion would increase the time required to reach the operational orbit.

Since MOSAIC must map at least 75% of the Martian surface before 2033, it is important that OPUS reaches the operational orbit quickly. Electric propulsion is also much more effective than chemical propulsion for longer missions because it drastically reduces the necessary amount of propellant needed. The MOSAIC mission objectives shall be completed within 10 years, which would make a change from chemical to electric propulsion result in a more negligible decrease in propellant. Chemical propulsion generally has a higher thrust-to-weight ratio than electric propulsion. The Mars orbit injection requires relatively high thrust, so chemical propulsion is more appropriate for that reason. Electric systems also require more power than chemical propulsion, which would require additional solar panels and batteries. This would increase the weight of OPUS as compared to a chemical propulsion system. The additional solar panels, batteries, and electric thrusters would cause an electric propulsion system to be more expensive than a chemical propulsion system. Electric systems also generally use Xenon, which is rare and frequently has shortages, whereas chemical propulsion generally uses hydrazine and nitrogen tetroxide which are more common. As a result, this could increase the price of electric propulsion.

The benefits of chemical propulsion outweighed the benefits of electric propulsion for MOSAIC because it's a relatively short mission to Mars with tight cost and weight requirements, so chemical propulsion was chosen for this mission.

2. Propellant Trades

When deciding on the propellant to use for MOSAIC, past Martian orbiter missions were considered to find an approach that has been effective in the past. One mission considered was the MRO [31] which used solely hydrazine. Another mission considered was the Mars Odyssey Orbiter [32]. This mission used hydrazine for attitude control and maneuvering and hydrazine with nitrogen tetroxide for their main engine. The Mars Climate Orbiter [33] also used hydrazine for attitude control and maneuvering and hydrazine with nitrogen tetroxide for their main engine. The final mission considered was Dawn [34], which went to asteroids rather than Mars but it used ion thrusters for the main thrusters and hydrazine thrusters for attitude control.

Since hydrazine was used for all of these missions for attitude control and maneuvering, OPUS shall use hydrazine thrusters as well because this technology has proven to be effective for Mars orbiters. Something to consider is that a combination of hydrazine and nitrogen tetroxide produces more thrust than hydrazine alone. However, hydrazine was able to provide the necessary amount of thrust for the orbit insertion maneuver, and using one propellant produced a simpler configuration than multiple propellants, therefore hydrazine was chosen as the propellant for OPUS.

3. Thruster Type

One primary thruster was chosen to fulfill the thrust requirements for orbit insertion and eight small thrusters were chosen to fulfill the thrust requirements for attitude control. The large thruster chosen was the Aerojet MR-107S. This

thruster provides 275 N of thrust, requires 34.8 W of power, and weighs 1.01 kg. The small thrusters chosen were the Aerojet MR-103D. These thrusters each provide 1 N of thrust, require 8.25 W of power, and weigh 0.33 kg. The total mass requirement for the propulsion system is 3.65 kg, and the total max power requirement is 100.8 W.

4. Tank Sizing

The sizing of the tanks was calculated from the required delta-v for the mission, the dry weight of the orbiter, and the selected thrusters with the Tsiolkovsky rocket equation

$$\Delta V = I_{sp} g_0 \ln \frac{m_0}{m_f} \tag{18}$$

where Δv is the required delta-v which was calculated to be 7 km/s with a 10% margin, I_{sp} is the specific impulse provided by the thruster which was given to be 225 s, g_0 is the standard gravity which is 3.728 m/s^2 in the Martian orbit, m_0 is the wet mass of the orbiter, and m_f is the dry mass of the orbiter which was calculated to be 1993.60 kg [15]. This gave a total mass of hydrazine for the mission of 2192.7 kg with a 10% margin. Using the density of hydrazine, the volume necessary for the tank was given to be 2.2235 m^3.

5. Thruster Configuration

Most of the past missions to Mars considered in this research used primary thrusters at the bottom of the orbiter arranged symmetrically around the center of mass as well as smaller thrusters to enable precise maneuvering in all axes for station keeping and attitude control. Using this information, the configuration chosen for OPUS includes 1 primary thruster and 8 small thruster arranged on the outside faces of the orbiter and angled at 45° from the main face. The thruster configuration can be seen in Figure 18. In Figure 18, the purple arrow on the top is the thrust direction for the primary thruster and the blue arrows on the sides show the thrust direction for 4 of the small thrusters. These 4 thrusters are mirrored on the other side of OPUS.

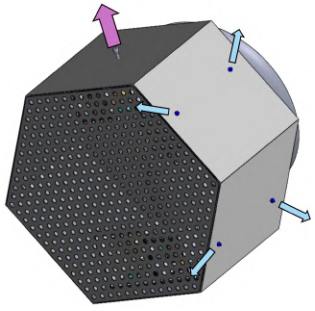

Fig. 18 Thruster Configuration for OPUS

C. Attitude Determination and Control (ADCS)

The OPUS ADCS system is designed to satisfy the following requirements:

Table 14 ADCS Requirements

Req Name	Parent Req	Traceability	Requirement	Rationale
GNC-1.0	MR-5.0	MR-5.0 - GNC-1.0	The OPUS shall have the ability to perform station keeping maneuvers and maintain low Mars orbit of 250 kilometers.	Ensures that OPUS can stay in the science orbit so that the instruments can collect data with minimized error and highest resolution.
GNC-2.0	MR-5.0	MR-5.0 - GNC-2.0	The OPUS shall maintain a 0.1-degree pointing accuracy during science orbit.	Ensures that OPUS can stay in the science orbit so that the instruments can collect data with minimized error and highest resolution.

1. Control Modes and Required Maneuvers

During a normal operating cycle, OPUS will be equipped for the following operation modes: Science Mode: to allow the science instruments to collect data; Momentum Dump: to release momentum in momentum wheels; Earth Relay: to send and receive information from Earth by orienting the X band transceiver towards earth; Tiles Relay: to send and receive information from the TILES by orienting the UHF transceiver towards the TILES; and Safe: where OPUS will be oriented so that the solar panels towards the sun for maximum solar power. The requirements for each operation mode are further detailed in Table 15.

Table 15 Operating Modes and Maneuvers

Operating Mode	Maneuver(s)	Actuators Used	ΔV	Max Power Consumption (W)	Frequency
Science	Orbit Trim	Thrusters and Momentum Wheels	0.2–0.6 m/s [17]	47	Weekly
	Maintain Required Instrument Pointing	Momentum Wheels	~	42	Once per orbit
Momentum Dump	Momentum Dumping	Thrusters	1 mm/s [17]	33	Once per orbit
Earth Relay	Communication with Earth	Momentum Wheels	~	42	Once per orbit
OPUS Relay	Communication with Probes	Momentum Wheels	~	42	Once per orbit
Safe	Point Solar Panels at Sun	Momentum Wheels	~	42	When needed

Additionally, OPUS must satisfy the pointing requirements for each subsystem involved in the maneuvers referenced in Table 15. This includes the science instruments, communications subsystem, and power subsystem. The OPUS

pointing budget is displayed in Table 16.

Table 16 OPUS Pointing Budget

Subsystem	Component	Target	Axis to Align and Frame of Axis	Accuracy
Payload	Gamma Ray and Neutron Spectrometer	Mars Surface	(+) Z Axis of Spacecraft to be aligned with Nadir of Mars	0.1 deg
	Laser Altimeter	Mars Surface	(+) Z Axis of Spacecraft to be aligned with Nadir of Mars	0.1 deg
	High Resolution Imaging Camera	Mars Surface	(+) Z Axis of Spacecraft to be aligned with Nadir of Mars	0.1 deg
	Infrared Spectrometer	Mars Surface	(+) Z Axis of Spacecraft to be aligned with Nadir of Mars	0.1 deg
COMMs	X Band Transceiver	Earth	(-) Z Axis of Spacecraft to be aligned with Nadir of Mars	0.1 deg
	UHF Transceiver	TILES probes	(-) Z Axis of Spacecraft to be aligned with Nadir of Mars	0.1 deg
EPS	Solar Panels	Sun	(+,-) X or Y Axis of Spacecraft to be aligned with Sun	45 deg

In addition to maneuvers performed during the normal operating cycle, OPUS will be required to perform the following maneuvers:

- Trajectory Correction Maneuver (TCM) 1: Correct initial launch trajectory.
- Aerobraking: Orient the solar panels normal to the velocity vector to act as an air brake. The main control modes used during aerobraking will be the aerobraking mode and communication with Earth.
- TCM 2: Place OPUS in science orbit after aerobraking phase is complete
- Probe Release: Orienting OPUS so that the TILES probes will eject at the correct atmospheric entry angle.

The primary thruster will be the main source of translational motion in these maneuvers, while rotational motion will result from the momentum wheels.

2. Internal and External Torque Quantification

The internal and external torques on OPUS were quantified in order to size the ADCS system actuators. OPUS experiences internal torques from slewing and external torques from the Mars gravity gradient, solar radiation pressure, and atmospheric drag during its orbit. Equations 20, 21, and 22 in Section VII.C.3, are used to quantify these external torques. Table 17 quantifies these torque values.

Table 17 Torques Acting On OPUS

Source	Torque (Nm)	Internal/External
Gravity Gradient	2.53E-04	External
Solar Radiation Pressure	3.64E-11	External
Atmospheric Drag	4.89E-13	External
Slewing (max 180 deg/hr)	9.01E-06	Internal

The principal moment of inertia matrix for OPUS is defined in equation 19.

$$\begin{bmatrix} 4322 & 0 & 0 \\ 0 & 7902 & 0 \\ 0 & 0 & 9768 \end{bmatrix} \text{kg·m}^2 \tag{19}$$

3. External Torque Equations

As defined in [8], Equations 20, 21, and 22 model the torques induced by the Mars gravity gradient, atmospheric drag, and solar radiation pressure, respectively.

$$T_{gg} = 3\mu \frac{|I_{zz} - I_{xx}| \sin(2\theta)}{2R^3}, \tag{20}$$

$$T_a = \frac{1}{2}\rho V^2 C_d A (c_{pa} - c_g), \tag{21}$$

$$T_s = \frac{SA\cos(i)}{c}(1+q)(c_{pa} - c_g), \tag{22}$$

In Equation 20, μ is the gravitational parameter of Mars, and I_{zz} and I_{xx} are the z and x-axis moments of inertia of the spacecraft, respectively. θ is the orbiter's maximum deviation from the z-axis, and R is the radius of the orbit from the center of Mars. In Equation 21, ρ is equal to the atmospheric density, V^2 is the flight velocity of OPUS, and A is the surface area of OPUS that is normal to its z-axis (as defined by Figure 19). C_d is the orbiter's coefficient of drag, and c_{pa} and c_g are the orbiter's center of pressure and center of gravity, respectively. Equation 22 defines the torque induced by solar radiation pressure. In Equation 22, S is the solar irradiance at the location of OPUS, i is the solar incidence angle, c is the speed of light, and q is the reflectance factor of the solar array.

4. Reaction Wheel Sizing

The reaction wheels were sized to counter the internal and external torques on OPUS during its flight. The total disturbance torque was calculated by summing the torque quantities in Table 17 Equation 23 was then used to calculate the worst case disturbance torque acting on OPUS.

$$h = 2(T_a + T_s + \frac{\sqrt{2}}{4}T_g) \tag{23}$$

The resulting worst case disturbance torque value was 0.1790 Nm. The reaction wheels were therefore sized to counteract this torque in each direction. Thus, 0.5 Nm of torque was selected for the reaction wheel. The selected Reaction Wheel was RWp500 from Blue Canyon Technologies [35].

5. ADCS Actuator and Sensor Configuration

In order to achieve the maneuvers and corresponding control modes defined above, the attitude control configuration was designed to provide OPUS six degrees of freedom while minimizing the required number of thrusters for mass and power reduction. As described in section VII.B.5 attitude control system of OPUS consists of one primary thruster, 8 small thrusters, and 4 reaction wheels. The specifications for the actuators are shown in Table 18. The orientation of these engines are displayed in Figure 19, where the 8 small thrusters are angled 45 degrees from the the normal of the surface they are on and outwards 45 degrees from the +x axis about the y axis. 4 of the small thrusters are visible in Figure 19, while the other 4 are mirrored across the ZY plane of the orbiter. This allows for six degrees of freedom, 3 for translational motion and 3 for rotational motion. This thruster configuration also provides redundancy as only four thrusters at a time are required for any given movement direction.

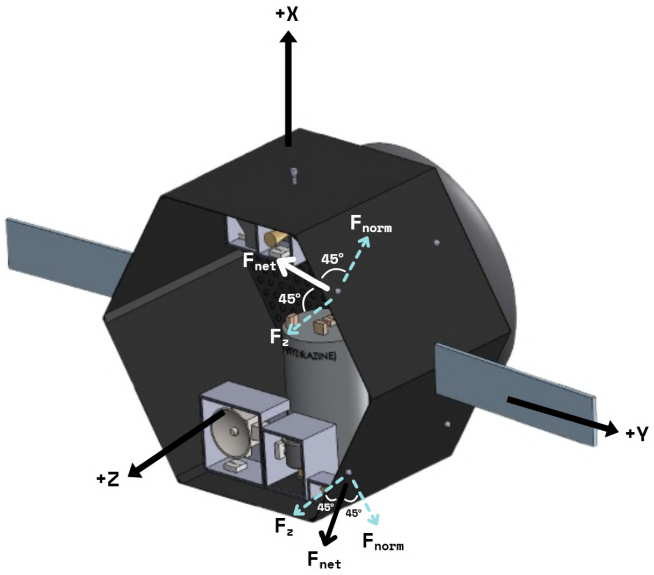

Fig. 19 OPUS Axis Orientation and Thrust Directions

Additionally, a suite of 5 star trackers, 2 inertial measurement units (IMU), and 4 sun sensors is used for OPUS attitude determination. The selected instruments and their quantities are displayed below in Table 18. As seen in Figure 20, the 3 momentum wheels are each aligned with an axis of the spacecraft, and the fourth is included for redundancy in the case that one of the momentum wheels fails. This configuration allows for passive three axis stabilization of OPUS, providing maximum 0.1 degree pointing accuracy required in Table 16. The thrusters will then allow momentum dumping and translational motion for orbit trim maneuvers.

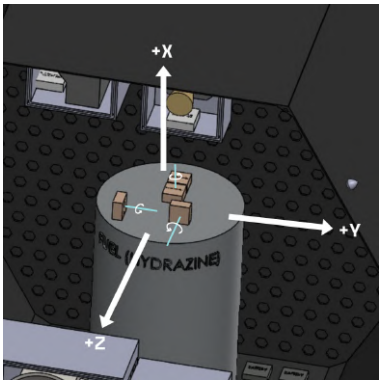

Fig. 20 OPUS Interior Momentum Wheel Configuration

The final selected components and their properties are displayed in Table 18.

Table 18 ADCS Component Specifications

Element	Quantity	Name	Distributor	Mass (kg)	Avg Power (W)
Reaction Wheel	4	RW1	Blue Canyon Technologies	1.1	14
Inertial Measurement Unit	2	MIMU	Honeywell Aerospace	4.6	25
Sun Sensor	4	Aquila-DO2	NewSpace Systems	0.037	0.15
Star Sensor	5	CT-2020	BAE Systems	3.75	8
Big Thruster	1	MR-107S	L3Harris	1.01	34.8
Small Thruster	8	MR-103D	L3Harris	0.33	8.25

6. ADCS Trades

Multiple trade studies were performed in deciding the thruster configuration and sensor suite of the ADCS system. First, a trade was initiated for the number and orientation of thrusters used for OPUS. The existing configurations for the Mars Reconnaissance Orbiter (MRO) and Mars Climate Orbiter (MCO) were compared and analyzed.

The thruster configuration of the MRO was studied and was determined to encompass6 main engine thrusters (Aerojet Rocketdyne MR-107N), 6 trajectory correction maneuver thrusters (Aerojet Rocketdyne MR-106E), and 8 attitude control thrusters (Aerojet Rocketdyne MR-103D) [36]. Under this configuration, this system would utilize approximately 426 Watts of power [37]. The MRO configuration has a substantial amount of redundancy, but also consumes a large amount of mass and power. The Mars Climate Orbiter, on the other hand, had a much simpler but less robust thruster configuration, with 4 medium thrusters for trajectory correction and 4 small thrusters for roll control. Based on the specifications, this system would utilize approximately 134.2 Watts, which is considerably less than the MRO [37].

A thruster configuration was then designed using the above trades. First, a thruster configuration for OPUS was then considered with one main engine thruster, 4 medium thrusters surrounding the main, and 6 small thrusters arranged on either end of the vehicle in two clusters. However, it was quickly found that this arrangement did not easily provide

the required 6 degrees of freedom for the vehicle motion. Additionally, medium thruster arrangement was found to be unnecessary due to the small external torques on OPUS and their arrangement. The current thruster configuration was then designed, minimizing power consumption from the previous design and allowing for the 6 degrees of freedom. The final total consumption for this design was 66 Watts for the ADCS thrusters.

Another trade was initiated for the instruments selected for attitude determination. Two Honeywell Mini Inertial Measurement Units (MIMU) are placed in the center, where the second is for redundancy. The Honeywell MIMU was chosen for its proven use on the MAVEN spacecraft, and performance capabilities. Other considered inertial measurement units included the Honeywell HG 1125 and HG 9900 [38]. The HG 9900 was considered for its performance, with bias performance being as low as 0.0006 deg/hr, while the HG 1125 was considered for its low size and power consumption (0.06 lbs and 0.5W). However, HG 9900 in turn was very large and the HG 1125 had considerably high biases. The MIMU was chosen as a middle ground between the two, with fairly low bias and small size. The MIMU specifications are stated in the mass budget [39]. The other sensors described in Table 18 were chosen based on heritage and market availability.

VIII. TILES Design

A. Instrumentation Selection & Trades

The TILES instruments shall have the following requirements:

Table 19 TILES Instrumentation Requirements

Req Name	Parent Req	Traceability	Requirement	Rationale
PRB-1.0	SYS-6.0	MR-9.0 - SYS-6.0 - PRB-1.0	The TILES shall collect data on the density and frequency of dust clouds on the Martian surface using photodetectors and by taking images at different times during the day.	Details how the TILES will observe dust clouds at its POFMO.
PRB-2.0	SYS-6.0	MR-9.0 - SYS-6.0 - PRB-2.0	The TILES shall collect radiation and meteorology data using a solid-state detector telescope, Cesium Iodide calorimeter, and scintillators to identify charged particles, neutrons, and gamma-rays over time.	Details how the TILES will collect radiation and weather data at its POFMO.

1. Radiation and Dust Sensor

For the instrumentation onboard the TILES probes, the team prioritized collecting scientific data that would be highly relevant to future exploration and doing so via highly proven instruments. The first of these two instruments is the Radiation and Dust Sensor, or RDS. This sensor previously visited Mars aboard the Perseverance rover, as part of its

Mars Environmental Dynamics Analyzer instrument suite [40]. The RDS has the following functions: estimating the optical and scattering properties of airborne dust as the seasons and local time change, detecting dust devils and other localized weather events, and characterizing cloud cover. On a high level, this instrument looks to investigate the dust accumulation rates and grain properties at specific locations that look to be favorable for future manned or unmanned exploration, given how harmful Martian regolith can be to life-sustaining electronics. This instrument's detectors can be split into two categories: the RDS-SkyCam and RDS-Photodetectors. The Skycam is an upwards-pointed camera designed to operate within the visible spectrum, primarily for taking pictures of cloud cover. The photodetectors are distributed around the body of the RDS, pointing slightly above parallel with the Martian surface. These detectors image at spectral bands ranging from ultraviolet to near-infrared to investigate the optical properties of dust and clouds as they change. The instrument is shown below in Figure 21.

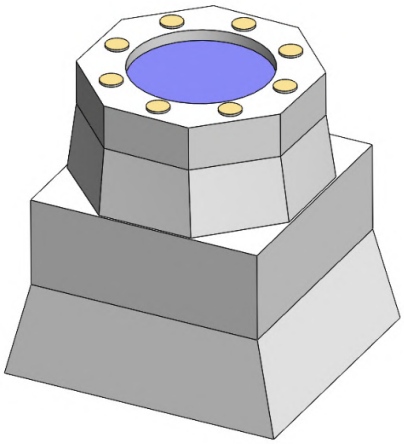

Fig. 21 RDS Structure

This instrument was chosen over other dust-investigating instruments because of its flight heritage and diverse measurement capabilities. The RDS has been operating without fault since Perseverance landed on Mars in 2021, making it a proven choice for short- to medium-term data collection at potential landing sites. Additionally, its ability to collect information on dust composition and visual-light images of the sky and surface provides scientists and mission planners with a wealth of information, especially as compared to instruments like Opportunity's Magnet Array which only investigate composition for similar mass and power requirements [41]. Due to its reliability over the last 4 years of operation on Perseverance, we decided this use of the RDS instrument to be a TRL of 8.

2. Radiation Assessment Detector

The second of the TILES probes' two instruments is the Radiation Assessment Detector, or RAD. This instrument was originally part of the Mars Science Laboratory (MSL) mission, landing on the Martian surface with the Curiosity

Rover. During this mission, it made the first direct measurements of radiation from the Martian surface, including solar energetic particles (SEPs), cosmic rays, and a variety of particles from both the atmosphere and regolith. This spans a range of 0.15-270 MeV, making it comprehensive in its data collection [42]. In the MOSAIC mission, this instrument would be deployed onboard TILES to collect long-term data on radiation exposure that future astronauts would experience while on the planet. This effort greatly informs future mission planning; radiation exposure is a great concern for interplanetary manned missions, so having consistent data at landing sites would be invaluable, especially given Mars' thin atmosphere and weak magnetic field. Figure 22 shows a model of the instrument itself.

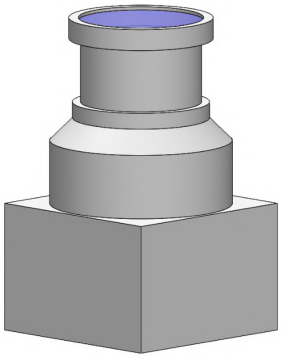

Fig. 22 RAD 3D Model

RAD was chosen to be the instrument to evaluate the effects of radiation and space weather on the Martian surface for multiple reasons. The first such reason is its low mass and power requirements, having a mass below 2kg and only requiring 4.2W of power when operating. [42]. Additionally, RAD has proven to be an effective and reliable instrument in the past aboard Curiosity; it has been operating consistently for twelve years, which is ten more than its intended lifespan. This fact means that our use of RAD would be TRL 9. In terms of its actual capabilities, RAD is the most suited to the wide spectrum of radiation that the Martian surface. especially in regards to radiation resulting from regolith or the atmosphere, similar instruments intended for other planetary missions do not adequately measure the most relevant particles for human health [42].

B. Entry, Descent, and Landing (EDL) Strategy

The requirements of the EDL subsystem are defined as follows:

Table 20 EDL Subsystem Requirements

Req Name	Parent Req	Traceability	Requirement	Rationale
EDL-1.0	MR-8.0	MR-8.0 - EDL-1.0	The TILES shall land safely at the desired POFMO.	Ensures that the EDL subsystem can land the TILES at a velocity that will not damage its subsystems or instruments.
EDL-2.0	MR-8.0	MR-8.0 - EDL-2.0	The EDL subsystem shall be able to land the TILES within a 50 kilometer radius of the intended POFMOs.	Ensures that the EDL subsystem can land the TILES at the intended radial accuracy so as to properly mark the locations for future Mars outposts.

EDL will begin on January 14, 2034, once the target landing sites have been determined by the Ground Station.

1. EDL Trades

A trade was initiated to compare previously existing Mars EDL systems a determine the best system to satisfy the TILES landing requirements. The first EDL system considered was for the Mars Science Laboratory (MSL) [43]. The MSL used a heat shield, followed by parachute deployment at an altitude of 11 kilometers. At around 18.6 meters altitude, the Sky Crane system was then used to decrease the vertical velocity of the lander from 20 m/s to 0.75 m/s. The major benefit of the MSL EDL system was the high precision in landing site arrival and the soft landing for the vehicle. However, this system is very complex and therefore expensive, and would not fit under the MOSAIC budget constraints. It was also designed to land a science payload of up to 300 kg, while the TILES science payload is under 10 kg [44]. Ultimately, the Sky Crane system was not chosen for the TILES EDL.

The Insight rover used a similar EDL system as the MSL. Instead of using the SkyCrane as it approached the Martian surface, Insight used thrusters attached to the landing vehicle itself to slow its descent velocity. Additionally, Insight used telescoping landing legs to stabilize the system upon landing [45]. The Insight rover was able to successfully safely within a 130x27 km ellipse [46].

The Pathfinder Lander used a different method for landing the vehicle. After parachute deployment, the lander deployed an array of airbags to cushion its fall as it approached the surface of Mars[47]. The landing accuracy for the Pathfinder Lander rover was a 200x70 km ellipse. [46]. Both the Pathfinder and Insight landers were designed for a science payload of 25-70 kg [44]. Therefore, a similar EDL system to the Insight rover was chosen to land the TILES.

2. EDL Sequence

Figure 23 summarizes the EDL sequence for the TILES.

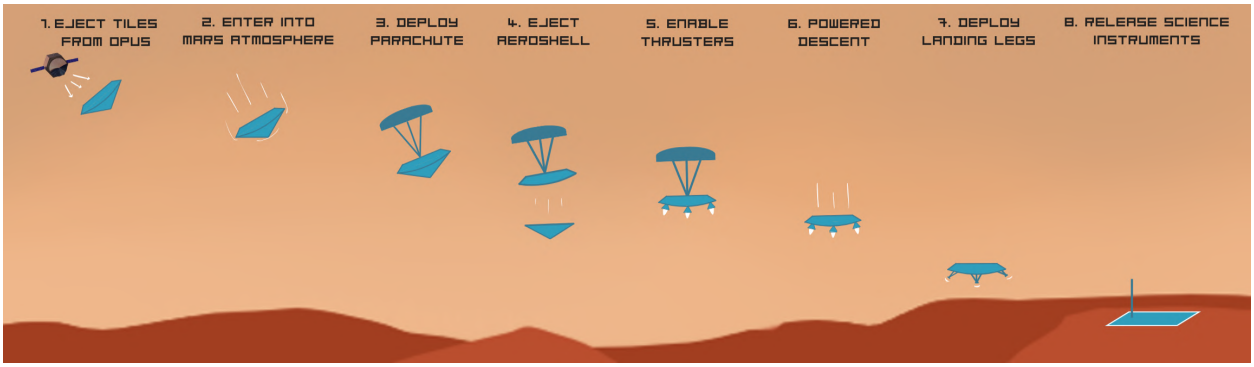

Fig. 23 TILES EDL Sequence

The probes will be ejected from OPUS using loaded springs and pyrotechnic bolts. It will then enter the atmosphere at an angle of 11.5 degrees. This angle was chosen as too high of an angle would cause excessive friction to overheat the landing vehicle (while too low an angle would cause the lander to bounce off of the atmosphere).

As will be mentioned in Section IX.B, the aeroshell/heat shield is be used to initially slow the TILES' descent, while protecting the interior of the landing vehicle from high entry temperatures. Once descent velocity of the probes is approximately Mach 2, a disk-band-gap parachute will be deployed. This parachute will bring the vehicle to a descent velocity of approximately 60 m/s. During this phase, the aeroshell will also be ejected using pyrotechnic bolts. Once the 60 m/s descent velocity is reached, the landing thrusters will be enabled to further decelerate the landing vehicle. This will ensure that instruments will not be damaged upon contact with the Martian surface. Once the lander has reached an altitude of about 20m, its landing legs will be deployed to further cushion its fall. Upon landing, the TILES will wait about an hour before unfolding the science instruments and beginning data collection, in order to ensure dust has fully settled and the TILES have achieved successfully communication to Earth.

The necessary equipment for the EDL system includes thrusters, a parachute and parachute mortor, propellant, and sensors. Four L3 Harris MR-80B thrusters shall be aboard the lander. Each is a gimbaled engine with the capability of providing 3100N of thrust. 50 kg of hydrazine is stored in the propellant tanks of each TILES to provide propulsion for the descent phase. Similar to on OPUS, a MIMU from Honeywell Aerospace is used to calculate the descent velocity of the probes. A LiDAR sensor is also attached onto the bottom of the lander, to determine the altitude of the probe as it approaches the surface.

Additionally, the EDL system will be able to land the probe within a 50km radius of the desired landing site. This value was confirmed using 50 iterations of a Monte Carlo simulation modeling the vehicle's descent.

IX. OPUS/TILES Integration

A. Telemetry, Tracking, and Command (TTC) & Data Handling

The design of the communications system was primarily drawn from past Mars missions, with communications modules, frequencies, and ground stations chosen for their heritage. A reliable link is needed for proper transfer of the high-resolution images captured for MOSAIC's mission, which for the mission's purposes is defined as a link margin of at least 3 dB for any given communications relay. The TT&C subsystem shall have the following requirements:

Table 21 TT&C Subsystem Requirements

Req Name	Parent Req	Traceability	Requirement	Rationale
CDH-1.0	MR-10.0	MR-10.0 - CDH-1.0	The OPUS shall be able to receive commands from the Ground Team at a frequency of 7.1 giga-Hertz.	Ensures that OPUS's communication subsystem can receive commands at a frequency specified by the equipment chosen.
CDH-2.0	MR-10.0	MR-10.0 - CDH-2.0	The OPUS shall be able to send data to the Ground Team using the Deep Space Network at a frequency of 8.1 giga-Hertz.	Ensures that OPUS's communication subsystem can send data at a frequency specified by the equipment chosen.
CDH-3.0	MR-10.0	MR-10.0 - CDH-3.0	All commands sent to the OPUS and TILES shall be verified by the Ground Team before being implemented.	Prevents commands sent in error that would jeopardize the mission.
CDH-4.0	MR-10.0	MR-10.0 - CDH-4.0	The Ground Team shall have the ability to monitor all subsystems on the OPUS and TILES.	Ensures that OPUS and TILES have a method to monitor internal system health and communicate that to the Ground Station.
CDH-5.0	MR-10.0	MR-10.0 - CDH-5.0	All communication methods shall maintain a link margin of at least 3 decibels.	Ensures that all communications are within a safe link margin to not interfere with other missions or frequencies.

Below is a diagram of the chosen ground stations and all communication pathways for MOSAIC. All communications to and from the Deep Space Network (DSN) utilize the designated X-band frequencies, while Mars surface communications between OPUS and TILES use the UHF range.

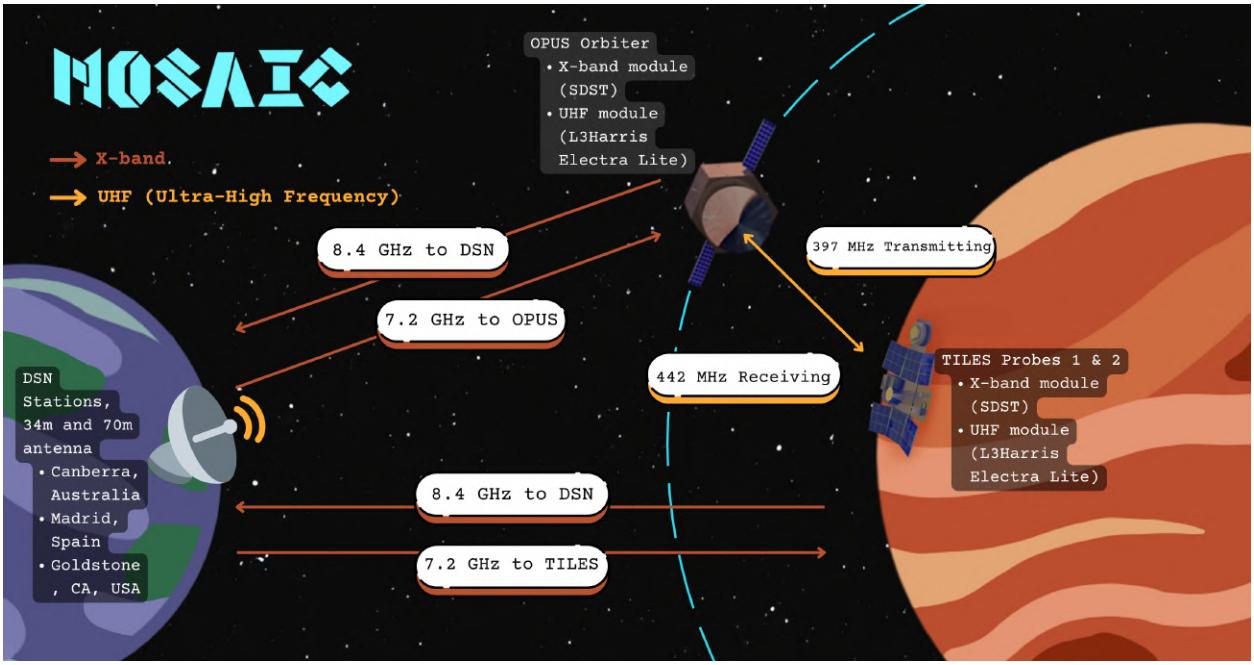

Fig. 24 Diagram of Communications Channels and Stations with Frequencies Outlined

1. Communications Module Selection

Since communications occur in both the X-band and UHF ranges, each system requires two communications modules to accommodate both. For the UHF range, the chosen communications module was the L3Harris Mars Electra Lite Transceiver. The Electra Lite has heritage from its use on Perseverance for Mars 2020, making it a viable candidate for UHF communications for both TILES and OPUS [48]. Additionally, the Lite configuration has a lower mass and power requirement compared to the Electra UHF transceiver launched with the MAVEN orbiter [49] [50]. This module is capable of communicating from existing orbiters to Perseverance in a millisecond, making it ideal for lower latency as well[49].

For X-band communications, the Small Deep Space Transponder (SDST) by General Dynamics and NASA JPL was chosen. The SDST has heritage with the Curiosity and Perseverance rovers, as well as MAVEN, OSIRIS-REx, and Psyche, proving its reliability for X-band communications. Additionally, it is compatible with the DSN [51].

OPUS will have a fixed high-gain antenna, as well as two gimbal-mounted low-gain antennas in the case that data cannot be received with the high-gain antenna. A fixed high-gain antenna was chosen as opposed to a gimbaled one due to the saved mass and power requirements for the system. From previous systems, such as the MRO, the mass added for gimbaling hardware was close to 45 kg, as well as 14 extra Watts of power [52]. Below is a mass breakdown of the communications systems for both OPUS and TILES.

Table 22 OPUS Communications System Components and Masses

Component	Mass per unit (kg)	Quantity
L3Harris UHF Communications Module	3.0	1
UHF antenna	1.4	1
Small Deep Space X-band Transponder (General Dynamics)	3.2	1
X-band HGA reflector	19.1	1
Antenna feed	1.6	1
LGA antenna	0.4	2
Antenna hardware (struts, support, etc)	1.1	-
X-band TWTAs	0.95	2
X-band power converters	3.0	1
Diplexers & brackets	1.8	1
Waveguides and coax	8.3	1
Waveguide transfer switches	1.5	1
Misc. microwave components	1.4	-
TOTAL	**48.5**	

Table 23 TILES Communications Components and Masses

Component	Mass per unit (kg)	Quantity
L3Harris UHF Communications Module	3.0	1
UHF helix antenna	1.1	1
UHF antenna	1.2	1
UHF diplexer	0.36	1
UHF transfer switch + bandpass filter	0.13	1
Small Deep Space X-band Transponder (General Dynamics)	3.2	1
X-band reflector/radar	5.0	1
MGA antenna + cabling	3.5	1
X-band diplexers	1.8	-
Waveguide, adaptor, support	0.59	1
RF transfer switch	0.42	1
Bandpass and notch filter	0.41	1
X-band cables	1.12	1
TOTAL	**22.24**	

2. On Board Data Handling

For commands and data handling, the BAE Systems RAD750 radiation-hardened single board computer was chosen for both OPUS and the TILES probes. The RAD750 has heritage from the Mars Reconnaissance Orbiter, Lunar Reconnaissance Orbiter, the Insight Lander, and Perseverance rover, making it reliable for high volumes of data (such as those from HiRISE on the MRO) and data handling of both surface and orbiter systems. RAD750 has a 200 MHz processing speed and 2 gigabytes of flash memory, as well as 256 MB of RAM and 256 kB of read-only memory [53]. There will be two of these computers on each system for redundancy.

Since HiRIC has a maximum image size of 1.035 GB in its highest-resolution imaging mode with 1:6 compression [24], the selected computers possess enough storage to both hold images and compress data to be sent back to Earth.

Image relay communications will occur during the designated Science mode for the orbiter.

3. Data and Link Budgets

The bandwidth for OPUS and TILES downlink was determined by the maximum data rates for each system, as outlined in Table 24. For OPUS, this is the sum of data rates for instrumentation and sensors on board the orbiter frame, as well as data transmitted by the TILES probes. For the uplink budget, the bandwidth was the maximum data transfer rate taken from the DSN 34m and 70m Information Manuals [54][55].

Table 24 Data Budget Summary

Instrument	Quantity	Output Rate (Hz)	Bits	Data Rate (bps)
ADCS – OPUS				
Star Tracker	5	10	32	1600
Sun Sensor	2	5	32	320
IMU	1	1000	32	64000
Propulsion – OPUS				
Tank Pressure Sensor	14	25	12	4200
Thruster Pressure Sensor	2	25	12	600
Flow Meters	2	10	25	500
Temperature Sensors	16	25	10	10000
Power – OPUS				
Voltage Sensors	20	1	10	200
Current Sensors	20	1	12	240
Temperature Sensors	20	1	10	200
Science – OPUS				
Neutron Spectrometer	1	—	—	122
CIRS-Lite	1	—	—	6000
High Resolution Imaging Camera (HiRIC)	1	—	—	1695938000
LiDAR	1	—	—	10000
Power – TILES				
Voltage Sensors	20	1	10	200
Current Sensors	20	1	12	240
Temperature Sensors	20	1	10	200
Science – TILES				
Radiation and Dust Sensor (RDS)	1	—	—	1100
Radiation Assessment Detector (RAD)	1	—	—	1.408
			Orbiter Total (kbps):	1695990.942
			Probe Total (kbps):	11.501408
			***Relay Total (kbps):**	1696013.945

*Note: 2 probe, 1 orbiter relay link configuration.

The link budgets below were calculated using the following equation,

$$\frac{E_b}{N_0} = EIRP + G_{\text{receiving}} + L_{\text{free space}} + L_{\text{atm}} + L_{\text{point}} + L_{\text{implementation}} - 10\log(kT_{\text{sys}}B), \tag{24}$$

where all parameters for the equation are outlined in the respective link budget tables [56]. Parameters for the probe were modeled after prior Mars landers and rovers, while orbiter parameters were based on MAVEN and MRO [52][40]

Table 25 OPUS–Earth Uplink Budget [54][55][52]

Parameter	34m DSN to LGA	70m DSN to LGA	34m DSN to HGA	70m DSN to HGA
System Noise Temperature (K)	25.000	35.000	25.000	35.000
Max Distance (km)	4.00E+08	4.00E+08	4.00E+08	4.00E+08
Transmit Frequency (GHz)	7.200	7.200	7.200	7.200
Free-Space Loss (dB)	-282.969	-282.969	-282.969	-282.969
EIRP (dBm)	139.400	139.400	139.400	139.400
Receiving Antenna Gain (dB)	8.400	8.400	45.200	45.200
Atmospheric Loss (dB)	-8.000	-8.000	-8.000	-8.000
Pointing Loss (dB)	-0.100	-0.100	-0.100	-0.100
Implementation Loss (dB)	-1.000	-1.000	-1.000	-1.000
Bandwidth (kHz)	128.000	128.000	256.000	256.000
BPSK Eb/N0 Requirement (dB)	10.000	10.000	10.000	10.000
Design Eb/N0 (dB)	14.487	18.457	50.377	54.346
LINK MARGIN (dB)	**4.487**	**8.457**	**40.377**	**44.346**

Table 26 OPUS–Earth Downlink Budget [54][55][52]

Parameter	Science Mode		Safe Mode	
Name	**HGA to 34m**	**HGA to 70m**	**LGA to 34m**	**LGA to 70m**
System Noise Temp (K)	135.000	135.000	135.000	135.000
Max Distance (km)	4.00E+08	4.00E+08	4.00E+08	4.00E+08
Transmit Frequency (GHz)	8.400	8.400	8.400	8.400
Tx Antenna Gain (dB)	46.700	46.700	8.800	8.800
Free-Space Loss (dB)	-282.969	-282.969	-282.969	-282.969
EIRP (dBm)	135.333	135.333	97.433	97.433
Rx Antenna Gain (dB)	66.980	74.360	66.980	74.360
Atmospheric Loss (dB)	-8.000	-8.000	-8.000	-8.000
Pointing Loss (dB)	-3.600	-3.600	-3.000	-7.000
Implementation Loss (dB)	-1.000	-1.000	-1.000	-1.000
Bandwidth (kbps)	1696013.945	1696013.945	36.820	36.820
BPSK Eb/N0 Req. (dB)	10.000	10.000	10.000	10.000
Design Eb/N0 (dB)	21.746	25.726	30.480	34.460
LINK MARGIN (dB)	**11.746**	**15.726**	**20.480**	**24.460**

Bandwidth values for the UHF link budget, receiving column, were calculated from the Probe section of the data budget 24. The transmitting bandwidth is the expected data rate of command from the orbiter, and the receiving bandwidth is the telemetry data. Note that the transmitting data rate of OPUS is the receiving data rate for TILES, and vice versa; therefore, the transmit and receive link margins for TILES are the reverse of OPUS.

Table 27 UHF Communications, OPUS Transmit and Receive [54][55][52]

Parameter	OPUS Transmit	OPUS Receive
System Noise Temperature (K)	54	54
Max Distance (km)	250	250
Frequency (GHz)	0.397	0.442
Transmit Antenna Gain (dB)	10.7	10.7
Free-Space Loss (dB)	-132.37	-133.31
EIRP (dBm)	20.448	20.448
Receiving Antenna Gain (dB)	0.01	0.01
Atmospheric Loss (dB)	-2	-2
Pointing Loss (dB)	-0.12597	-0.12597
Implementation Loss (dB)	-1	-1
Bandwidth (kbps)	32	11
BPSK E_b/N_0 Requirement (dB)	10	10
Design E_b/N_0 (dB)	46.9165	41.34632
MARGIN (dB)	**36.9165**	**31.34632**

In the case that OPUS cannot relay information and science data from TILES to Earth, TILES will use its medium gain antenna to communicate direct-to-Earth.

Table 28 TILES–Earth Link Budgets: Uplink and Downlink

Parameter	Uplink DSN to MGA		Downlink MGA to DSN	
Name	**34m DSN**	**70m DSN**	**34m DSN**	**70m DSN**
System Noise Temp (K)	25.000	35.000	135.000	135.000
Max Distance (km)	4.00E+08	4.00E+08	4.00E+08	4.00E+08
Transmit Frequency (GHz)	7.200	7.200	8.400	8.400
Tx Antenna Gain (dB)	66.980	73.230	24.800	24.800
Free-Space Loss (dB)	-282.969	-282.969	-282.969	-282.969
EIRP (dBm)	139.400	145.800	73.433	73.433
Rx Antenna Gain (dB)	20.500	20.500	66.980	74.360
Atmospheric Loss (dB)	-8.000	-8.000	-8.000	-8.000
Pointing Loss (dB)	-5.000	-5.000	-3.600	-3.600
Implementation Loss (dB)	-1.000	-1.000	-1.000	-1.000
Bandwidth (kHz)	256.000	256.000	11.501	11.501
BPSK Eb/N0 Req. (dB)	10.000	10.000	10.000	10.000
Design Eb/N0 (dB)	25.677	29.646	14.385	18.365
LINK MARGIN (dB)	**15.677**	**19.646**	**4.385**	**8.365**

4. Latency and Communication Periods

The DSN has three stations in Goldstone, Madrid, and Canberra. According to the GMAT simulations, the orbiter will not make contact with the Madrid station, but will make contact multiple times a day with the Canberra and Goldstone locations.

The longest data transmission operation would be the downlink of images from HiRIC, which has a maximum image size of 3 gigabytes [24]. To send one full image at the maximum TLM data rate of 30 Mbps for the SDST would take a total of 800 seconds, or about 14 minutes [51]. Thus, even at a lower rate of 10 MBps , the operation would

take 40 minutes. GMAT simulation also requires that the contact with the DSN station lasts about an hour for each session, leaving enough time to transmit full images in one pass, and other science data through different communication windows within the same day.

Roughly once every two years, a solar conjunction period between Mars and Earth occurs, lasting about two weeks. During this time, MOSAIC will conduct minimal science operations until communications are resumed[57].

5. Operational Node Connectivity Diagram

The node connectivity diagram below outlines the flow of information from the engineering team and mission control to OPUS and TILES, and vice versa. It is important to note that landing site determination occurs after science data from OPUS provides necessary elevation profiles, high-resolution images, and surface compositions of the planet. Candidate landing sites are decided on the requirements listed above in Section III.F.

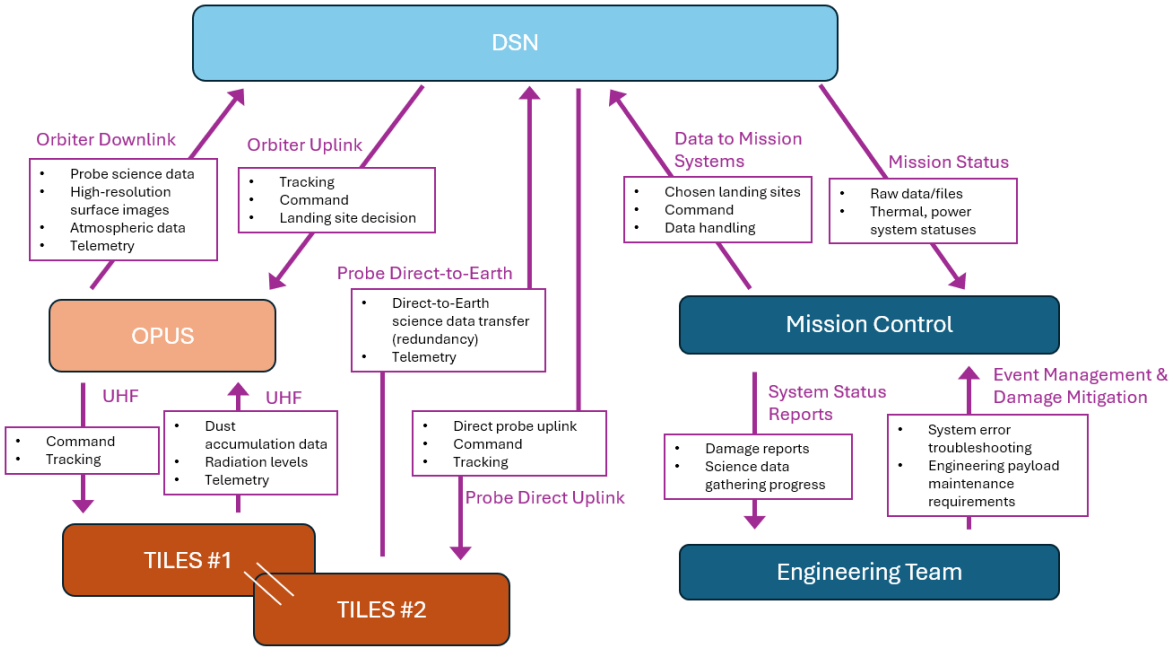

Fig. 25 MOSAIC Operational Node Connectivity Diagram (OV-2)

B. Thermal Management

1. Thermal Requirements

The MOSAIC mission is a multiphase operational procedure with different thermal requirements for each vehicle in every environment they may encounter. A thermal control system to manage and enforce these requirements is essential to maintain the survival of each vehicle. This means that material temperatures should not reach a certain level where deformation or melting may occur, and internal temperatures should not reach a certain degree where they may become

unable to operate. The temperature requirements to prevent either of these failures are outlined below in Table 29.

Table 29 Temperature Requirements for OPUS and TILES Instruments [42] [58] [59] [60]

OPUS Instruments	Operational Temperature (K)
External AlLi Surface	≤ 650
Neutron Spectrometer	≤ 100
CIRS-lite	≤ 150
HiRIC	243 to 293
LiDAR	278 to 301
TILES Instruments	**Operational Temperature (K)**
External AlLi Surface	≤ 650
RDS	218 to 323
RAD	253 to 328

In order to achieve these temperature requirements, a unique thermal control strategy is implemented for each of the vehicles, incorporating both passive and active control. Therefore, the thermal subsystem has the following requirements:

Table 30 Thermal Subsystem Requirements

Req Name	Parent Req	Traceability	Requirement	Rationale
THR-1.0	MR-4.0	MR-9.0 - MR-4.0 - THR-1.0	The subsystems on the OPUS and TILES shall be able to withstand a maximum of 355 Kelvin experienced during launch from Earth.	From the Falcon Heavy User Guide. Ensures that the thermal system protects against the heat from launch (as experienced inside the payload fairing).
THR-2.0	MR-4.0	MR-4.0 - THR-2.0	The spacecraft shall be able to withstand deep space temperatures of at least 2 degrees Kelvin during transit to Mars.	Ensures that the spacecraft and its components will not freeze - which would damage it - during transit to Mars.
THR-3.0	MR-4.0	MR-4.0 - THR-3.0	The TILES shall be able to withstand Mars surface temperatures between 170 and 270 Kelvin.	Ensures that the TILES will not freeze or overheat during Martian days and nights.
THR-4.0	MR-4.0	MR-4.0 - THR-4.0	The OPUS and the TILES shall be protected against radiation experienced during all phases of the mission.	Ensures that the subsystems and instruments aboard OPUS and the TILES will not be affected by space radiation, which may harm these components.
THR-5.0	MR-4.0	MR-4.0 - THR-5.0	The TILES shall have thermal protection to withstand entry into the Martian atmosphere.	Ensures that the TILES will not overheat while descending to their POFMO.

2. OPUS Thermal Environments

The primary vehicle OPUS goes through four main stages in the mission procedure: launch onboard Falcon Heavy, transfer orbit to Mars, aerobraking into science orbit, and operating science orbit.

The first significant phase for thermal considerations is during launch from within the Falcon Heavy payload fairing. During this stage, the payload fairing may experience significant temperatures as an effect of the rocket's engine firing.

SpaceX provides an estimated composite temperature profile for the payload fairing shown in Figure 34. Although the figure truncates at 240 seconds, the available temperature profile is still valid because the peak heating is likely to occur around 210 seconds as the rocket exits Earth's atmosphere. However, the estimated maximum temperature/worst-case heating scenario is still taken to be 240 seconds. This results in a surface temperature of $\approx 185°F$ or $85°C$.

The next significant phase for OPUS is during the transfer from Earth to Mars, where the spacecraft is effectively in deep space. During this stage, the spacecraft is subject to deep space temperatures of $\approx 3K$ and must keep the internal instruments warm enough to survive the extreme cold.

The third and most significant stage for OPUS is during the aerobraking maneuver performed to enter a 250km science orbit. During this phase, the spacecraft skims the Martian atmosphere at high speeds at its periapsis to lower the apoapsis using atmospheric drag forces. This results in a very large aeroheating effect, as the air particles on the surface of the spacecraft are compressed and heated as they are pushed to the side. Figure 26 shows the aeroheating effects on a sample solar array panel (which is likely to be the most affected area), and Figure 27 shows the resulting temperature profiles on either side of the insulated surface using a sample MLI strategy. This mapping demonstrates an expected temperature of $97°C$ affecting the outer surface of the insulation.

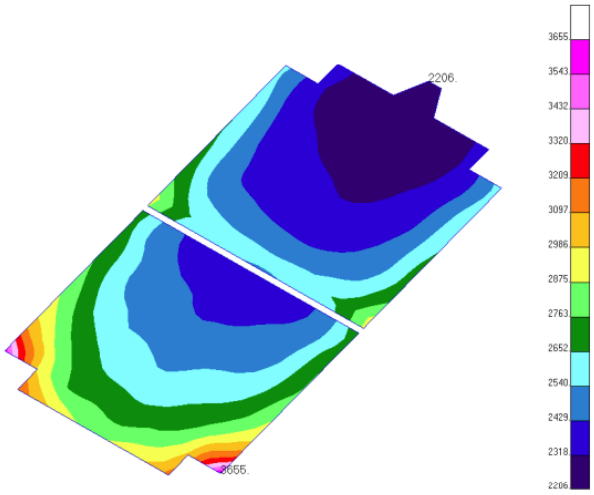

Fig. 26 Aeroheating Profile During Aerobraking Phase of Mission

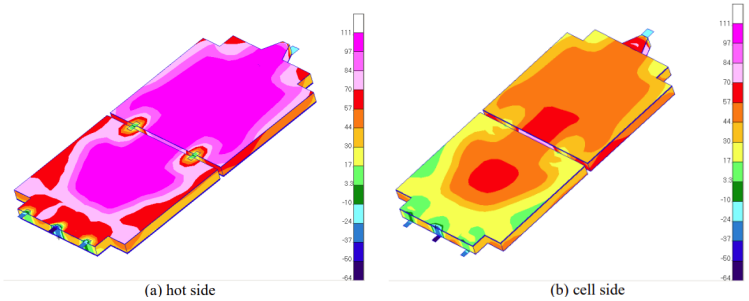

(a) Outer Surface (b) Inner Surface

Fig. 27 Temperature Profile Facing Each Surface During Aerobraking [61]

Finally, the last phase of the spacecraft's operations includes its scientific operation in steady orbit just outside the Martian atmosphere. This phase is when the instruments will be active and require the most precise thermal balance. However, the spacecraft will also be impacted by a much less extreme environment without the effects of aeroheating or the frigid temperature of deep space.

3. OPUS Thermal Management Trades

Based on the temperature mapping of the solar arrays developed via simulation, the Team used the preliminary MLI layout from Mars Global Surveyor and Mars Odyssey to develop an analytical representation of the system. This initial layout incorporates five layers of material in a sandwiched structure, including an M55J graphite composite facesheet on the outer surface directly exposed to aeroheating (0.19 mm), aluminum honeycomb core (19.5 mm), M55J facesheet (0.19 mm), kapton sheet (0.051 mm), and finally a solar cell layer on the inside [61]. This structure is also pictured in Figure 28.

Using this structure, the Team developed and validated an analytical process to calculate the inner surface temperature using the expected results from the simulation. In order to determine the expected inner surface temperature, conduction was considered to be the dominating method of heat transfer. This allowed the inner surface temperature to be calculated based on the total external heat input from aeroheating and solar radiation, reflected heat output, outer wall temperature, and thermal conductivity of each material in the insulation structure 25. This formulation resulted in <10% error compared to the simulated results, thereby validating the usage of the analytical representation.

Additionally, a trade study was conducted to determine the active cooling system for the orbiter. Loop Heat Pipes (LHPs) and Miniature Cryocoolers were selected as the primary options due to their heritage in past missions. LHPs are passive thermal transport devices capable of efficiently moving heat from high-power electronics to radiators without requiring electrical power. Their simplicity, lack of moving parts, and proven reliability make them ideal for spacecraft temperature regulation in the dynamic Mars orbital environment. LHPs are lightweight, require minimal integration

effort, and are highly adaptable. These characteristics make them particularly attractive for long-duration missions where mechanical reliability and low power consumption are critical. In contrast, Miniature Cryocoolers are active devices that provide targeted, low-temperature cooling, sometimes down to cryogenic levels ($\approx$ 40 K). This makes them essential for missions that carry sensitive scientific instruments, such as infrared detectors or spectrometers, which require precise and sustained low-temperature environments. However, cryocoolers come with higher mass, continuous power requirements, and mechanical complexity, which can introduce vibration and reduce system longevity due to moving components. As a result, miniature cryocoolers were used selectively for instruments with stringent temperature requirements such as CIRS and the neutron spectrometer, while loop heat pipes were used to cool the overall body of the spacecraft.

4. OPUS Thermal Control Strategy

OPUS's thermal control strategy development began with considering the aeroheating effects impacting the orbiter during aerobraking. This was selected as the worst case condition for thermal design as the due to the fact that temperatures reached during aeroheating were roughly $12°C$ higher than the maximum temperature expected during the launch phase. Additionally, design choices were made to take into account the effect of heating on the solar panels, as these components would likely be impacted the most due to their large area and orientation.

Based on the preliminary insulation structure, the conductive heat transfer calculations resulted in an inner wall temperature of $32.69°C$. However, the requirements for the allowable temperatures necessitate a maximum temperature of $20°C$, enforced by the High Resolution Imaging Camera. In order to meet this requirement, adjustments were made to the insulation layering structure. Therefore, the final MLI structure incorporated six layers of varying thickness: a M55J graphite composite facesheet on the outer surface directly exposed to the aeroheating (0.19 mm), aluminum honeycomb core (23.5 mm), kapton sheet (0.051 mm), M55J facesheet (0.19 mm), kapton sheet (0.051 mm), and finally the solar cell layer on the inside (a germanium coated kapton film is used for additional reinforcement while being RF transparent). This final layout provided sufficient thermal insulation from external heating to maintain an internal surface temperature of $16°C$ during the worst-case peak heating situation, staying below the allowable temperature limit of the instruments and allowing for a slight margin. This layout was then extended to cover the main body of the orbiter in addition to the solar panels to protect the vehicle during aeroheating and launch. The final global MLI structure is shown below in Figure 35. Additionally, AZ-93 white thermal coating is applied to locations of higher risk where aeroheating may be more centralized or the orbiter's structure may be weaker, such as hinges and joints [62].

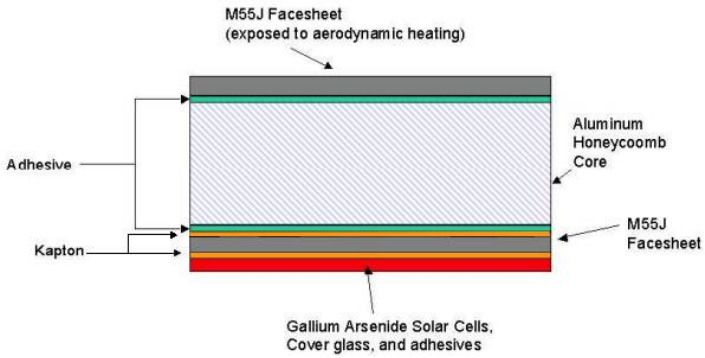

Fig. 28 Final MLI Layering Surrounding OPUS's Body [61]

Although the passive thermal control system is expected to provide sufficient thermal protection to maintain the internal temperature of the spacecraft, active thermal control is still in place for redundancy. The active thermal control strategy includes loop heat pipes filled with ammonia and adjustable radiators. The loop heat pipes function by absorbing excess thermal energy to heat and vaporize ammonia fluid, which creates a pressure difference due to the phase change, which then pushes the vaporized ammonia through the loop. The vaporized fluid then radiates heat out to space and condenses back into a liquid, where it is then pushed back toward the evaporator section due to capillary pressure in the piping. This schematic is pictured below in Figure 29. Finally, the radiators can be mechanically actuated to open or close a specific amount and determine how much heat is emitted out of the spacecraft.

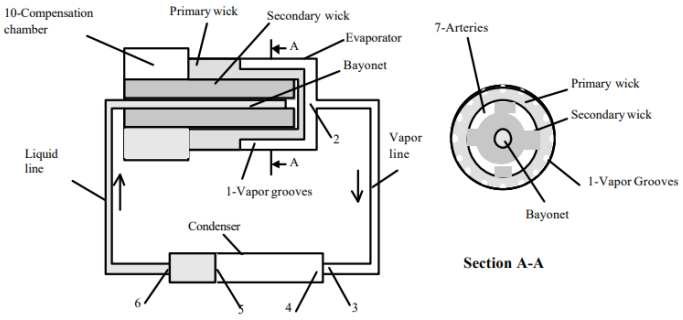

Figure 1. Flow Schematic of an LHP

Fig. 29 Schematic of Loop Heat Pipe Operation [63]

The second extreme condition that must be considered for thermal control is the intense cold during deep space operations. Although the MLI insulation already in place around the spacecraft will provide an initial barrier against the heat loss towards space, it may not be sufficient due to the significant temperature difference between the spacecraft internals and the external environment. However, it is not feasible to heat the entire spacecraft as a result of its large size. Therefore, an alternate solution was developed involving secondary insulation that encapsulates individual components.

The Multi-Environment MLI (MEMLI) thermal insulation system utilizes a novel lightweight vacuum shell supported by integrated MLI (IMLI) and spacers to significantly reduce heat flux [64]. This 10 layer MEMLI prototype (TRL 5) was able to reduce heat flux to as low as $0.19 W/m^2$ while maintaining a low mass of $1.5 kg/m^2$ and was proven feasible in vacuum and Martian atmospheric environments, providing additional support during additional orbiting phases of the mission. The MEMLI will be used to encapsulate individual instruments and components to isolate them from the external environment within their own system with minimal heat transfer in or out. This implementation is shown in Figure 30.

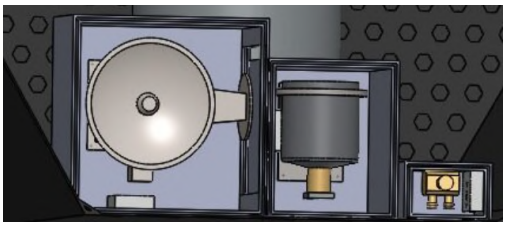

Fig. 30 MEMLI Implementation for OPUS Instrumentation

Though the MEMLI is extremely effective at isolating components into a new isothermal subsystem, it cannot be be used for the entirety of the mission. Once the orbiter enters its science orbit and begins operation of instruments, the vacuum sealed shell will need to be opened up in order to give visibility to instruments such as the laser spectrometer and High Resolution Imaging Camera. This means that the instrument sub-compartment will be opened directly to the cold environment of the science orbit. At this altitude, the temperature can be modeled at an ambient external temperature of $-78.9°C$[65].

Based on this temperature, we calculated the necessary heat input to maintain the instrument temperature by accounting for direct/indirect solar radiation, convective heat loss, and radiative heat loss using equations 26, 27, 28, and 29 [66].

The result of these calculations was that OPUS would need 443.96 W to maintain the internal temperature of above 248K within the High Resolution Imaging Camera. The neutron spectrometer and CIRS-lite were not considered, because they are equipped with their own miniature pulse tube cryocoolers to maintain low temperature. The thermal requirements to maintain the operational temperature of LiDAR above 283 K was less than 1 W and thus considered negligible. In order to meet these requirements for thermal energy, electrically powered resistive heater units (RHUs) were implemented to maintain the equilibrium temperature at a constant degree during operations and prevent issues resulting from sudden heat flux. The RHUs are each capable of providing up to 250 W of thermal energy at an efficiency ratio close to one and incorporate thermocouples to read ambient temperature and provide energy as needed.

5. TILES Thermal Environments

The secondary vehicle, TILES, will be deployed into an EDL phase through the Martian atmosphere before settling on the Martian surface for scientific operations.

During the EDL phase, the probe undertakes massive amounts of thermal energy caused by the friction and compression of air particles similar to the effects in aerobraking. However, the high velocity of EDL combined with the thicker atmosphere as the altitude decreases results in a much greater level of heating, mapped in Figure 31.

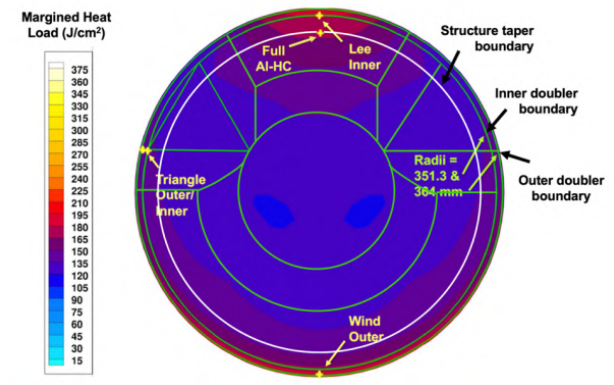

Fig. 31 Aeroheating Profile During EDL Phase of Mission [67]

The primary duration of the probe's lifetime will be spent on the Martian surface as scientific operations are conducted. During this phase, the probe must survive the cold winter nights of Mars as well as maintaining operation during the milder summers and days. The expected conditions are mapped in Figures 32(a) and 32(b). These figures demonstrate that the worst-case cold condition can be expected to be around 170 K and the median condition around 200 K.

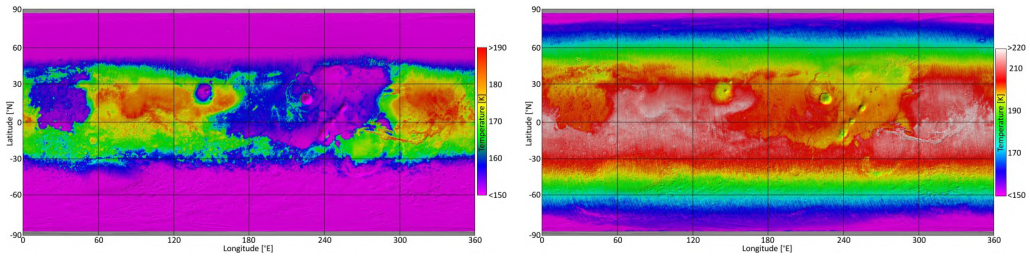

(a) Minimum Temperature Profiles of Martian Surface [68] (b) Median Temperature Profiles of Martian Surface [68]

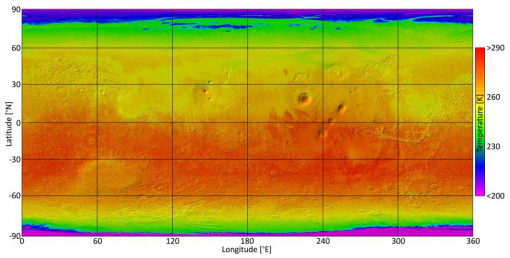

(c) Hot Temperature Profiles of Martian Surface [68]

Fig. 32 Various Temperature Maps

6. TILES Thermal Management Trades

For the TILES Mars lander, the passive thermal control system was drawn primarily from the thermal protection systems of past missions such as Curiosity and Insight. However, a trade study was conducted for the active thermal control system to compare the use of RTGs (radioisotope thermoelectric generators) and RHUs (resistive heater units), both common systems on Mars Landers with significant heritage. For a small-scale Mars lander or probe with modest power and thermal control requirements such as TILES, selecting between RTGs and RHUs requires weighing power generation needs, thermal performance, system complexity, and mission constraints.

RTGs are compact power systems that convert heat from the radioactive decay of plutonium-238 into electricity, providing both power and significant heat. They are best suited for missions requiring continuous electrical power, particularly in low-light environments or over extended durations where solar panels may be ineffective. However, RTGs are relatively heavy, complex, and expensive. They also generate more power and thermal energy than typically needed for small-scale, low-demand landers, making them potentially excessive for minimal payloads. In contrast, RHUs are small, lightweight capsules that provide localized heating through the conversion of electrical energy to thermal. Although RHUs consume power rather than producing, the amount of power necessary to fully heat the probe is still relatively low due to the high efficiency of energy conversion. Overall, RHUs are significantly simpler, cheaper, and easier to integrate than RTGs, which would only be necessary if the thermal energy and power requirements were significantly higher.

7. TILES Thermal Control Strategy

The thermal control strategy for TILES begins with the thermal protection necessary to withstand the extreme heating of atmospheric entry. In order to mitigate these effects and prevent excess heat from penetrating into structure of the probe, we designed an aeroshell with thermal shielding. The heat shield structure is composed of an aluminum honeycomb sandwich with graphite fiber-reinforced composite facesheets. The facesheet thickness and honeycomb core density varies across the heat shield to balance structural integrity and thermal performance. The TPS for the heat shield, with an average thickness of 25 mm, utilizes Phenolic Impregnated Carbon Ablator (PICA). PICA is a lightweight, high-performance material composed of a carbon fiber preform infused with phenolic resin. This material's low density and high ablation efficiency make it ideal for managing extreme heat loads, particularly in areas that experience peak heating. The backshell structure is also constructed out of an aluminum honeycomb sandwich, with graphite composite facesheets of varying ply thicknesses. It is primarily protected by Super Lightweight Ablator (SLA-561V), a heritage material made from chopped silica fibers in a silicone resin matrix, with an average thickness of approximately 16 mm [67].

The aeroshell's heat dissipation strategy relies on ablation, where material erosion carries heat away from the spacecraft. PICA's carbon-fiber structure effectively chars and vaporizes under extreme conditions, while SLA-561V, though less efficient at high heat fluxes, provides sufficient protection for the backshell's relatively milder thermal environment. Additional coatings are also applied to the TPS to enhance radiative heat rejection and minimize material degradation. The overall aeroshell structure is pictured below in Figure 33 [67].

Fig. 33 Aeroshell Design for TILES, Including Thermal Shielding and Backplate

Once the probe has deployed onto the Mars surface, it will be faced with the temperatures of the Martian climate for the duration of its operation. During this period, the probe will be impacted by various thermal effects, including direct/indirect solar radiation (assumed zero during worst case cold condition), planetary radiation, surface conduction, convective heat loss, and radiative heat loss.

The first measure to protect against these effects will be a passive thermal control system incorporating MLI blanketing, aerogel insulation, and thermal coatings. Germanium coated kapton film (MLI) blanketing will also be wrapped around the surface of the probe to minimize radiative heat loss, while aerogel insulation provides additional thermal protection due to its low conductivity and lightweight nature. Specialized AZ-93 white thermal control paint

will also be applied to critical components to regulate heat absorption and emission.

The sum of all these effects can be analytically modeled and used to calculate any necessary internal thermal energy production using the equations 26, 27, 28, 29, 30, and 31 [66].

The results of this computation provide a required internal thermal energy production value of 218.88 W during worst case cold conditions and 70.33 W during hot conditions. This thermal energy will be supplemented by the same RHUs utilized in the OPUS thermal control system, producing 250 W of thermal energy at an efficiency ratio near one.

Supplemental Thermal Equations & Data

$$T_{\text{inner}} = T_{\text{outer}} - \frac{(\dot{q}t)}{k}, \tag{25}$$

- k = thermal conductivity
- t = material thickness

$$\dot{Q}_{\text{solar}} = \alpha I_s A_{\text{solar}} Fs/v, \tag{26}$$

- α = absorptivity
- I_s = solar intensity
- A_{solar} = area impacted by sunlight
- Fs/v = view factor between sun and vehicle

$$\dot{Q}_{\text{albedo}} = b\alpha I_s A_{\text{solar}} Fs/v, \tag{27}$$

- b = albedo coefficient

$$\dot{Q}_{\text{conv}} = h(T_{\text{eq}} - T_{\text{amb}})SA, \tag{28}$$

- h = convection coefficient
- SA = surface area

$$\dot{Q}_{\text{out}} = \sigma\varepsilon_{sc}(T_{eq}^4 - T_{\text{amb}}^4)SA, \tag{29}$$

- σ = Stefan-Boltzmann constant
- ϵ_{sc} = spacecraft emissivity

$$\dot{Q}_{\text{planetary}} = J_p A_{\text{planetary}}, \tag{30}$$

- J_p = planetary coefficient

$$\dot{Q}_{\text{conduction}} = \frac{T_{\text{gnd}} - T_{\text{probe}}}{R_{\text{gnd}} + R_{\text{probe}}}, \tag{31}$$

- R = Resistive coefficient

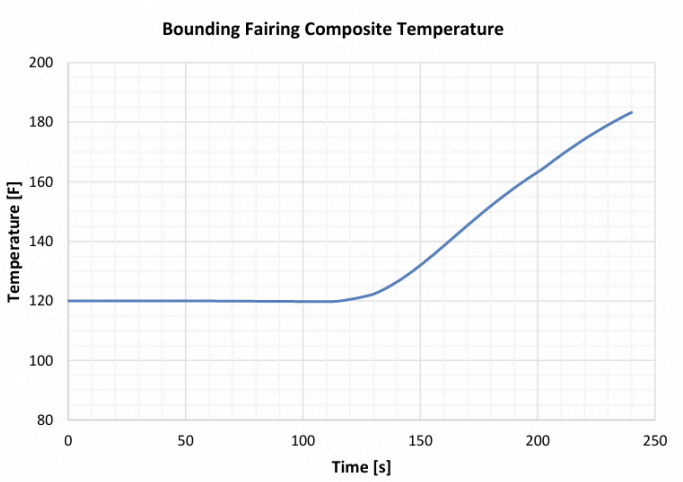

Fig. 34 Payload Fairing Temperature Within the Falcon Heavy During Initial Launch Burn [2]

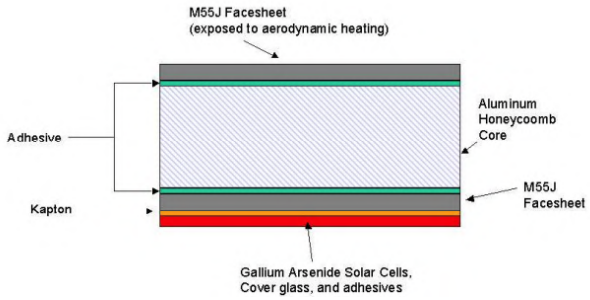

Fig. 35 MLI Layers for Solar Cell Array Modeling [61]

C. Power

The power subsystem shall have the following requirements:

Table 31 Power Subsystem Requirements

Req Name	Parent Req	Traceability	Requirement	Rationale
POW-1.0	MR-10.0	MR-10.0 - POW-1.0	The spacecraft shall be able to have electrical connectivity to the electrical ground support equipment.	From the Falcon Heavy User Guide. Ensures that the spacecraft can connect to the ground support electrical equipment.
POW-2.0	MR-4.0	MR-4.0 - POW-2.0	The OPUS shall have maximum 1000 W to power its subsystems.	Ensures that all OPUS subsystems and instruments have sufficient operating power.
POW-3.0	MR-4.0	MR-4.0 - POW-3.0	The TILES shall have maximum 500 W each to power all its subsystems.	Ensures that all TILES subsystems and instruments have sufficient operating power.
POW-4.0	MR-4.0	MR-4.0 - POW-4.0	The power sources for both the OPUS and TILES shall be stored in a compartment with an internal temperature between 253 and 313 Kelvin.	Ensures that the power subsystem does not overheat or freeze.
POW-5.0	MR-4.0	MR-4.0 - POW-5.0	The main power source for the OPUS and TILES will be supplied via solar panels.	Details how power will be individually generated for OPUS and TILES.
POW-6.0	MR-4.0	MR-4.0 - POW-6.0	The OPUS and TILES shall have a power reserve for eclipsed periods.	Details how OPUS and TILES will be able to operate when the solar panels cannot generate solar energy.

1. Power Subsystem Trades

When deciding on the batteries to use for OPUS and TILES, a trade was conducted on lithium-ion batteries as compared to supercapacitors. Supercapacitors have high power density, which would help to decrease the mass of the power system [69]. However, supercapacitors have first been used on a space mission in 2020, whereas lithium-ion batteries are the standard on space missions. Lithium-ion batteries were ultimately chosen because they've been proven to be effective and reliable, despite the lower weight of the supercapacitors. The lithium-ion batteries chosen for this mission were optimized to have the highest power density per unit mass, to decrease the weight of the power system.

When deciding on the solar panels to use for OPUS and TILES, the maximum power point, the efficiency, and the weight of the solar cells were considered in a trade for the system. Ultimately, the power produced per mass was the deciding factor for the solar panels chosen.

2. Power Budgets

Table 32 OPUS Power Budget - Required

				Idle Operation		Science Operation	
Subsystem	Component	Quantity	Voltage (V)	Duty Cycle (%)	Average Power (W)	Peak Duty Cycle (%)	Peak Power (W)
Structure	Probe Dismount	4	22	99.99	0	0.01	22
Instrumentation	Neutron Spectrometer	1	-	95	4.5	5	6.75
Instrumentation	CIRS-Lite	1	-	91	26.37	9	32.89
Instrumentation	High Resolution Imaging Camera	1	-	99.53	38	0.47	52.2
Instrumentation	LiDAR	1	-	17	26.2	83	29.9
Propulsion	Large Thruster (MR 107S)	1	28	99.99	0	0.01	34.8
ADCS	IMU (Honeywell MIMU)	2	28-100	75	25	75	25
ADCS	Small Thruster (MR 103D)	8	28	10	8.25	10	8.25
ADCS	Reaction Wheel (RW1)	4	22-34	25	9	25	9
ADCS	Star Tracker (BAE CT-2020)	2	22-34	0	0	100	8
ADCS	Sun Tracker (Adcole Digital Sun Sensor)	1	21-35	0	0	100	1
Thermal	Heater Units	1		60	443.96	40	491.6
Comms	Low-gain Antenna Gimbal	2	22-36	10	12.5	25	15
Comms	Electra Lite UHF Transceiver	1	22-36	5	15	95	65
Comms	Small Deep Space Transponder	1	22-36	5	12.5	95	15.8
Comms	X-band TWTAs	2	22-35	5	22	95	86
Comms	BAE Systems RAD750 Microprocessor	2	1.9-3.3	0	13	100	18
			Total Power Consumed (W)		656.28		921.19
				Power Margin	10%		10%
			Total Power Required (W)		721.908		1013.309

Table 33 TILES Power Budget - Required

				Idle Operation		Science Operation	
Subsystem	Component	Quantity	Voltage (V)	Duty Cycle (%)	Average Power (W)	Peak Duty Cycle (%)	Peak Power (W)
Structures	Explosive Bolts	2	22	99.99	0	0.01	22
Instrumentation	Radiation and Dust Sensor (RDS)	1	-	91.67	0	8.33	17
Instrumentation	Radiation Assessment Detector (RAD)	1	-	75	0	25	4.13
Thermal	Resistive Heater Units	1	-	50	128	50	234
EDL	Parachute Mortar	2	-	99	0	1	10
Comms	Electra Lite UHF Transceiver	1	22-36	10	15	90	65
Comms	Small Deep Space Transponder	1	22-36	75	12.5	25	15.8
Comms	Landing Radar	1	22-36	99.99	22.7	0.01	25.4
Comms	BAE Systems RAD750 Microprocessor	2	1.9-3.3	0	13	100	18
				Total Power Consumed (W)	191.2		411.33
				Power Margin	10%		10%
				Total Power Required (W)	210.32		452.463

The biggest draw of power is the heater units for thermal control so this held a large role in the power system sizing. The heater units require the most power during times of darkness to keep the systems at operational temperatures. This required larger batteries because solar panels weren't collecting energy while the heater units were fully powered. Other large draws of power include the CIRS-Lite, the High Resolution Imaging Camera, and the Electra Lite UHF Transceiver. Most of these components will be fully powered during the hours of light to collect and transmit data and idle in the darkness, which allows for the total power requirement at any time to be lower than the sum of the max powers.

The operational demand for OPUS in the light is 814.5 W, and 895.95 W is provided by the solar panels. The operational demand for OPUS in the dark is 873.05 W, and 960.355 W is provided by the batteries. The operational demand for TILES in the light is 212.96 W, and 234.256 W is provided by the solar panels. The operational demand for TILES in the dark is 340.38 W, and 374.418 W is provided by the batteries. These breakdowns of power requirements can be seen in Tables 34, 35, 36, and 37. The peak power demand for OPUS is 873.05 W, which can be provided by the solar panels and batteries, and the peak power demand for TILES is 340.38 W, which can be provided by the solar panels and batteries.

Table 34 OPUS Illuminated Power Budget - Provided

Subsystem	Component	Quantity	Power Required (W)	Power Provided (W)
Structure	Probe Dismount	4	0	0
Instrumentation	Neutron Spectrometer	1	4.5	4.95
Instrumentation	CIRS-Lite	1	32.89	36.179
Instrumentation	High Resolution Imaging Camera	1	52.2	57.42
Instrumentation	LiDAR	1	29.9	32.89
Propulsion	Large Thruster (MR 107S)	1	0	0
ADCS	IMU (Honeywell MIMU)	2	25	27.5
ADCS	Small Thruster (MR 103D)	8	8.25	9.075
ADCS	Reaction Wheel (RW1)	4	9	9.9
ADCS	Star Tracker (BAE CT-2020)	2	8	8.8
ADCS	Sun Tracker (Adcole Digital Sun Sensor)	1	1	1.1
Thermal	Heater Units	1	443.96	488.356
Comms	Low-gain Antenna Gimbal	2	15	16.5
Comms	Electra Lite UHF Transceiver	1	65	71.5
Comms	Small Deep Space Transponder	1	15.8	17.38
Comms	X-band TWTAs	2	86	94.6
Comms	BAE Systems RAD750 Microprocessor	2	18	19.8
		Total Power (W)	814.5	895.95

Table 35 OPUS Umbra/Penumbra Power Budget - Provided

Subsystem	Component	Quantity	Power Required (W)	Power Provided (W)
Structure	Probe Dismount	4	0	0
Instrumentation	Neutron Spectrometer	1	4.5	4.95
Instrumentation	CIRS-Lite	1	26.37	29.007
Instrumentation	High Resolution Imaging Camera	1	38	41.8
Instrumentation	LiDAR	1	29.9	32.89
Propulsion	Large Thruster (MR 107S)	1	0	0
ADCS	IMU (Honeywell MIMU)	2	25	27.5
ADCS	Small Thruster (MR 103D)	8	8.25	9.075
ADCS	Reaction Wheel (RW1)	4	9	9.9
ADCS	Star Tracker (BAE CT-2020)	2	8	8.8
ADCS	Sun Tracker (Adcole Digital Sun Sensor)	1	1	1.1
Thermal	Heater Units	1	525.73	578.303
Comms	Low-gain Antenna Gimbal	2	12.5	13.75
Comms	Electra Lite UHF Transceiver	1	65	71.5
Comms	Small Deep Space Transponder	1	15.8	17.38
Comms	X-band TWTAs	2	86	94.6
Comms	BAE Systems RAD750 Microprocessor	2	18	19.8
		Total Power (W)	873.05	960.355

Table 36 TILES Day Power Budget - Provided

Subsystem	Component	Quantity	Power Required (W)	Power Provided (W)
Structures	Explosive Bolts	2	0	0
Instrumentation	Radiation and Dust Sensor (RDS)	1	17	18.7
Instrumentation	Radiation Assessment Detector (RAD)	1	4.13	4.543
Thermal	Resistive Heater Units	1	70.33	77.363
EDL	Parachute Mortar	2	0	0
Comms	Electra Lite UHF Transceiver	1	65	71.5
Comms	Small Deep Space Transponder	1	15.8	17.38
Comms	Landing Radar	1	22.7	24.97
Comms	BAE Systems RAD750 Microprocessor	2	18	19.8
	Total Power (W)		212.96	234.256

Table 37 TILES Night Power Budget - Provided

Subsystem	Component	Quantity	Power Required (W)	Power Provided (W)
Structures	Explosive Bolts	2	0	0
Instrumentation	Radiation and Dust Sensor (RDS)	1	0	0
Instrumentation	Radiation Assessment Detector (RAD)	1	0	0
Thermal	Resistive Heater Units	1	218.88	240.768
EDL	Parachute Mortar	2	0	0
Comms	Electra Lite UHF Transceiver	1	65	71.5
Comms	Small Deep Space Transponder	1	15.8	17.38
Comms	Landing Radar	1	22.7	24.97
Comms	BAE Systems RAD750 Microprocessor	2	18	19.8
	Total Power (W)		340.38	374.418

3. Power System Selection and Sizing

The solar array power requirement was calculated using the equation

$$\tilde{P}_{\text{sa}} = \frac{P_{\text{sa}}}{A_{\text{sa}}} = [\eta_{\text{degradation}}] * [\eta_{\text{pointing}}] * [\eta_{\text{cell}}\eta_{\text{array}}S], \tag{32}$$

where $\tilde{P}_{\text{sa}}$ is the power produced by the solar array per square meter, P_{sa} is the power produced by the solar array which was calculated by the power requirement, A_{sa} is the solar array area, $\eta_{\text{degradation}}$ is the loss factor due to degradation which was estimated to be 0.8% at most, η_{pointing} is the loss factor due to pointing which was estimated to be 6% on average, η_{cell} is the loss factor due to the cell which was estimated to be 4.5% at most, η_{array} is the loss factor due to the array which was estimated to be 4.85% at most, and S is the solar irradiance [70] [15] [71] [72].

The necessary power from the solar panels determined the solar panels chosen for MOSAIC. The power requirement for OPUS was determined to be 510.73 W/m^2 and the power requirement for TILES was determined to be 537.51 W/m^2. The solar panels are then sized to produce more power than necessary for daytime operations, so power can be stored in the batteries for the night. Over the course of a day, the energy stored can be calculated by subtracting the required daytime power from the available power and multiplying it by the number of hours of light and the number of

hours in a cycle. The shortest period of light and the longest period of darkness were used when calculating the required battery capacity. The required energy for the night can be calculated by multiplying the required power for the night by the number of hours of darkness. The required energy to be stored is 2041.6 W-hr for OPUS and 4334.6 for TILES. The batteries and solar panels were then sized to accommodate those energies with a 10% margin. The solar panels had a required area of 6.1098 m^2 for OPUS and 1.5714 m^2 for TILES. The required battery capacity was calculated using the relation

$$C_{\text{bat}} = \frac{\text{Energy Req}}{(\text{DOD})\eta_{\text{conv}}}, \tag{33}$$

where C_{bat} is the required battery capacity, Energy Req is the energy required, DOD is the depth of discharge, and η_{conv} is the efficiency of drawing power from the battery [73] [69]. The required battery capacity for OPUS was 9073.7 W-hr and 25045 W-hr for TILES, also including a 10% margin.

The batteries chosen to fulfill these requirements are the Eaglepicher Technologies 60 Ah Space Cell [74]. Using these battery cells, OPUS requires 3 battery cells, which results in a mass of 20.25 kg and provides 2041.6 W-hr of energy and TILES requires 13 battery cells, which results in a mass of 87.75 kg and provides 4334.6 W-hr of energy. The solar panels chosen to fulfill these requirements are the Spectrolab Photovoltaic Products 26.8% Improved Triple Junction (ITJ) Solar Cells [75]. Using these solar cells, OPUS requires 631 solar cells, which results in a mass of 164.099 kg, and TILES requires 453 solar cells, which results in a mass of 117.948 kg.

The power system is colored pink and can be seen in Figure 42(b).

D. Structures and Design

For MOSAIC, a primary goal within the structural system was maintaining low mass profiles for the frame and integrative components of OPUS and TILES. Enabling this cause could be broken into volume minimization and material composition. Aluminum is most commonly used within space missions for structural purposes happening within and around the Moon and Mars environments [76]. Aluminum is resistive to corrosion, can handle large loads, and is relatively easy to manipulate and work with. However, for the purposes of this mission, pure aluminum appeared to not be as effective as it would be too dense given the mass limitations that the Falcon Heavy imposes. Understanding that the mission needed to be primarily created within a structure of high strength, lighter-weight metal, both the probe and orbiter have been determined to be created with frames and sub-structures of 2195-T8 Aluminum-Lithium alloy (Al-Li).

The structures subsystem shall have the following requirements:

Table 38 Structures Subsystem Requirements

Req Name	Parent Req	Traceability	Requirement	Rationale
STR-1.0	MR-4.0	MR-4.0 - STR-1.0	The structure of the OPUS and TILES shall keep all subsystems secure and attached.	Ensures that the design chosen for OPUS and the TILES will protect it against velocity changes.
STR-2.0	MR-4.0	MR-4.0 - STR-2.0	The structure of the OPUS and TILES shall protect all subsystems from vibrations during launch, transit, and orbits.	Ensures that the design and material chosen for OPUS and the TILES will protect it against strong vibrations.
STR-3.0	LV-1.0	MR-9.0 - LV-1.0 - STR-3.0	The structure of the OPUS and TILES shall be able to withstand loads of 5.4 g's.	Ensures that the design and material chosen for OPUS and the TILES will protect it against loads experienced during launch from Earth.
STR-4.0	MR-7.0	MR-7.0 - STR-4.0	The OPUS will have mounting hardware to attach the two TILES to it as well as a method of releasing the TILES over their POFMOs.	Ensures that the TILES have a method of attaching and releasing from OPUS.

1. OPUS Design

In addition to using a lighter weight alloy, a honeycomb structure was also implemented to force stability into the formation of the orbiter while minimizing mass. The outer shell is solid Al-Li, but for visualization purposes, the honeycombed structure of the material is shown in Figure 36.

The overall shape of OPUS was determined to be that of a 3D Hexagon in order to maximize stability, distribute load evenly and withstand the forces charged onto the vehicle that would be caused by aerobraking. The cage of the orbiter has solid sides that are capable mounting the instruments required of the mission, as well as general wiring, pipes, etc. that come with the individual subsystems. The visual empty volume that can be seen in Figure 36 was estimated using volume capacity from previous missions (like Viking), which, like previously stated, is used to connect sources through wiring and piping. In practice, the orbiter would not be majority open spacing.

An additional requirement is that the system is to be fully enclosed during aerobraking to prevent extreme temperature damage, however this would not allow for the instruments on board to collect data, as they need to point towards Mars and their cameras must not be obstructed. This is mitigated by the outer panels having gates that will open once the science orbit has begun and extreme temperature changes are minimal.

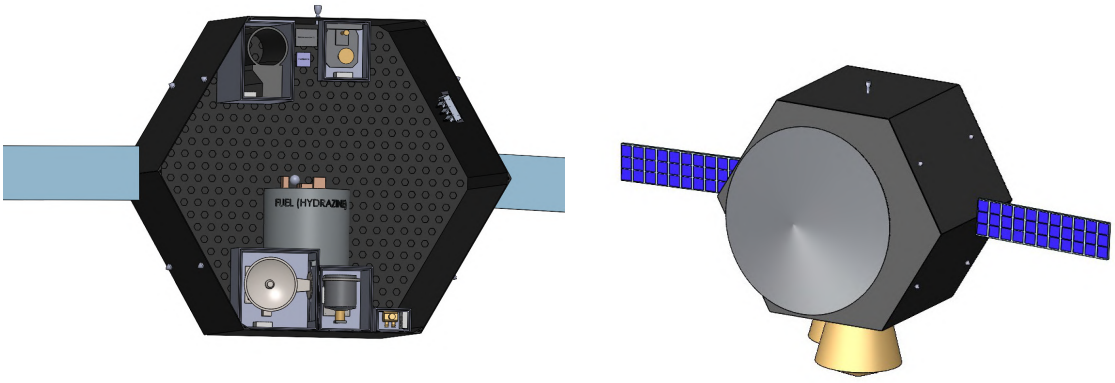

Fig. 36 Inside View of OPUS with Instruments, Fuel Storage, Reaction Wheels, and Venting System Visible (left) and the Front View with Solar Arrays and Communications Dish (right)

As seen in Figure 36., the instruments are orientated so that their cameras and other pointing devices are directed at Mars.

On the opposite side, OPUS has been designed so that the High Gain Reflector Dish and the solar panels are pointing towards Earth and the Sun respectively to ensure communication and power absorption when the orbiter is aligned with the Sun and/or Earth. This is reflected in Figure 36 as well.

The overall dimensionality of the structure can be attributed as 3.330x2.880x2.005 m^3, not including the solar panels and probe attachments. With the solar panels folded and the probe being attached to the bottom of the structure, the overall orbiter fits within the Falcon Heavy payload bay, amounting to about a box of 3.520x2.880x2.975 m^3. To effectively hold the mass and structure of the entire orbiter-probe system, the large "Payload Isolation Stand" created by Moog is used to integrate the system with the launch vehicle [77]. This adapter was chosen based on what is currently on market that can hold our total orbiter and probe masses, as well as being a company that has collaborated with SpaceX in past missions.

A fully rendered OPUS can be seen in Figure 37.

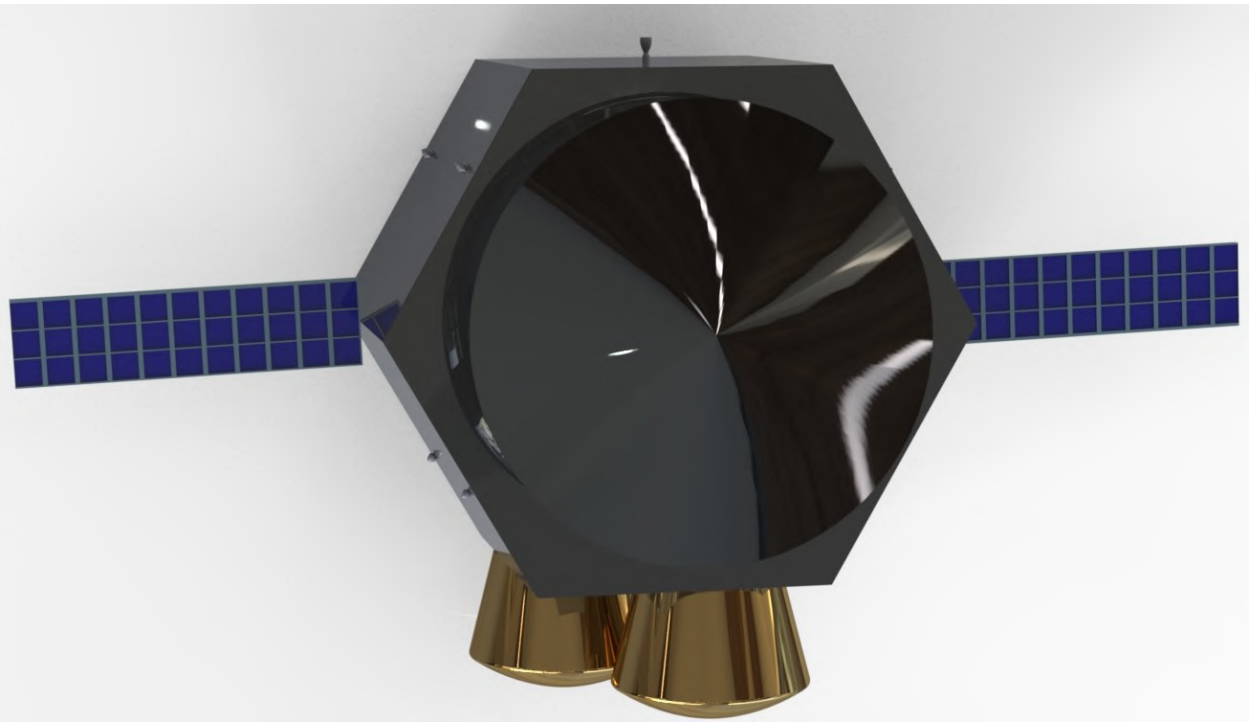

Fig. 37 Rendered Assembly of OPUS and Both TILES with Expanded Solar Arrays

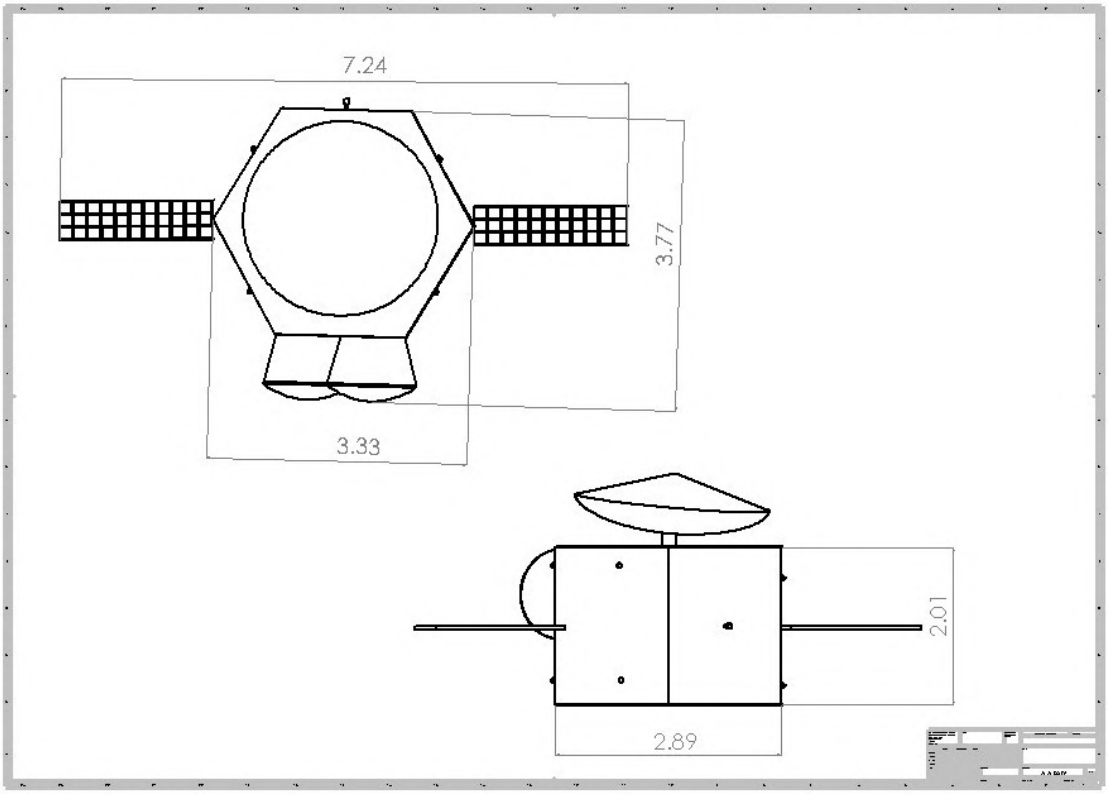

Fig. 38 OPUS Engineering Drawing in Meters

2. TILES Design

For the TILES probe, an outer structure was created with inspiration derived from the Cassini-Huygens mission, which resulted in 3D Trapezoid shape as the general formation [58]. This, like the 3D Hexagon, was chosen for structural and force distributional methodologies. The resultant formation, without the heat shield, can be seen in Figure 39 with the outer shell shown as transparent for visualization purposes.

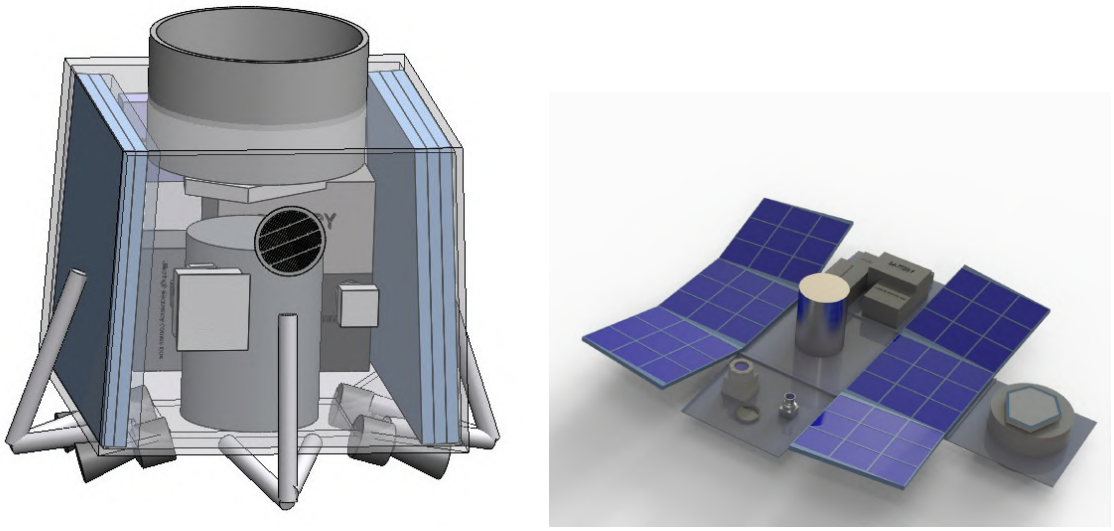

Fig. 39 TILES with Transparent Shell for Visualization (left) and Open Configuration (right)

Like the OPUS, the probe will be powered by solar energy. After the probe descends to the Martian surface, it will unfold, becoming near flat, where the faces of the structure which do no mount instruments or other devices, will hold solar arrays. The entire open system creates a geometric pattern, similar to that of a simple, rectangular mosaic. This can be seen in Figure 39. Below shows an engineering drawing of the assembly. The size of the assembly amounted to a folded dimensionality of 0.78x0.60x0.60 m^3 and an unfolded configuration of 2.01x1.56x0.30 m^3.

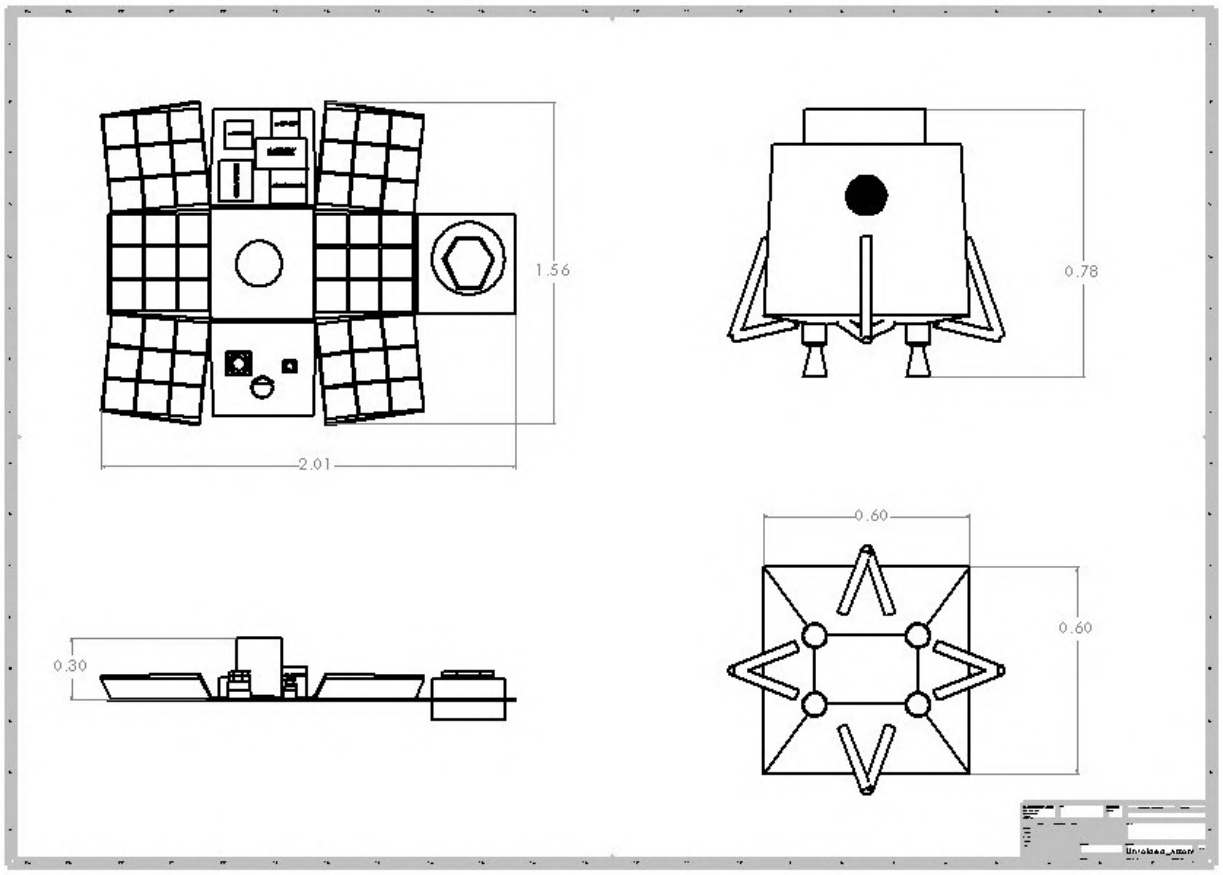

Fig. 40 Engineering Drawing of TILES, with Opened Configuration (left) and Folded (right) in Meters

Surrounding the outside of the structure is the heat shield as pictured in Figure 33. The angle of the conical portion of the shield was determined to be 70 degrees for EDL. The shield is encompassing of two parts, a top portion which connects to the orbiter, and bottom angular shield used directly for descent. The top attaches to the orbiter via a loaded spring system that would project the probes into their descent paths when released, and pyrotechnic bolts, that when cut also release the probes into their flight paths. Once released into descent, the top portion of the shield detaches from the bottom heat shield to then allow the parachutes to release. After the second parachute releases, the remaining heat shield shall unattach from the probe via 2 additional pyrotechnic bolts. Figure 41 shows the attachment of the TILES probes to the body of OPUS. More specifics on the thermal shields and the EDL can be found in sections IX.B and VIII.B, respectively.

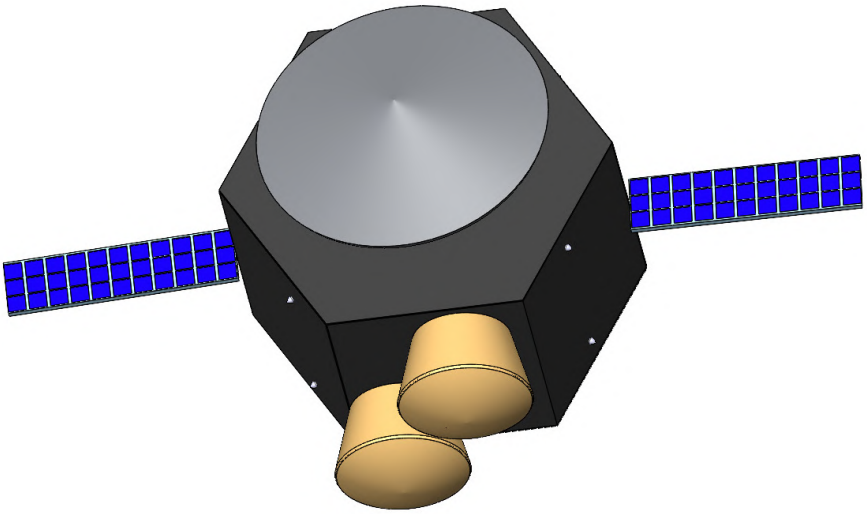

Fig. 41 Angled View to Show TILES Attachments to OPUS

3. Subsystem Labeling

For clarity, the following figures show how the previously expounded subsystems will be integrated in the overall orbiter system:

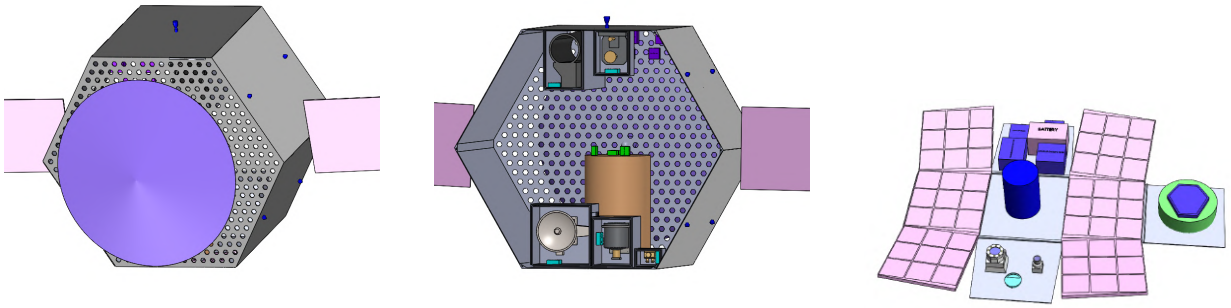

(a) Color-coded OPUS from the Sun Facing View

(b) Color-coded OPUS from the Mars Facing View

(c) Color-coded TILES

Fig. 42 Color-coded views of OPUS and TILES

Subsystems are colored as follows:

Communications	EDL/Reaction Wheels	Power	Fuel	Propulsion	Thermal

X. Mission and Operations Summary

A. Mass Budget

Below are the actual estimated masses of every subsystem analyzed in this report:

Table 39 Actual Mass Budget Estimates

Begin of Table			
Component	Level 3 (kg)	Level 2 (kg)	Level 1 (kg)
1.0 Spacecraft Dry Mass			1993.60
1.1 TILES			858.68
1.11 TILES #1		396.84	
1.111: Structures	48.38		
1.112: Thermal Control	3.50		
1.113: Power	205.70		
1.114: TT&C	22.24		
1.115: On-Board Processing	11.00		
1.116: EDL	99.00		
1.117: Radiation and Dust Sensor (RDS)	5.50		
1.118: Radiation Assessment Detector (RAD)	1.52		
1.12 TILES #2		396.84	
1.111: Structures	48.38		
1.112: Thermal Control	3.50		
1.113: Power	205.70		
1.114: TT&C	22.24		
1.115: On-Board Processing	11.00		
1.116: EDL	99.00		
1.117: Radiation and Dust Sensor (RDS)	5.50		
1.118: Radiation Assessment Detector (RAD)	1.52		
1.13 TILES Mounting Hardware			65.00
1.2 OPUS			1134.92
1.21: Structures			758.00
1.22: Thermal Control			36.50
1.23: Power			184.35
1.24: TT&C			48.50
1.25: On-Board Processing			11.00
1.26: ADCS			11.22

Continuation of Table 39			
Component	Level 3 (kg)	Level 2 (kg)	Level 1 (kg)
1.27: Propulsion			3.65
1.28: Gamma-Ray and Neutron Spectrometer (GRNS)			13.10
1.29: CIRS-Lite			17.00
1.210: High Resolution Imaging Camera			42.00
1.211: LiDAR			9.6
2.0 Consumables			0.0
3.0 Propellant			2192.70
4.0 Loaded Mass			4186.30
5.0 Kick Stage			0
6.0 Injected Mass			4186.30
7.0 Launch Vehicle Adapter			430.00
8.0 Boosted Mass			4616.30
9.0 Margin (10% of 10.0)			512.92
10.0 Total Mass			**5129.22**
End of Table			

As seen in Table 39, the total mass (including the reduced 10-percent mass margin) is approximately 30 percent of the total capacity of the Falcon Heavy. The Falcon Heavy appears to have more capacity than necessary, so there are now two options for MOSAIC: change the launch vehicle to one that is more suitable for the total mass, or partner with another Mars mission to use the remaining ~1,000 kilograms available in the Falcon Heavy's payload fairing. Choosing another launch vehicle this late in the development process would cause many turnbacks and delay operations significantly, so the MOSAIC Team opted to partner with another supposed Mars mission. This decision would also split the responsibility for the launch vehicle, operations, and other equipment costs, thus lowering the cost of the mission overall. For the purposes of this report, the cost analysis done in Section XI does not factor in this shared financial responsibility.

B. Risk Analysis

The MOSAIC Team identified 25 risks across all subsystems that would have the most significant impact on the mission (zoom in to read):

Table 40 Top 25 Risks and Mitigation Strategies

Ranking	Risk ID	Description	Con.	Lik.	Risk Score	Pre-Launch Mitigation
1	C-1	TILES cannot relay data to OPUS	5	3	15	More rigorous IA&T.
2	PO-1	Batteries lose charge when idle	4	3	12	Perform fatigue testing on batteries to understand if/when that would happen
3	EDL-1	Parachutes deploy too late	4	3	12	Ensure altitude sensors have redundancy and resistance to dust clouds
4	P-1	Fails to ignite	5	2	10	Ensure ignition redundancy.
5	OP-1	All instruments out of focus	5	2	10	Perform multiple and repetitive focusing simulations with instruments
6	TI-1	TILES fail to take images	5	2	10	Ensure strong power and comms connections
7	EDL-2	Landing legs fail to absorb landing impact	5	2	10	Recalculate TILES landing force and investigate upgrading to a stronger landing legs
8	P-2	Velocity into aerobraking is too high	3	3	9	Double-check Delta-V calculations and burn times; adjust orbit accordingly
9	OP-2	One instrument out of focus	3	3	9	Perform multiple and repetitive focusing simulations with instruments
10	TH-2	Radiation interferes with subsystems	3	3	9	Double-check shielding thickness
11	TR-1	Entry inclination into science orbit is incorrect	4	2	8	Ensure pointing accuracy is minimized during testing
12	TH-1	Spacecraft overheats during aerobraking	4	2	8	Double-check Delta-V calculations and shielding thickness
13	OR-1	Incorrect orbit altitude	4	2	8	Double-check Delta-V calculations
14	C-2	OPUS releases TILES over incorrect locations	4	2	8	Account for latency at all orbit locations
15	PO-2	Solar panels not charging to maximum capacity	4	2	8	Research how dust affects solar panel charging
16	ST-1	Subsystem attachments become loose	3	2	6	Test and purchase stronger attachment hardware
17	P-3	Velocity into aerobraking is too low	3	2	6	Assess minimum velocity that aerobraking is required
18	C-3	Temporarily lose contact with the spacecraft	2	3	6	Monitor
19	LV-1	Fails to launch	5	1	5	Do launch checks and rehearsals with SpaceX to catch errors
20	LV-2	Fails to deploy spacecraft	5	1	5	Do launch checks and rehearsals with SpaceX to catch errors
21	S-1	Bit rate error causes software failure	5	1	5	Double-check shielding thickness
22	OT-2	Inclement weather delays launch	1	4	4	Acceptance
23	ST-2	Damage sustained during launch loads	3	1	3	Test and reinforce frame, if necessary
24	OT-1	Launch facilities incorrectly electrically connect spacecraft to launch vehicle	3	1	3	Ensure SpaceX understands electrical connectivity with spacecraft before launch
25	C-3	Data is being transmitted/received slower than anticipated	3	1	3	Double-check data budget and create contingency plan for slow data transfers
			AVERAGE RISK SCORE		7.68	

The risks in Table 40 were sorted by risk score, then consequence, and finally by likelihood. The risks were then placed in a risk matrix:

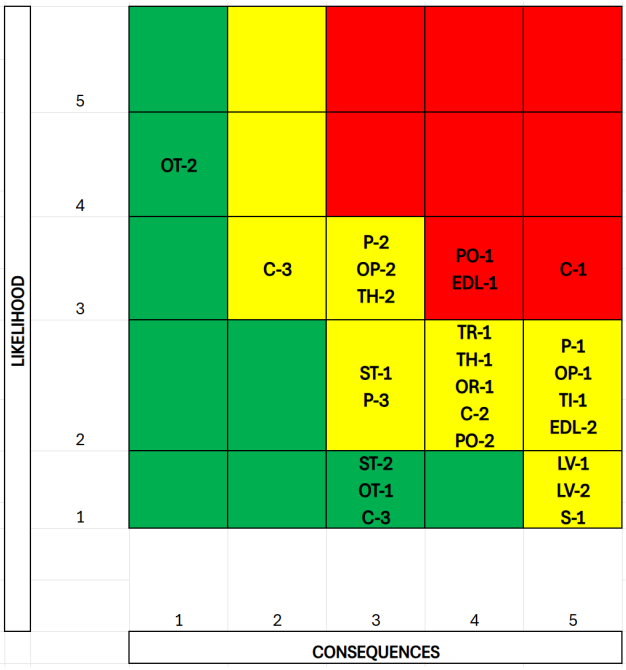

Fig. 43 MOSAIC Risk Matrix

The Team recognizes that not all possible risks are captured as there is an inherent level of uncertainty with every mission, and life can be unpredictable. However, since the majority of these risks identified are not in the red cells in Figure 43, MOSAIC appears to be feasible at this stage in the design process.

C. Schedule

MOSAIC's launch date is December 31, 2028, which means that all schedule phases, dates, and milestones need to be constructed around that date. Should this date be missed, the launch date (and therefore the structure of this schedule) can be shifted to the new launch date of January 16, 2029 (see Section VI). NASA provides guidelines on mission phases, milestones, and necessary reviews in Figure 44:

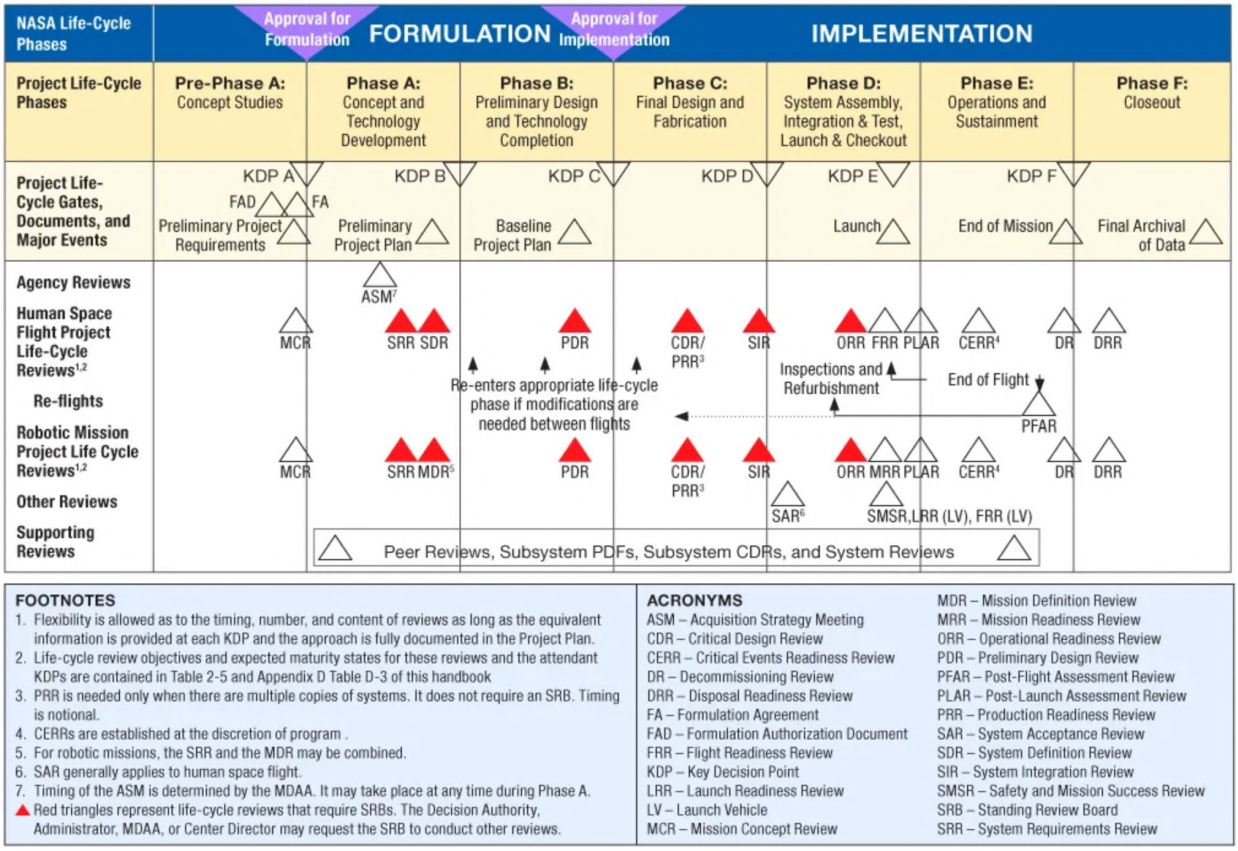

FOOTNOTES

1. Flexibility is allowed as to the timing, number, and content of reviews as long as the equivalent information is provided at each KDP and the approach is fully documented in the Project Plan.
2. Life-cycle review objectives and expected maturity states for these reviews and the attendant KDPs are contained in Table 2-5 and Appendix D Table D-3 of this handbook
3. PRR is needed only when there are multiple copies of systems. It does not require an SRB. Timing is notional.
4. CERRs are established at the discretion of program .
5. For robotic missions, the SRR and the MDR may be combined.
6. SAR generally applies to human space flight.
7. Timing of the ASM is determined by the MDAA. It may take place at any time during Phase A.

▲ Red triangles represent life-cycle reviews that require SRBs. The Decision Authority, Administrator, MDAA, or Center Director may request the SRB to conduct other reviews.

ACRONYMS

ASM – Acquisition Strategy Meeting
CDR – Critical Design Review
CERR – Critical Events Readiness Review
DR – Decommissioning Review
DRR – Disposal Readiness Review
FA – Formulation Agreement
FAD – Formulation Authorization Document
FRR – Flight Readiness Review
KDP – Key Decision Point
LRR – Launch Readiness Review
LV – Launch Vehicle
MCR – Mission Concept Review
MDR – Mission Definition Review
MRR – Mission Readiness Review
ORR – Operational Readiness Review
PDR – Preliminary Design Review
PFAR – Post-Flight Assessment Review
PLAR – Post-Launch Assessment Review
PRR – Production Readiness Review
SAR – System Acceptance Review
SDR – System Definition Review
SIR – System Integration Review
SMSR – Safety and Mission Success Review
SRB – Standing Review Board
SRR – System Requirements Review

Fig. 44 NASA Mission Phases, Milestones, and Reviews Structure [78]

Historical data on previous NASA missions in qualitative categories has also been supplied in Figure 41:

Table 41 Historical Phase Data for NASA Missions, in Months [56]

Mission Type	Example(s)	Phase A	Phase B	Phase C	Fab.	ATLO	Total
All Inherited Technology	MGS	3	3	6	5	9	26
New Engineering	Stardust, Genesis	5	7	10	6	12	40
New Technology	CloudSAT, GRACE	6	8	10	9	12	
Moderately Complex Payload with New Engineering	Magellan, Odyssey, Phoenix	7	7	12	9	15	48
Moderately Complex Payload with New Technology	Pathfinder, Deep Impact, MER	8	8	12	12	15	55
Highly Complex Payload with New Engineering	Mars Observer, Voyager	7	7	18	24	22	78
Highly Complex Payload with New Technology	Galileo, Cassini, MSL (Curiosity)	8	8	18	27	22	81

The instrumentation for MOSAIC is quite new, but the other components have been used on many other modern space missions. Therefore, MOSAIC is classified as a "moderately complex payload with new technology," which is highlighted in orange in Table 41. With these guidelines, the estimated start and end dates of the mission schedule phases and their appropriate tasks can be set:

Table 42 MOSAIC Schedule Phases, Tasks, and Reviews

Begin of Table		
Phases	**Start Date**	**End Date**
Major Reviews		
Mission Concept Review	2/3/2025	2/3/2025
Systems Requirements Review	5/1/2025	5/1/2025
Mission/System Definition Review	8/1/2025	8/1/2025
Preliminary Design Review	8/12/2026	8/12/2026
*Falcon Heavy Contract Signed	12/31/2026	12/31/2026
Critical Design Review	2/1/2027	2/1/2027
*Falcon Heavy Mission Integration Kickoff	2/28/2027	2/28/2027
Systems Integration Review	12/1/2027	12/1/2027
*SpaceX Completion of Mission Integration Analyses	12/31/2027	12/31/2027
Operational Readiness Review	7/1/2028	7/1/2028
*SpaceX Launch Campaign Readiness Review	9/30/2028	9/30/2028
Flight Readiness Review	11/1/2028	11/1/2028
*SpaceX Launch Readiness Review	12/29/2028	12/29/2028
*Falcon Heavy Orbit Injection Report	12/31/2028	12/31/2028
*Falcon Heavy Flight Report	12/31/2028	12/31/2028
Post-Launch Assessment Review	4/1/2039	4/1/2039
Phase A: Finalized Concept	**2/4/2025**	**9/30/2025**
Trajectory and Orbit Determination	2/4/2025	9/30/2025
Mars Atmospheric Conditions Investigation	2/4/2025	2/15/2025
OPUS and TILES Instruments R&D	2/15/2025	7/1/2025
OPUS ADCS R&D	2/15/2025	7/1/2025
TILES EDL R&D	2/15/2025	7/1/2025
Comms R&D	2/15/2025	7/1/2025
Power R&D	2/15/2025	7/1/2025
OPUS Propulsion R&D	2/15/2025	7/1/2025
Thermal/Radiation Control R&D	2/15/2025	7/1/2025

Continuation of Table 42

Phases	Start Date	End Date
Structural Materials & Design R&D	7/1/2025	9/30/2025
Phase B: Preliminary Design	**10/1/2025**	**4/30/2026**
OPUS/TILES Instruments Finalization	10/1/2025	1/1/2026
OPUS ADCS Preliminary Design	10/1/2025	1/1/2026
TILES EDL Preliminary Design	10/1/2025	1/1/2026
Comms Preliminary Design	10/1/2025	1/1/2026
Power System Preliminary Design	10/1/2025	1/1/2026
OPUS Propulsion System Preliminary Design	10/1/2025	1/1/2026
Thermal Control System Preliminary Design	10/1/2025	1/1/2026
Radiation Control Materials Determined	10/1/2025	1/1/2026
TILES Structure Preliminary Design	1/1/2026	4/30/2026
OPUS Structure Preliminary Design	2/1/2026	4/30/2026
Phase C: Finalized Design and Fabrication	**5/1/2026**	**4/30/2028**
OPUS Design & Systems Finalization	5/1/2026	4/30/2027
TILES Design & Systems Finalization	5/1/2026	4/30/2027
OPUS Components & Instruments Fabrication	5/1/2027	4/30/2028
TILES Components & Instruments Fabrication	5/1/2027	4/30/2028
Phase D: Assembly, Test & Launch	**5/1/2028**	**1/1/2029**
Spacecraft Assembly	5/1/2028	10/1/2028
OPUS/TILES Integration & Testing	10/1/2028	12/30/2028
Operations Preparation	10/1/2028	12/30/2028
Launch	12/31/2028	12/31/2028
Phase E: Operations and Sustainment	**1/1/2029**	**12/31/2038**
Transit to Mars & Separation from Falcon Heavy	1/1/2029	7/1/2029
Spacecraft Insertion into Science Orbit	7/1/2029	1/1/2030
OPUS Instrument Calibration	1/1/2030	1/6/2030
OPUS Mapping	1/6/2030	12/31/2033
Determination of POFMOs	12/31/2033	1/14/2034
TILES Release & Descent to POFMOs	1/14/2034	1/14/2034
TILES Record Environmental Data	1/15/2034	12/31/2038
Phase F: End of Life	**1/1/2039**	**12/31/2039**
OPUS/TILES Powered Off	1/1/2039	1/2/2039
Final Data Analysis & Next Mission Pre-Phase A	1/2/2039	12/31/2039

Continuation of Table 42

Phases	Start Date	End Date

End of Table

The asterisked (*) tasks indicate deadlines set by the Falcon Heavy User Guide [2]. Although the schedule may seem inflexible, time margins are included in these dates with the most flexibility being included in Phase F. The Gantt chart with all the phases, milestones, and reviews in Table 42 are represented in Figure 45

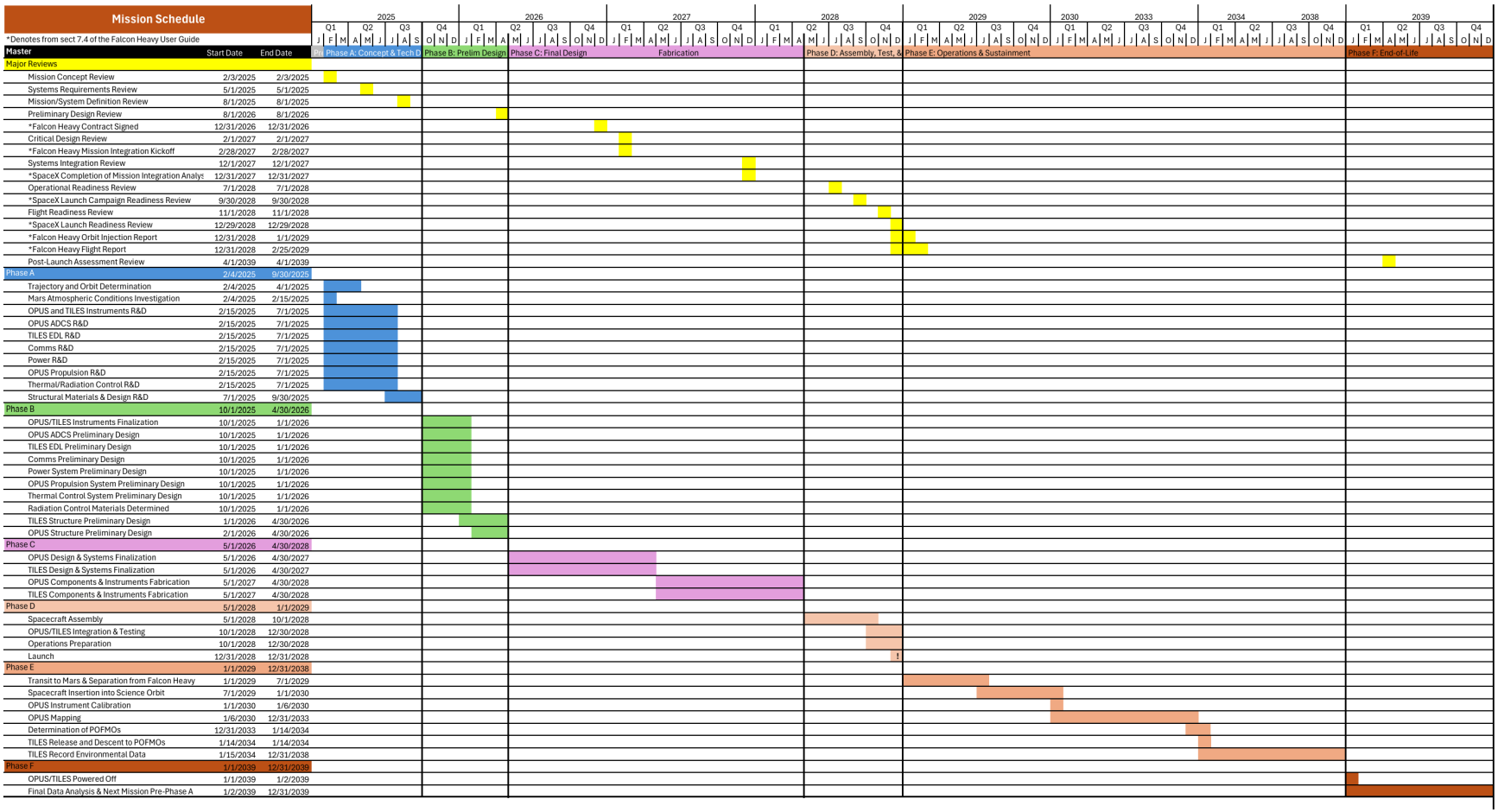

Fig. 45 MOSAIC Mission Schedule Gantt Chart

Please note that the columns for Q2: 2030 through Q1: 2033 and Q3: 2034 through Q2: 2038 have been condensed to allow Figure 45 to fit on the page. No milestones or task transitions are hidden in these columns.

XI. Mission Cost

The estimated cost of the mission is calculated using the Space Vehicle Cost Model (USCM8) for non-recurring and recurring costs [8]. The USCM8 utilizes various system parameters - typically mass or volume - into a formula to predict the cost, in units of thousands of dollars ($K).

A. Work Breakdown Structure & Labor

Below is MOSAIC's WBS:

Fig. 46 Work Breakdown Structure, According to the USCM8

Although NASA's basic WBS elements are accounted for, the USCM8 does not account for elements 3.0 (Ground Command) and 7.0 (Operations), as they require more complex calculations. To account for some of these costs, the Team ran a simulation on how many personnel (administrative and engineering) would be needed to complete the mission. Below is a list of assumptions made for this labor calculation:

- Each employee works 8 hours per day for 5 days a week (40-hour work weeks).
- Each employee's total cost is 150% of their annual salary, which accounts for other employee benefits like healthcare.
- An engineer's salary is $80,000 annually ($200k total).
- A technician's salary is $60,000 annually ($150k total).
- There is a mission staff of administrative engineers that will stay employed for the course of the entire mission (2025 to 2040).
- The Design and Fabrication (D&F) Team will be hired through mission phases A through D (2025 through 2028).
- The Launch and Operations (L&O) Team will be hired through mission phases E through F (2029 through 2039).
- There will be an approximately 6-month overlap between the two teams to ensure a smooth transition.
- Some engineers/technicians from the D&F Team will be hired onto the L&O Team to save overall costs.
- Continuity between teams and managerial roles will result in a salary increase between 5-25%, depending on the weight of the role.

Assuming continuity between teams, the MOSAIC mission is estimated to need at least 38 engineers and 8 technicians

throughout all phases of the mission, resulting in $7,940,00 in labor costs (see Figure 47).

Staffing and Labor

Notes: Estimated from the new SMAD and our mission timeline

Avg Engineer Salary ($K)	80	Avg Engineer Annual Cost ($K)	200
Avg Technician Salary ($K)	60	Avg Technician Annual Cost ($K)	150

Team Name	Position #	Position Name	Subposition (if any)	bposition (	Category	Start Date	End Date	# of Years	Total Hours	Shift Hours per Week	Shift Hours per Year	Shift Hours of Employment	Rec #	No Continuity			Continuity		
														Act #	Position Annual Cost ($K)	Employees Annual Cost ($K)	Act #	Position Annual Cost ($K)	Employees Annual Cost ($K)
Mission Staff	MS-1.1	Engineering Manager			E	1/1/2025	1/1/2040	15.00	131040	40	2080	31200	4.2	1	250	250	Not applicable for these positions		
	MS-1.2	Operations Manager			E	1/1/2025	1/1/2040	15.00	131040	40	2080	31200	4.2	1	250	250			
	MS-2.1	Operations Engineer			E	1/1/2025	1/1/2040	15.00	131040	40	2080	31200	4.2	2	230	460			
	MS-2.2	Mission Planner			E	1/1/2025	1/1/2040	15.00	131040	40	2080	31200	4.2	2	230	460			
													Engineers	6		1420			1420
													Technicians	0		0			0
													Team Total	6		1420			1420
Design & Fabrication Team	DT-1.0	OPUS Program Engineer			E	1/1/2025	1/1/2029	4.00	34944	40	2080	8320	4.2	1	220	220	1	240	240
		DT-1.1	Structures & Thermal Syste		E	1/1/2025	1/1/2029	4.00	34944	40	2080	8320	4.2	1	210	210	1	230	230
			DT-1.11 Structures		E	1/1/2025	1/1/2029	4.00	34944	40	2080	8320	4.2	1	200	200	1	200	200
			DT-1.12 Thermal C		E	1/1/2025	1/1/2029	4.00	34944	40	2080	8320	4.2	1	200	200	1	200	200
		DT-1.2	Trajectory, Orbit Maintenar		E	1/1/2025	1/1/2029	4.00	34944	40	2080	8320	4.2	1	210	210	1	230	230
			DT-1.21 Trajectory		E	1/1/2025	1/1/2029	4.00	34944	40	2080	8320	4.2	1	200	200	1	200	200
			DT-1.22 Orbit Analy		E	1/1/2025	1/1/2029	4.00	34944	40	2080	8320	4.2	1	200	200	1	200	200
			DT-1.23 ADCS/GNC		E	1/1/2025	1/1/2029	4.00	34944	40	2080	8320	4.2	1	200	200	1	200	200
			DT-1.24 Propulsion		E	1/1/2025	1/1/2029	4.00	34944	40	2080	8320	4.2	1	200	200	1	200	200
		DT-1.3	Communications & Softwa		E	1/1/2025	1/1/2029	4.00	34944	40	2080	8320	4.2	1	210	210	1	230	230
			DT-1.31 Power Sub		E	1/1/2025	1/1/2029	4.00	34944	40	2080	8320	4.2	1	200	200	1	200	200
			DT-1.32 Instrument		E	1/1/2025	1/1/2029	4.00	34944	40	2080	8320	4.2	1	200	200	1	200	200
			DT-1.33 TT&C Engi		E	1/1/2025	1/1/2029	4.00	34944	40	2080	8320	4.2	1	200	200	1	200	200
			DT-1.34 Software E		E	1/1/2025	1/1/2029	4.00	34944	40	2080	8320	4.2	1	200	200	1	200	200
			DT-1.35 On-Board I		E	1/1/2025	1/1/2029	4.00	34944	40	2080	8320	4.2	1	200	200	1	200	200
	DT-2.0	TILES Program Engineer			E	1/1/2025	1/1/2029	4.00	34944	40	2080	8320	4.2	1	220	220	1	240	240
		DT-2.1	Structures & Thermal Syste		E	1/1/2025	1/1/2029	4.00	34944	40	2080	8320	4.2	1	210	210	1	230	230
			DT-2.11 Structures		E	1/1/2025	1/1/2029	4.00	34944	40	2080	8320	4.2	1	200	200	1	200	200
			DT-2.12 Thermal C		E	1/1/2025	1/1/2029	4.00	34944	40	2080	8320	4.2	1	200	200	1	200	200
			DT-2.13 EDL Engine		E	1/1/2025	1/1/2029	4.00	34944	40	2080	8320	4.2	1	200	200	1	200	200
		DT-2.2	Communications & Softwa		E	1/1/2025	1/1/2029	4.00	34944	40	2080	8320	4.2	1	210	210	1	230	230
			DT-2.21 Power Sub		E	1/1/2025	1/1/2029	4.00	34944	40	2080	8320	4.2	1	200	200	1	200	200
			DT-2.22 Instrument		E	1/1/2025	1/1/2029	4.00	34944	40	2080	8320	4.2	1	200	200	1	200	200
			DT-2.23 TT&C Engi		E	1/1/2025	1/1/2029	4.00	34944	40	2080	8320	4.2	1	200	200	1	200	200
			DT-2.24 Software E		E	1/1/2025	1/1/2029	4.00	34944	40	2080	8320	4.2	1	200	200	1	200	200
			DT-2.25 On-Board I		E	1/1/2025	1/1/2029	4.00	34944	40	2080	8320	4.2	1	200	200	1	200	200
	DT-3.0	IA&T Engineer			E	1/1/2025	1/1/2029	4.00	34944	40	2080	8320	4.2	1	210	210	1	210	210
		DT-3.1	Simulations Technician		T	1/1/2025	1/1/2029	4.00	34944	40	2080	8320	4.2	2	150	300	2	150	300
		DT-3.2	IA&T Technician		T	1/1/2025	1/1/2029	4.00	34944	40	2080	8320	4.2	2	150	300	2	150	300
													Engineers	27		5500	27		5640
													Technicians	4		600	4		600
													Team Total	31		6100	31		6240
Launch & Operations Team	LO-1.0	Flight Operations Supervisor			E	5/1/2028	1/1/2040	11.67	101920	40	2080	24266.66667	4.2	1	220	220	1	220	220
	LO-2.0	Spacecraft Controller			E	5/1/2028	1/1/2040	11.67	101920	40	2080	24266.66667	4.2	4	220	880	4	220	880
	LO-3.0	Spacecraft Operations Engi			E	5/1/2028	1/1/2040	11.67	101920	40	2080	24266.66667	4.2	1	220	220	DT-1.0	--	--
		LO-3.1	Power, TT&C, & Instrument		E	5/1/2028	1/1/2040	11.67	101920	40	2080	24266.66667	4.2	1	200	200	DT-1.3	--	--
		LO-3.2	Orbit Analyst		E	5/1/2028	1/1/2040	11.67	101920	40	2080	24266.66667	4.2	1	200	200	DT-1.2	--	--
		LO-3.3	Structures & Thermal Cont		E	5/1/2028	1/1/2040	11.67	101920	40	2080	24266.66667	4.2	1	200	200	DT-1.1	--	--
	LO-4.0	TILES Operations Engineer			E	5/1/2028	1/1/2040	11.67	101920	40	2080	24266.66667	4.2	1	220	220	DT-2.0	--	--
		LO-4.1	Power, TT&C, & Instrument		E	5/1/2028	1/1/2040	11.67	101920	40	2080	24266.66667	4.2	1	200	200	DT-2.2	--	--
		LO-4.2	Structures, Thermal, & EDL		E	5/1/2028	1/1/2040	11.67	101920	40	2080	24266.66667	4.2	1	200	200	DT-2.1	--	--
	LO-5.0	OPUS Data Analyst			T	5/1/2028	1/1/2040	11.67	101920	40	2080	24266.66667	4.2	2	150	300	2	150	300
	LO-6.0	TILES Data Analyst			T	5/1/2028	1/1/2040	11.67	101920	40	2080	24266.66667	4.2	2	150	300	2	150	300
													Engineers	12		2540	5		1100
													Technicians	4		600	4		600
													Team Total	16		3140	9		1700
													Total Engineers	45		8040	38		6740
													Total Technicians	8		1200	8		1200
													Mission Total	53		9240	46		7940

Fig. 47 Staffing and Labor Calculations (in $K)

B. Cost Estimation

The formulas from the USCM8 are from 2010 and are therefore not representative of present-day pricing due to inflation. To account for this, *46% inflation is accounted for at the end of this section*, but the inflation percentage is halved to account for more accessible technologies available now than in 2010 (and therefore lower relative costs).

Below is the cost budget breakdown in accordance with USCM8:

USCM8 Non-Recurring & Recurring Subsystem CERs (Cost Estimating Relationships)

In FY2010 numbers, in thousands ($K)

WBS Element	Component	Subsystem	CER Input Parameter	Value	Units	Research, Dev, Test, & Eval (RDT&E) Cost	1st Unit Cost (Prod)	2nd Unit Cost (Protoflight)	Total Cost	Std Error	Best-Case	Worst-Case
1.0 Spacecraft	OPUS	Structure	Mass	758	kg	62215.24	17955.70	--	80170.94	17458.05	62712.89	97628.98
		Thermal Control	Mass	36.5	kg							
		ADCS	Mass	11.22	kg	3635.28	3334.36	--	6969.64	2799.89	4169.75	9769.54
		Power	Mass	184.35	kg	11853.71	5972.94	--	17826.65	6711.63	11115.01	24538.28
		Propulsion	Tank Volume	2682600	cm^3	26234.91	28320.85	--	54555.76	15412.81	39142.96	69968.57
			Apogee kick motor mass	3.65	kg							
		TT&C & Data Handling	Average Cost	26916.00	$K	26916.00	6570.41	--	33486.41	6027.55	27458.86	39513.97
			Mass	59.5	kg							
		Communications	Mass	48.5	kg	26695.50	9166.50	--	35862.00	14253.14	21608.87	50115.14
			Number of Channels	2	channels							
		Flight Software	Source Lines of Code (SLOC)	50000	lines of code	27500.00		--	27500.00	--	27500.00	27500.00
		Gamma-Ray and Neutron Spectrometer (GRNS)	Mass	13.1	kg	--	5317.23	--	5317.23	2073.72	3243.51	7390.95
			Power	6.75	W							
			Design Life	11	months							
		CIRS-Lite	Mass	17	kg	--	19887.26	--	19887.26	7756.03	12131.23	27643.29
			Power	32.89	W							
			Design Life	48	months							
		High Resolution Imaging Camera	Mass	42	kg	--	27294.36	--	27294.36	10644.80	16649.56	37939.15
			Power	52.2	W							
			Design Life	24	months							
		LiDAR	Mass	9.6	kg	--	11257.28	--	11257.28	4165.19	7092.09	15422.47
			Power	29.9	W							
			Data Rate	10	kilobits per second							
			Technology Readiness Level (TRL)	8	range of 4-9							
					OPUS Totals	185050.63	135076.89	0.00	320127.53	87302.81	232824.71	407430.34
	Per TILES	Structure	Mass	48.38	kg	9622.60	1172.49	--	10795.09	2363.19	8431.89	13158.28
		Thermal Control	Mass	3.5	kg							
		Power	Mass	205.7	kg	13226.51	6664.68	--	19891.19	8218.95	11672.24	28110.14
		FDI	Mass	99	kg	32076.00	12127.71	--	44203.71	16910.75	27292.96	61114.46
		TT&C & Data Handling	average cost	26916.00	$K	26916.00	4936.74	--	31852.74	5733.49	26119.25	37586.24
			Mass	33.24	kg							
		Radiation and Dust Sensor (RDS)	Mass	5.5	kg	--	7101.04	--	7101.04	2769.41	4331.64	9870.45
			Power	17	W							
			Design Life	23	months							
		Radiation Assessment Detector (RAD)	Mass	1.52	kg	--	2285.55	--	2285.55	891.36	1394.18	3176.91
			Power	4.13	W							
			Design Life	23	months							
					Per TILES Totals	81841.11	34288.21	0.00	116129.32	36887.16	79242.16	153016.48
					TILES Combined Totals	163682.22	68576.42	0.00	232258.65	73774.32	158484.33	306032.96
	Int, Assembly, and Test		OPUS & TILES non-recur cost	261549.64	$K	51002.18	18939.76		69941.94	27860.43	42081.50	97802.37
			OPUS & TILES recur cost	152739.99	$K							
2.0 Launch Vehicle & Services									97000.00		97000.00	97000.00
4.0 Program Level			OPUS & TILES & IA&T non-recur cost	38251.64	$K	13655.83	4545.54		18201.38	8646.13	9555.24	26847.51
			OPUS & TILES & IA&T recur cost	14204.82	$K							
5.0 Launch Operations & Orbital Support			Average Value	5850	$K	5850.00			5850.00	--	5850.00	5850.00
6.0 Ground Support Equipment			OPUS & TILES non-recur cost	196162.23	$K	61222.18			61222.18	22652.21	38569.97	83874.38
7.0 Labor									7940.00			
					Mission Totals	480463.04	227138.62	0.00	812541.66	220235.90	592305.76	1032777.56
					Mission Totals, Assuming 46% Inflation Between 2010 to 2025 But More Accessible Technology So It's Halved	590969.55	279380.50	0.00	999426.24	270890.16	728536.08	1270316.40

Fig. 48 USCM8 Non-Recurring & Recurring Subsystem Cost Budget Summary Table (in $K)

The flight software is estimated to have 50,000 lines of code, which is the middle of the range given in the USCM8 for a non-communications satellite. The "Best-Case" and "Worst-Case" columns in Figure 48 reflect what the total cost for that line item would be given plus-or-minus the standard error, respectively. Some line items did not have a standard error provided in the USCM8, as indicated by "–". The "1st Unit Cost" columns are the production costs, and the "2nd Unit Cost" accounts for a protoflight, which will not be done in this mission.

As seen in Figure 48, OPUS and TILES to have the following cost distribution across its subsystems:

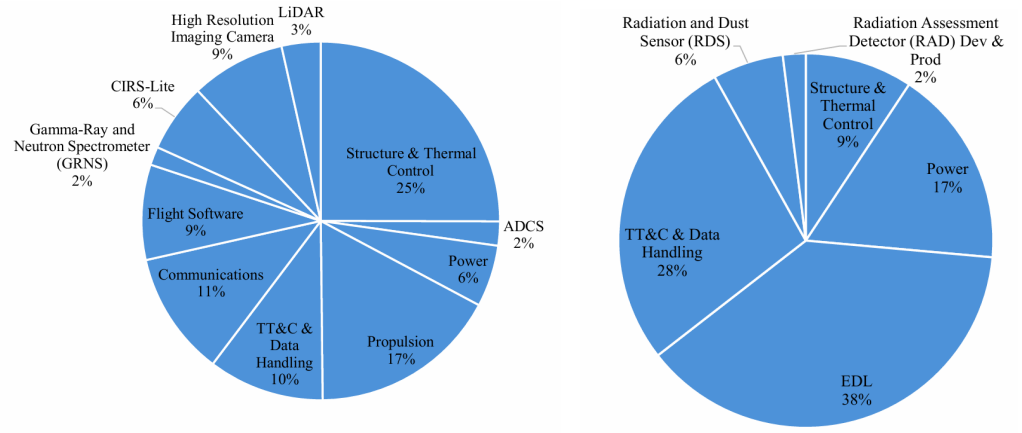

(a) Subsystem Cost Breakdown as Percent of Total OPUS Cost (b) Subsystem Cost Breakdown as Percent of Total TILES Cost

Fig. 49 OPUS and TILES Subsystems Cost Percentages

Finally, the USCM8 estimates the WBS elements to have the following cost distribution (including MOSAIC's labor cost calculations):

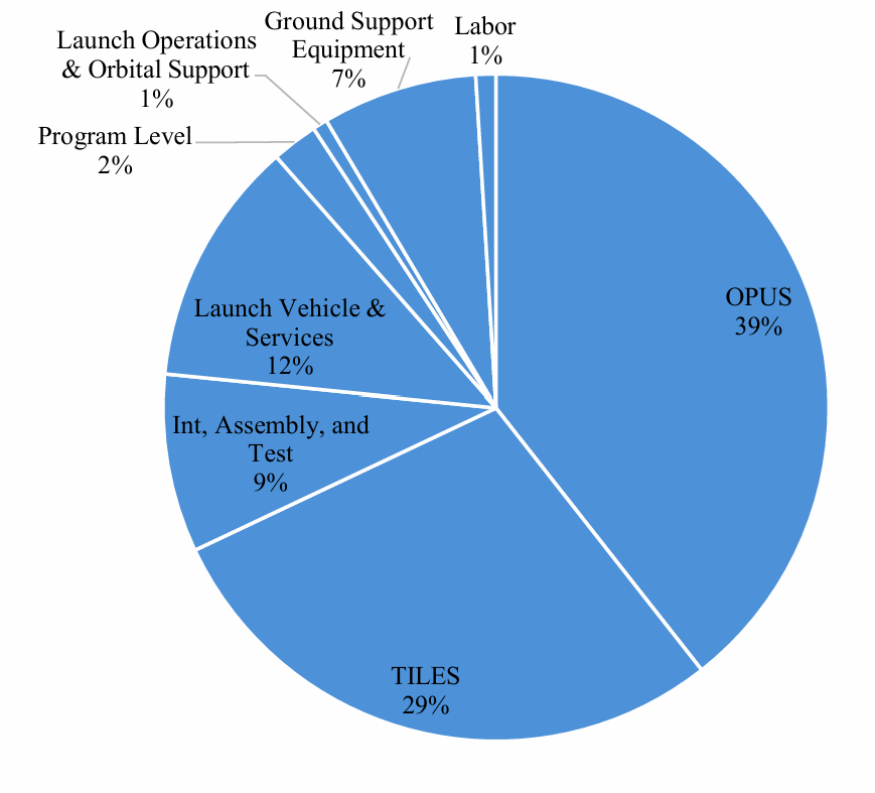

Fig. 50 WBS Elements Cost Breakdown as Percent of Total Cost

The IA&T and ground support equipment costs consider the price of OPUS and BOTH TILES, and the Program

Level estimation considers the IA&T cost in a similar formulation. The Falcon Heavy cost, which includes launch vehicle staffing, fuel, and most adjacent services, is directly from SpaceX's website [79].

At a total cost of **$999,426,240**, this mission is quite close to the upper echelon set by RFP-7 in Table 1. However, if the Falcon Heavy's payload fairing is shared with another mission, the cost of the WBS elements 2.0, 5.0, and 6.0 in Figure 46 could decrease as much as 50%, which would significantly reduce the cost of the mission. The MOSAIC Team understands that finding another mission to include in the payload fairing may be a difficult but necessary component to make the mission a reality.

Conclusion

The Mars Orbital Survey and Imaging Cartographer (MOSAIC) mission represents a comprehensive and innovative step forward in Martian exploration. Its core purposes were defined as mapping 75% of the Martian surface and carrying out environmental studies of prospective sites for human missions. Safe sites to land with traverse paths, referred to as POFMOs, were determined by mapping over three-quarters of the planet with high-resolution imaging and topographic measurements. Dust accumulation and radiation from space phenomena are monitored over time at these POFMOs to study Martian weather patterns to understand the environments of Mars in a novel, unique way. Overall, the data obtained on this mission will be vital to future manned missions to Mars and the continued exploration of the planet, helping humanity piece together a future on Mars, one step at a time.

XII. Compliance Matrix

Below is the Compliance Matrix with every requirement and constraint listed in the RFP [1].

Req ID	Requirement Description	Section(s) of Compliance
RFP-1	Design an integrated comprehensive mission to send one or more exploration assets to Mars vicinity with the primary objective to accurately characterize the atmospheric composition, detailed geographic survey, and/or determine the potential subsurface resources that may exist on Mars. The designed mission must address at minimum one of these primary objectives: - Characterization of the atmospheric composition and detailed density profile will provide mission planners the necessary data to plan and design the entry, descent, and landing system to support human exploration. - Detailed geographic survey, including terrain and elevation profile of the entire Martian surface will provide mission planner the ability to pinpoint potential landing location and traverse paths for each mission to maximize the potential to achieve exploration objectives. - Investigation, identification, and quantification of potential surface and subsurface resources will enable mission planners to determine the potential of utilizing such resources in support of the human exploration activities.	Fulfilled throughout report
RFP-2	The designed mission must be able to provide data on at least one primary objective area with minimum of 75% coverage of the entire Mars globe at the conclusion of the primary mission phase.	Fulfilled throughout report
RFP-3	Perform trade studies on various mission designs at the architecture and system levels to demonstrate the fitness of the chosen mission and system design. Trades should include system architecture, launch vehicles, instruments, orbital mechanics, spacecraft subsystem level designs, and other mission level system trades, including analysis of single vs multiple assets. It is highly desirable to use technologies that are already demonstrated on previous programs or currently in the NASA technology development portfolio. Trades should be assessed on the bases of benefit, risk, and cost.	IV, VII.A, VII.B.1, VII.C, VIII.A, VIII.B, IX.A, IX.B.3, , IX.C.1, IX.D
RFP-4	Perform mission analysis to evaluate the flight profile for the asset(s) and describe the mission profile for observation measurement and to show how the mission provide adequate coverage as specified by the RFP.	VI
RFP-5	Discuss selection of subsystem components and the values of each of the selection and how the design requirements or scientific objectives drove the selection of the subsystem.	III.C, VII, VIII, IX
RFP-6	Discuss the instruments selected to address the primary objectives, and the data collection, analysis, and transmission process to address the objectives.	III.C, IX.D.1, IX.D.2, IX
RFP-7	The cost for the mission and capability development in support of its activities shall not exceed $1.0 Billion US Dollar (in FY24), including development, hardware, launch, and operation cost of the mission through the primary mission phase.	XI.B
RFP-8	The mission should complete deployment and primary data gathering activities no later than December 31, 2033, with the system designed to operate into the late 2030s, though operation cost past the primary mission phase will be outside the scope of this RFP.	X.C
RFP-9	Requirements Definition – the report should include the mission and design requirements at the vehicle, system, and subsystem level. The requirements definition should demonstrate the team's understanding of the RFP Design Requirements and Constraints and lay the foundation for the design decisions that follow.	III.A, III.B
RFP-10	Concept of Operation – A detailed concept of mission operation should be included to describe all phases of the mission and to demonstrate the realization of the mission requirements in the RFP Design Requirements and Constraints. The report should show that the team has performed historical analysis of similar concepts to evaluate the merits and deficiencies of previous designs, and demonstrate that alternative concepts were considered while providing justification for the chosen concept.	III.E
RFP-11	Trade Studies – the report should include the trade studies for the vehicle architecture, mission operations, and subsystem selections, and must discuss in detail how the system level requirement are developed from mission requirements by describing the pro and cons of each subsystem options. The report must discuss how each subsystem level decision is made, with description of the selection metrics and their associated weightings when appropriate, and provide detailed discussions on how each decision impact system level metrics such as cost, schedule, and risk.	IV, VII.A, VII.B.1, VII.C, VIII.A, VIII.B, IX.A, IX.B.3, , IX.C.1, IX.D
RFP-12	Design Integration and Operation – The report should discuss how the trades selected in section 3 are integrated into a complete architecture. This section should discuss design of all subsystems: structures, mechanisms, thermal, attitude control, telemetry, tracking, and command, electric power, propulsion, payload and sensors, and the mission concept of operations. Discussion on the extensibility of the overall system design and how it can support future exploration mission should be included. The report must clearly describe all of the tools and methods utilized for the system and subsystem design and provide brief description of the inputs, outputs, and assumptions for the design. A discussion on the validation of the tools and methods must be included.	IX
RFP-13	Cost Estimate – a top level cost estimate covering the life cycle for all cost elements should be included. A Work Breakdown Structure (WBS) should be prepared to capture each cost element including all flight hardware, ground systems, test facilities, and other requirements for the design. Estimates should cover design, development, manufacture, assembly, integration and test, launch operations and checkout, in-space operations, and final delivery to the Martian surface and return to the Earth. Use of existing/commercial off-the-shelf hardware is strongly encouraged. Advanced technology utilization must be fully costed with appropriate cost margin applied. A summary table should be prepared showing costs for all WBS elements distributed across the various project life cycle phases. The report should discuss the cost model employed and describe the cost modeling methods and associated assumptions in the cost model. The cost analysis should provide the appropriate cost margin based on industry standards.	XI.B
RFP-14	Mission and operation summary – an integrated roll up of all the subsystems into a mass and power Work Breakdown Structure, showing mass and power budget, broken into subsystems, with description of the margin assigned to each system based on industry standards. A summary table should be prepared showing all mass, power, and other resource requirements for all flight elements/subsystems with the appropriate mass and power margins clearly labeled and discussed.	Table 39, X, IX.C.2, XI.B
RFP-15	Schedule – A mission development and operation schedule should be included to demonstrate the mission meets the schedule deadline established in the RFP. Schedule margin should be applied to appropriate areas with funded schedule reserve detailed in the cost estimate. Any advanced technology assumption should have corresponding technology development schedules and costs associated with the technology and appropriate contingency plans should be discussed.	X.C
RFP-16	Summary and References. A concise, 5 page "Executive Summary" of the full report must be included and clearly marked as the summary at the beginning of the report. The executive summary should provide a clear sense of the project's motivation, process, and results. References should be included at the end. A compliance matrix, listing the page numbers in the report where each these section as well as the items identified under the Design Requirements and Constraints and Deliverables sections can be found, is mandatory.	I, References (next page), XII

References

[1] American Institute of Aeronautics and Astronautics, "2024-2025 AIAA Undergraduate Team Space Design Competition," , 2024. URL https://www.aiaa.org/docs/default-source/uploadedfiles/membership-and-communities/university-students/design-competitions/2024-25-aiaa-undergraduate-team-space-design-competition.pdf, accessed: 2025-03-10.

[2] SpaceX, "Falcon User's Guide," , September 2021. URL https://www.spacex.com/media/falcon-users-guide-2021-09.pdf, Accessed: 2025-03-10.

[3] Mane, S., "Theoretical Overview on Polar Satellite Launch Vehicle (PSLV)," International Journal of Enhanced Research in Science, Technology and Engineering, 2024.

[4] Force, C. C. A., "Vulcan Centaur Program Operations and Launch on Cape Canaveral Air Force Station," , 2024. URL https://www.nasa.gov/wp-content/uploads/2024/01/national-aeronautics-and-space-administration-vulcan-fonsi-bg-word.pdf?emrc=1d8873.

[5] SpaceX, "Capabilities & Services," , 2024. URL https://www.spacex.com/media/Capabilities&Services.pdf, accessed: February 10, 2025.

[6] SpaceX, "Starship," , 2025. URL https://www.spacex.com/vehicles/starship/?utm=syndication, accessed: February 9, 2025.

[7] Massachusetts Institute of Technology, "Lecture Notes for 16.07: Dynamics," , 2004. URL https://dspace.mit.edu/bitstream/handle/1721.1/60691/16-07-fall-2004/contents/lecture-notes/d27.pdf, accessed: March 10, 2025.

[8] Wertz, J. R., Everett, D. F., and Puschell, J. J., Space Mission Engineering: The New SMAD, Microcosm Press, 2011.

[9] Motiwala, S. A., Mathias, D. L., and Mattenberger, C. J., "Conceptual Launch Vehicle and Spacecraft Design for Risk Assessment," Tech. Rep. NASA/TM-2014-218366, NASA Ames Research Center, 2014. URL https://ntrs.nasa.gov/api/citations/20150000182/downloads/20150000182.pdf.

[10] Team, P., "PorkChopPlot: Interplanetary Trajectory Tool," , 2025. URL https://wavwebs.com/PorkChopPlot/, accessed: 2025-03-08.

[11] NASA, "NASA Trajectory Browser," , 2025. URL https://trajbrowser.arc.nasa.gov/, accessed: Mar. 10, 2025.

[12] Srivastava, V. K., and Mishra, P., "Mars orbiter mission long eclipse prediction and aerobraking feasibility study," Journal of Space Safety Engineering, Vol. 10, No. 2, 2023, pp. 182–196. https://doi.org/10.1016/j.jsse.2023.03.010, URL https://doi.org/10.1016/j.jsse.2023.03.010.

[13] NASA, "Mars Reconnaissance Orbiter Aerobraking," , 2025. URL https://science.nasa.gov/resource/mars-reconnaissance-orbiter-aerobraking/, accessed: 2025-03-08.

[14] Laboratory, N. J. P., "Mars Global Surveyor Successfully Completes Aerobraking," , 2025. URL https://www.jpl.nasa.gov/news/mars-global-surveyor-successfully-completes-aerobraking/, accessed: 2025-03-08.

[15] Center, N. G. S. F., "Mars Fact Sheet," , 2025. URL https://nssdc.gsfc.nasa.gov/planetary/factsheet/marsfact.html, accessed: 2025-03-08.

[16] Laboratory, N. J. P., "Mars Telecommunications: Section 4 - Telecommunications Analysis," , 2025. URL https://descanso.jpl.nasa.gov/propagation/mars/MarsPub_sec4.pdf, accessed: 2025-03-08.

[17] Jesick, M., Demcak, S., Young, B., Jones, D., McCandless, S., and Schadegg, M., "Navigation Overview for the Mars Atmosphere and Volatile Evolution Mission," Journal of Spacecraft and Rockets, Vol. 54, 2016. https://doi.org/10.2514/1.A33618.

[18] NASA Goddard Space Flight Center, "General Mission Analysis Tool (GMAT)," , 2025. URL https://sourceforge.net/projects/gmat/, accessed: March 10, 2025.

[19] Laboratory, J. H. A. P., "Psyche GRNS," , "2025". URL "https://www.jhuapl.edu/destinations/instruments/psyche-grns", accessed: 2025-02-27.

[20] of Arizona Lunar, U., and Laboratory, P., "GRS PDS Data Node," , 2025. URL https://grs.lpl.arizona.edu/, accessed: 2025-03-10.

[21] Smith, D. E., "LOLA Fact Sheet," , 2024. URL https://science.nasa.gov/wp-content/uploads/2024/01/lola-fact-sheet.pdf, accessed: 2025-02-27.

[22] Cremons, D. R., "The future of lidar in planetary science," Frontiers in Remote Sensing, Vol. 3, 2022. https://doi.org/10.3389/frsen.2022.1042460, URL https://www.frontiersin.org/journals/remote-sensing/articles/10.3389/frsen.2022.1042460.

[23] Daly, M. G., Barnouin, O. S., Dickinson, C., Seabrook, J., Johnson, C. L., Cunningham, G., Haltigin, T., Gaudreau, D., Brunet, C., Aslam, I., Taylor, A., Bierhaus, E. B., Boynton, W., Nolan, M., and Lauretta, D. S., "The OSIRIS-REx Laser Altimeter (OLA) Investigation and Instrument," Space Science Reviews, Vol. 212, No. 1, 2017, pp. 899–924. https://doi.org/10.1007/s11214-017-0375-3, URL https://doi.org/10.1007/s11214-017-0375-3.

[24] Meng, Q., Wang, D., Wang, X., Li, W., Yang, X., Yan, D., Li, Y., Cao, Z., Ji, Q., Sun, T., Yan, W., Wang, K., Li, X., Huang, J., Wang, Z., Zhao, W., Wang, Y., He, Y., Hao, X., Liu, W., Zhang, B., Zhou, P., Li, Y., Zhao, H., Lu, L., Guan, H., Zhou, D., Wu, F., Zhang, F., Zhu, S., and Dong, J., "High Resolution Imaging Camera (HiRIC) on China's First Mars Exploration Tianwen-1 Mission," Space Science Reviews, Vol. 217, No. 3, 2021, p. 42. https://doi.org/10.1007/s11214-021-00823-w, URL https://doi.org/10.1007/s11214-021-00823-w.

[25] McEwen, A., Byrne, S., Hansen, C., Daubar, I., Sutton, S., Dundas, C., Bardabelias, N., Baugh, N., Bergstrom, J., Beyer, R., Block, K., Bray, V., Bridges, J., Chojnacki, M., Conway, S., Delamere, W., Ebben, T., Espinosa, A., Fennema, A., Grant, J., Gulick, V., Herkenhoff, K., Heyd, R., Leis, R., Ojha, L., Papendick, S., Schaller, C., Thomas, N., Tornabene, L., Weitz, C., and Wilson, S., "The high-resolution imaging science experiment (HiRISE) in the MRO extended science

phases (2009–2023),” Icarus, Vol. 419, 2024, p. 115795. https://doi.org/https://doi.org/10.1016/j.icarus.2023.115795, URL https://www.sciencedirect.com/science/article/pii/S0019103523003731.

[26] Brasunas, J. C., Flasar, F. M., and Jennings, D. E., “CIRS-lite: A Fourier Transform Spectrometer for a Future Mission to Titan,” Advances in Imaging, Optica Publishing Group, 2009, p. FTuA1. https://doi.org/10.1364/FTS.2009.FTuA1, URL https://opg.optica.org/abstract.cfm?URI=FTS-2009-FTuA1.

[27] Brasunas, J., Ely, V., Edgerton, M., Gong, Q., Hagopian, J., Mamakos, W., Morell, A., Pasquale, B., and Strojny, C., “CIRS-lite, a Fourier Transform Spectrometer for Low-Cost Planetary Missions,” NASA Technical Reports, 2011. URL https://ntrs.nasa.gov/citations/20110013404.

[28] Pasquale, B., Brasunas, J., Hagopian, J., Gong, Q., Mamakos, W., Edgerton, M., and Bly, V., “Optical design for the Composite InfraRed Spectrometer Lite (CIRS-Lite),” Proceedings of SPIE - The International Society for Optical Engineering, Vol. 7652, 2010. https://doi.org/10.1117/12.879044.

[29] Chai, P. R., Merrill, R., and Qu, M., “Mars Hybrid Propulsion System Trajectory Analysis Part I: Crew Missions,” , 2015. URL https://ntrs.nasa.gov/api/citations/20160006328/downloads/20160006328.pdf, accessed: 2025-03-10.

[30] Aerospace, D., “A Comparison of Electric and Chemical Propulsion in the Era of Low Launch Costs,” , 2024. URL https://www.dawnaerospace.com/latest-news/electricorchemical, accessed: 2025-03-10.

[31] Williams, D. R., and Bell II, E., “Mars Reconnaissance Orbiter,” , 2022. URL https://nssdc.gsfc.nasa.gov/nmc/spacecraft/display.action?id=2005-029A, accessed: 2025-03-10.

[32] Williams, D. R., and Bell II, E., “2001 Mars Odyssey,” , 2022. URL https://nssdc.gsfc.nasa.gov/nmc/spacecraft/display.action?id=2001-013A, accessed: 2025-03-10.

[33] Williams, D. R., and Bell II, E., “Mars Climate Orbiter,” , 2022. URL https://nssdc.gsfc.nasa.gov/nmc/spacecraft/display.action?id=1998-073A, accessed: 2025-03-10.

[34] Williams, D. R., and Bell II, E., “Dawn,” , 2022. URL https://nssdc.gsfc.nasa.gov/nmc/spacecraft/display.action?id=2007-043A, accessed: 2025-03-10.

[35] Blue Canyon Technologies, “Reaction Wheels Datasheet,” Tech. rep., Blue Canyon Technologies, 2024. URL https://www.bluecanyontech.com/static/pdf/Reaction-Wheels-Combined-2024.pdf, accessed: 2025-02-10.

[36] You, T.-H., Graat, E., Halsell, A., Highsmith, D., Long, S., Bhat, R., Demcak, S., Higa, E., Mottinger, N., and Jah, M., “Mars Reconnaissance Orbiter Interplanetary Cruise Navigation,” The International Symposium on Space Flight Dynamics, 2007, pp. 1–16.

[37] Aerojet Rocketdyne Holdings, Inc., “MR-103D Datasheet,” Tech. Rep. 2008-015, Aerojet Rocketdyne Holdings, Inc., Redmond, WA, 2008. Approved for public release and export.

[38] Honeywell Aerospace, "Inertial Measurement Units (IMUs)," , 2025. URL https://aerospace.honeywell.com/us/en/products-and-services/product/hardware-and-systems/sensors/inertial-measurement-units, accessed: 2025-02-15.

[39] Honeywell Aerospace, "MIMU Datasheet," Tech. rep., Honeywell Aerospace, 2023. URL https://aerospace.honeywell.com/content/dam/aerobt/en/documents/learn/products/space/datasheet/N61-1613-000-000_MIMU-ds.pdf, accessed: 2025-03-10.

[40] NASA, "Mars 2020: Perseverance Rover," , 2025. URL https://science.nasa.gov/mission/mars-2020-perseverance/, accessed: 2025-02-27.

[41] NASA, "Mars Exploration Rovers: Science Instruments," , 2025. URL https://science.nasa.gov/mission/mars-exploration-rovers-spirit-and-opportunity/science-instruments/, accessed: March 10, 2025.

[42] Hassler, D., Zeitlin, C., Wimmer-Schweingruber, R., Böttcher, S., Martin, C., Andrews, J., Böhm, E., Brinza, D., Bullock, M., Burmeister, S., Ehresmann, B., Epperly, M., Grinspoon, D., Köhler, J., Kortmann, O., Neal, K., Peterson, J., Posner, A., Rafkin, S., and Cucinotta, F., "The Radiation Assessment Detector (RAD) Investigation," Space Science Reviews, Vol. 170, 2012, p. 503. https://doi.org/10.1007/s11214-012-9913-1.

[43] Nelessen, A., Sackier, C., Clark, I., Brugarolas, P., Villar, G., Chen, A., Stehura, A., et al., "Mars 2020 Entry, Descent, and Landing System Overview," 2019 IEEE Aerospace Conference, 2019, pp. 1–20. https://doi.org/10.1109/AERO.2019.8742167.

[44] Parrish, J. C., "Long-Range Rovers for Mars Exploration and Sample Return," SAE Technical Papers, SAE International, 2001. https://doi.org/10.4271/2001-01-2138, URL https://spacecraft.ssl.umd.edu/design_lib/ICES01-2138.Mars_09_rover.pdf, accessed: 2025-04-24.

[45] SEIS InSight Mission Team, "Landing – SEIS / Mars InSight," , 2018. URL https://www.seis-insight.eu/en/public-2/the-insight-mission/landing, accessed: 2025-04-24.

[46] NASA Jet Propulsion Laboratory, "Mars 2020 Perseverance Rover Landing Press Kit," , 2020. URL https://www.jpl.nasa.gov/news/press_kits/mars_2020/landing/mission/, accessed: 2025-04-24.

[47] NASA Science, "Mars Pathfinder - NASA Science," , December 2017. URL https://science.nasa.gov/mission/mars-pathfinder/.

[48] L3Harris, "L3Harris Perseverance Support," , 2021. URL https://www.l3harris.com/sites/default/files/2021-02/L3Harris-IMS-EO-Sellsheet-Rover.pdf.

[49] L3Harris, "Electra Ultra-High Frequency Mars Transmitter," , 2020. URL https://www.l3harris.com/sites/default/files/2020-07/ims_eo_datasheet_UHF_Mars_Transmitter.pdf.

[50] JPL, N., "Electra Proximity Link for Mars Missions," , 2007. URL https://discovery.larc.nasa.gov/PDF_FILES/29Electra_Description.pdf.

[51] Dynamics, G., "Small Deep Space Transponder for X-band and S-band Communications," , 2025. URL https://gdmissionsystems.com/products/communications/spaceborne-communications/tracking-telemetry-and-control/small-deep-space-transponder.

[52] DESCANSO, J., "Mars Reconnaissance Orbiter," , 2014. URL https://descanso.jpl.nasa.gov/monograph/series13/DeepCommo_Chapter6--141029.pdf.

[53] NASA, "Perseverance Rover Components," , 2025. URL https://science.nasa.gov/mission/mars-2020-perseverance/rover-components/.

[54] Laboratory, N. J. P., "DSN Telecommunications Link Design Handbook - 104N," , 2021. URL https://deepspace.jpl.nasa.gov/dsndocs/810-005/104/104N.pdf, accessed: 2025-03-10.

[55] Laboratory, N. J. P., "DSN Telecommunications Link Design Handbook - 101E," , 2021. URL https://deepspace.jpl.nasa.gov/dsndocs/810-005/101/101E.pdf, accessed: 2025-03-10.

[56] Christian, J. A., "AE 4321: Space System Design I Lecture Slides," , 2024. Associate Professor, Guggenheim School of Aerospace Engineering, Director, Space Exploration Analysis Laboratory (SEAL).

[57] Laboratory, N. J. P., "What's Mars Solar Conjunction and Why Does It Matter?" , 2025. URL https://www.jpl.nasa.gov/news/whats-mars-solar-conjunction-and-why-does-it-matter/, accessed: 2025-03-10.

[58] Henry, C., "An Introduction to the Design of the Cassini Spacecraft," Space Science Reviews, Vol. 104, 2002, pp. 129–153. https://doi.org/10.1023/A:1023696808894.

[59] Murchie, S., et al., "CRISM: Compact Reconnaissance Imaging Spectrometer for Mars," Journal of Geophysical Research, Vol. 112, 2007. URL https://agupubs.onlinelibrary.wiley.com/doi/full/10.1029/2006JE002682.

[60] Livox, "Mid LiDAR specs - Livox," , 2025. URL https://www.livoxtech.com/mid-40-and-mid-100/specs, baseline specs used for STM.

[61] Amundsen, R. M., and Dec, J. A., "Aeroheating Thermal Analysis Methods for Aerobraking Mars Missions," , 2005. URL https://ntrs.nasa.gov/api/citations/20040085708/downloads/20040085708.pdf, accessed: 2025-03-10.

[62] Technology, A., "AZ-93 White Thermal Control, Inorganic Paint / Coating," , 2025. URL https://www.aztechnology.com/product/1/az-93, accessed: 2025-03-10.

[63] Ku, J., "Operating Characteristics of Loop Heat Pipes," , 2007. URL https://www.jpl.nasa.gov/nmp/st8/tech_papers/ices-1999-01-2007.pdf, accessed: 2025-03-10.

[64] Deans, M. C., Dye, S. A., and et al., W. L. J., "Multi-Environment MLI: Novel Multi-Functional Insulation for Mars Missions," , 2021. URL https://techport.nasa.gov/projects/101904, accessed: 2025-03-10.

[65] Center, N. G. R., "Mars Atmospheric Model," , "2021". URL "https://www.grc.nasa.gov/www/k-12/airplane/atmosmrm.html", accessed: 2025-03-10.

[66] Quattrocchi, G., Pittari, A., dalla Vedova, M. D., and et al., "The thermal control system of NASA's Curiosity rover: a case study," , 2021. URL https://www.researchgate.net/publication/358749133_The_thermal_control_system_of_NASA's_Curiosity_rover_a_case_study, accessed: 2025-03-10.

[67] Mahzari, M., Beck, R., and et al., H. H., "Development and Sizing of the Mars 2020 Thermal Protection System," , 2022. URL https://ntrs.nasa.gov/api/citations/20220006688/downloads/Development%20and%20Sizing%20of%20the%20Mars%202020%20Thermal%20Protection%20System_AIAA%20Aviation%202022.pdf, accessed: 2025-03-10.

[68] et al., S. P. D. M. K. A. K., "Mars thermal inertia and surface temperatures by the Mars Climate Sounder," , 2024. URL https://www.sciencedirect.com/science/article/pii/S001910352300430X#s0080, accessed: 2025-03-10.

[69] Caldwell, S., "State-of-the-Art of Small Spacecraft Technology 3.0 Power," , 2025. URL https://www.nasa.gov/smallsat-institute/sst-soa/power-subsystems/, accessed: 2025-03-10.

[70] Kerslake, T. W., and Gustafson, E. D., "On-Orbit Performance Degradation of the International Space Station P6 Photovoltaic Arrays," , 2003. URL https://ntrs.nasa.gov/api/citations/20030068268/downloads/20030068268.pdf, accessed: 2025-03-10.

[71] Barrett, M., Spacecraft Solar Cell Arrays, Vol. 8074, National Aeronautics and Space Administration, 1971.

[72] Xu, K., Zheng, J., Gong, Z., Cao, Y., Zhang, P., Wu, Q., and Yang, W., "Investigation on solar array damage characteristic under millimeter size orbital debris hypervelocity impact," 7th European Conference on Space Debris, 2017, p. 172.

[73] Yang, J., Du, C., Liu, W., Wang, T., Yan, L., Gao, Y., Cheng, X., Zuo, P., Ma, Y., Yin, G., et al., "State-of-health estimation for satellite batteries based on the actual operating parameters–Health indicator extraction from the discharge curves and state estimation," Journal of Energy Storage, Vol. 31, 2020, p. 101490.

[74] TECHNOLOGIES, E., "High energy, long-cycle life and low maintenance lithium-ion cell for demanding applications," , 2022. URL https://www.eaglepicher.com/sites/default/files/LP3303760AhSpaceCell1222.pdf, accessed: 2025-03-10.

[75] Technologies, S. P., "26.8% Improved Triple Junction (ITJ) Solar Cells," , 2008. URL https://www.spectrolab.com/DataSheets/TNJCell/tnj.pdf, accessed: 2025-03-10.

[76] Uppal, R., "Material technologies for harsh space environment in Moon, and Mars missions," , 2022. URL https://idstch.com/space/material-technologies-for-harsh-space-environment-in-moon-and-mars-missions/, accessed: 2025-03-10.

[77] Moog, "PAYLOAD ISOLATION STAND." , 2025. URL https://www.moog.com/content/dam/moog/literature/sdg/space/structures/moog-payload-isolation-stand-datasheet.pdf, accessed: 2025-03-10.

[78] NASA, "NASA Program/Project Life Cycle," , 2024. URL https://www.nasa.gov/reference/3-0-nasa-program-project-life-cycle/, accessed: March 10, 2025.

[79] SpaceX, "Falcon 9 & Falcon Heavy Capabilities & Services," , 2022. URL https://web.archive.org/web/20220322170331/https://www.spacex.com/media/Capabilities&Services.pdf, accessed: March 10, 2025.